AN INNOVATIVE APPROACH TO PREDICTING MEAT TENDERNESS USING BIOMECHANICAL PROPERTIES OF MEAT

A Dissertation

by

RANDI MARBURGER BOLEMAN

Submitted to the Office of Graduate Studies of
Texas A&M University
in partial fulfillment of the requirements for the degree of

DOCTOR OF PHILOSOPHY

May 2006

Major Subject: Food Science and Technology

AN INNOVATIVE APPROACH TO PREDICTING MEAT TENDERNESS USING BIOMECHANICAL PROPERTIES OF MEAT

A Dissertation

by

RANDI MARBURGER BOLEMAN

Submitted to the Office of Graduate Studies of
Texas A&M University
in partial fulfillment of the requirements for the degree of

DOCTOR OF PHILOSOPHY

Approved by:

Chair of Committee,	Jimmy T. Keeton
Committee Members,	Rhonda K. Miller
	Stephen B. Smith
	David H. Allen
Intercollegiate Faculty Chair,	Rhonda K. Miller

May 2006

Major Subject: Food Science and Technology

ABSTRACT

An Innovative Approach to Predicting Meat Tenderness Using Biomechanical Properties of Meat. (May 2006)

Randi Marburger Boleman, B.S., Texas A&M University;

M.S., Texas A&M University

Chair of Advisory Committee: Dr. Jimmy T. Keeton

Biomechanical compression studies at different temperatures were conducted to correlate the biomechanical response of raw bovine *Longissimus dorsi* muscles varying in USDA Quality Grade with overall sensory tenderness scores. Phase 1 assessed the biomechanical properties of raw 2.54 cm^3 samples obtained with a Texture Analyzer fitted with a 10 cm diameter platen which applied a constant strain of 3% for four minutes. Muscle specimens were arranged with fibers in parallel and perpendicular orientations to the applied force and tested at 0, 2, 4, 6, 8 and 10°C. Initial stiffness, final stiffness and energy dissipated of raw steak cubes with fiber orientation in parallel and perpendicular fiber orientations were calculated using the models and technique of Spadaro (1996) and correlated to overall sensory tenderness scores for each compression temperature. All compression values had higher correlation coefficients with overall sensory tenderness than did Warner-Bratzler Shear Force (WBSF). Of the prediction equations developed, it was concluded that samples compressed perpendicularly at 2ºC were better predictors of overall sensory tenderness ($R^2 = 0.77$) than WBSF ($R^2 = 0.11$).

Phase 2 assessed the biomechanical properties of raw steaks (2.54 cm thick) using a 2 mm diameter stainless steel probe in lieu of the platen and compressing samples 0.635 cm for 0.25 sec at -6.6, 4.4 or 10°C. Initial stiffness (ISTFPR), final stiffness (FSTFPR) and energy dissipated (EDPR) of raw intact steaks were calculated using a modification of the models and technique of Spadaro (1996) and correlated to overall sensory tenderness scores for each compression temperature. ISTFPR, FSTPF and EDPR values regressed against overall sensory tenderness produced higher R-square values (R^2 = 0.71 at 4.4ºC and R^2 = 0.70 at 10ºC) than prediction equations using WBSF (R^2 = 0.65). The significance of this study was that sensory tenderness could be predicted rapidly and more accurately on intact raw loin samples using a nondestructive probe measurement than could be predicted with WBSF. This innovative technique could potentially be used as a selection tool to ensure beef tenderness, be integrated into an on-line USDA Quality Grading system and be utilized as a powerful non-destructive research technique.

DEDICATION

To Pud, thank you for your support and love. I am so blessed to have found you and even more blessed that you chose me. You are truly my best friend and soulmate. Thank you for being there when I needed you the most. You do nothing but make me happy. I love you.

To Ricki 2, thank you for being such a joy. You were my 'more precious'. I love you.

To Ricki 3, thank you for not stealing my memory stick. You came into my life when we needed you most. I love you.

To Lucy, thank you for bringing us most joy. You keep us laughing and we are grateful for you. I love you.

To my family, for all their love and support. You would not settle for any less than my best and always supported my decisions along the way. You were always proud of me and continued to encourage me to be successful. I love you.

To Dr. Keeton, thank you for believing in me. You pushed me, knowing that I wouldn't back down from a challenge. In the end, it makes me a better, stronger person. I thank you for the opportunities you gave me and the gamble you took in taking me as a student. I hope that I never disappointed you and that I will continue to make you proud. Thank you so much.

ACKNOWLEDGMENTS

I would like to express my sincere gratitude to Dr. Jimmy Keeton for all of his support and guidance. He shared his dream project with me and made me feel capable of anything. He has been like a father and will always be a role model for me.

I am greatly appreciative for the help that Dr. Rhonda Miller has given me. She provided sample for my project, provided amazing statistical explanations, and provided a female ear when needed. Thank you for being an outstanding example of what a woman can do.

I will always be grateful for Dr. David Allen's input and agreement to serve on my committee. His knowledge of the subject is immeasurable and he was able to demonstrate such patience with someone who is unfamiliar with his field.

I thank Dr. Stephen Smith for continuing to support me in all of my graduate study endeavors. His input during my Master of Science work and Doctoral project was greatly appreciated. I learned so much from him while assisting at the USDA-FSIS.

I am fortunate to have worked with Dr. Chad Searcy, who was so enthused with helping me and remaining patient throughout the process. I know that I could not have done it without his help. I owe him alot.

I would also like to express my appreciation to John Vila with Vilas Motor Works for graciously and enthusiastically assisting me in constructing my probe.

I would also like to thank Betsy Booren for helping me with data collection, sensory analysis and food runs.

TABLE OF CONTENTS

Page

ABSTRACT iii

DEDICATION v

ACNOWLEDGMENTS vi

TABLE OF CONTENTS vii

LIST OF TABLES ix

LIST OF FIGURES xii

INTRODUCTION 1

OBJECTIVES 8

REVIEW OF LITERATURE 9

- Factors Influencing Meat Tenderness 9
- Importance of Sensory Testing 19
- Correlating Instruments to Sensory Evaluation 23

MATERIALS AND METHODS 50

- Phase 1 50
- Phase 2 50
- Analytical Techniques 51
- Compression Tenderness Test with a Platen and Texture Analyzer (TA) 57
- Compression Tenderness Test with a Probe and Texture Analyzer (TA) 62
- Sensory Evaluation 67
- Statistical Analysis 68

RESULTS AND DISCUSSION 71

- Phase 1 – Assessment of Cubed Specimen Temperature on Compressive Strain Measurements 71
- Phase 2 - Assessment of Biomechanical Properties of Intact Raw Muscle Sample with a Probe 84

Page

CONCLUSIONS 119

REFERENCES 124

APPENDIX A 134

APPENDIX B 143

APPENDIX C 145

APPENDIX D 184

APPENDIX E 187

APPENDIX F 201

VITA 214

LIST OF TABLES

TABLE		Page
1	Least square means of platen Texture Analyzer compression values as affected by fiber orientation.	146
2	Least square means of platen Texture Analyzer compression values as affected by temperature (ºC) during compression.	147
3	R-square values for prediction equations for juiciness based on fiber orientation and temperature (ºC).	148
4	R-square values for prediction equations for connective tissue based on fiber orientation and temperature (ºC).	149
5	R-square values for prediction equations for muscle fiber tenderness based on fiber orientation and temperature (ºC).	150
6	R-square values for prediction equations for overall sensory tenderness based on fiber orientation and temperature (ºC).	151
7	R-square values for prediction equations for Warner-Bratzler Shear based on fiber orientation and temperature (ºC).	152
8	Prediction equations incorporating fiber orientation and temperature (ºC) during platen compression with the highest R^2 values for sensory attributes using Warner-Bratzler shear values and TA compressions values.	153
9	Mean values of physical, chemical, sensory and biomechanical traits of *Longissimus dorsi* samples evaluated at three holding temperatures (Phase 2).	154
10	Pairwise correlation coefficients of "Raw Data" pooled over compression temperatures for physical traits of *Longissimus dorsi* samples (Phase 2).	156
11	Pairwise correlation coefficients of "Raw Data" pooled over compression temperatures for chemical traits of *Longissimus dorsi* samples (Phase 2).	157

TABLE Page

12 Pairwise correlation coefficients of "Raw Data" pooled over compression temperatures for sensory traits of *Longissimus dorsi* samples (Phase 2). 158

13 Pairwise correlation coefficients of "Raw Data" pooled over compression temperatures for biomechanical traits of *Longissimus dorsi* samples (Phase 2). 159

14 Pairwise correlation coefficients of "Adjusted Data" pooled over compression temperatures for biomechanical traits of *Longissimus dorsi* samples (Phase 2). 161

15 Pairwise correlation coefficients of "Raw Data" biomechanical traits of *Longissimus dorsi* samples (Phase 2) tempered to -6.6°C prior to compression. 163

16 Pairwise correlation coefficients of "Raw Data" biomechanical traits of *Longissimus dorsi* samples (Phase 2) tempered to 4.4°C prior to compression. 165

17 Pairwise correlation coefficients of "Raw Data" biomechanical traits of *Longissimus dorsi* samples (Phase 2) tempered to 10°C prior to compression. 167

18 Pairwise correlation coefficients of "Adjusted Data" biomechanical traits of *Longissimus dorsi* samples (Phase 2) tempered to -6.6°C prior to compression. 169

19 Pairwise correlation coefficients of "Adjusted Data" biomechanical traits of *Longissimus dorsi* samples (Phase 2) tempered to 4.4°C prior to compression.. 171

20 Pairwise correlation coefficients of "Adjusted Data" biomechanical traits of *Longissimus dorsi* samples (Phase 2) tempered to 10°C prior to compression.. 173

21 Prediction equations for sensory traits utilizing TA platen and probe compression values for pooled data at all compression temperatures (Phase 2). 175

TABLE Page

22 Prediction equations for sensory traits utilizing TA platen and probe compression values[1] for pooled data at -6.6°C (Phase 2). 176

23 Prediction equations for sensory traits utilizing TA platen and probe compression values[1] for pooled data at 4.4°C (Phase 2). 177

24 Prediction equations for sensory traits utilizing TA platen and probe compression values[1] for pooled data at 10°C (Phase 2). 178

25 Prediction equations for sensory traits using TA probe compression values for pooled data at all compression temperatures (Phase 2). 179

26 Prediction equations for sensory traits using TA probe compression values for pooled data at -6.6°C (Phase 2). 180

27 Prediction equations for sensory traits using TA probe compression values for pooled data at 4.4°C (Phase 2). 181

28 Prediction equations for sensory traits using TA probe compression values for pooled data at 10°C (Phase 2). 182

29 R-square values of prediction equations for sensory traits utilizing Warner-Bratzler shear force values, segregated by temperature treatment (Phase 2). 183

LIST OF FIGURES

FIGURE		Page
1	(a) Ice, salt and water are contained in a plastic tub with tubing to a circulating water bath system, and (b) Cubed samples of *Longissimus dorsi* muscle submerged in a water impermeable resealable plastic pouch (Ziploc®), submerged in a circulating water bath.	58
2	Force applied (a) parallel (PL) or (b) perpendicular (PP) to the myofiber orientation	59
3	Aluminum platen utilized in platen compressive measurements	60
4	Platen compressive measurement using aluminum platen	64
5	Stainless steel compression probe unit utilized in Phase 2	65
6	Probe compressive measurements using stainless steel compression probe	65
7	Four measurement locations taken on muscle surface	66
8	Comparison of initial stiffness mean values of each fiber orientation at each of the various holding temperatures.	185
9	Comparison of final stiffness mean values of each fiber orientation at each of the various holding temperatures.	185
10	Comparison of energy dissipated values of each fiber orientation at each of the various temperatures.	186

INTRODUCTION

Tenderness is one of the most important textural attributes of beef products and influences a consumer's decision to choose a particular cut (Kingston 1989). Variation and inconsistency of beef tenderness causes consumer dissatisfaction (Savell and others 1989; Smith and others 1995; Park and others 1998; Li and others 1999) and unfortunately USDA Quality Grade, the present sorting method for carcasses, is subjective and insufficient to ensure consistently tender cuts (Miller and others 1976; Reagan and Buyck 1995). Studies show that the relationship between quality grade and tenderness varies from being linear to simply a scattered array of data (McBee and Wiles 1967; Carpenter and others 1972; Parrish and others 1973; Parrish 1974; Dikeman and Crouse 1975; Jennings and others 1978; Davis and others 1979; Tatum and others 1980; Smith and others 1984; Dolezal and others 1982; Morgan and others 1991). Because USDA Quality Grade is based on anatomical criteria and is the primary means for establishing economic value of the carcass, development of an objective, compatible technique or methodology that would accurately and rapidly discriminate levels of tenderness in a cost efficient manner, could be of a significant economic benefit to the beef industry.

Current methods for assessing meat tenderness are categorized as subjective or objective. Subjective methods rely on a trained sensory or consumer panels while objective methods rely on mechanical means for assessing meat tenderness. Use of an analytical descriptive sensory panel to evaluate meat products allows for differentiating

---

This thesis follows the style and form of the Journal of Food Science.

between treatments, evaluating changes in processing procedures or ingredient content, improving quality control procedures, and defining the sensory properties of the sample (Bett 1993). Although this technique is accurate, it is time consuming, expensive, relies on humans as test instruments, requires special preparation facilities, and involves destruction of the sample. Subjective methods of assessing meat tenderness are often regarded as opinion and potentially biased, since it is the human instrument that is determining the measurement. Consumer evaluations of a product serve to predict acceptance or rejection, or like or dislike, and are inappropriate for addressing quantitative sensory aspects (Bett 1993). Similar constraints exist with consumer evaluations as do with an analytical sensory panel. Meat scientists and technologists desire an objective method of evaluating tenderness that is comparative to subjective methods, but that has the attributes of speed, accuracy, reduced cost and can be performed in a non-destructive manner on a raw sample.

Objective methods that measure tenderness employ a mechanical device that quantitates a physical property that in turn can be related to one or more textural sensory attributes. Current objective methods lack the desired accuracy, are time consuming and destroy the sample. The most common objective tenderness measurement device is the Warner-Bratzler shear apparatus (Bratzler 1932; Bouton and Harris 1972a; Voisey and Larmond 1974), which measures the maximum shear force exerted during complete severance of a cored muscle sample. However, this technique is only partially effective at predicting tenderness as characterized by correlations with other objective tests and sensory parameters. A survey of the scientific literature indicates that correlations

between Warner-Bratzler shear force (WBSF) readings and sensory tenderness range from highly significant to non-significant and are related, in varying degrees (range of r = 0.16 to 0.94), to readings from other mechanical instruments that test meat texture or measure other biomechanical properties (Pool and Klose 1969; Moller 1981; Berry 1983; Beilken and others 1991; Lepetit and Culioli 1992; Bett 1993; Pearson 1963; Purchas 1973; Rhodes and others 1972; Shackelford and others 1991a,b; Shackelford and others 1995; Szczesniak 1963, 1966, 1968, 1969, 1972; Szczesniak and Torgeson 1965; Szczesniak and others 1963; Tornberg and others 1985; Voisey 1976; Voisey and Larmond 1974). The ability of the Warner-Bratzler shear to predict tenderness of muscles other than *Longissimus dorsi* also varies with R square values ranging from 0.00 to 0.73 (Shackelford and others 1995).

Shear force values and muscle tenderness can be influenced or affected by several physical, chemical and biomechanical properties of meat. These include muscle fiber orientation, myofibrillar contraction, muscle type, post-mortem aging, cooking method, degree of cooked doneness, connective tissue properties, amount and solubility of collagen, age of animal, insulatory value of subcutaneous fat, degree of marbling, tissue pH, water holding capacity, sarcomere length, and myofibrillar fragmentation index (Cover and others 1962; Locker and Hagyard 1963; Marsh and Leet 1966; Herring and others 1965; Davey and Gilbert 1969; Field and others 1970; Bouton and Harris 1972a,b,c; Dikeman and others 1972; Cross and others 1973; Carpenter 1974; Huffman 1974; Bouton and others 1975; Campion and others 1975; Olson and others 1976; Szczesniak 1977; Culler and others 1978; Parrish and others 1979; Moller 1981;

Koohmaraie and others 1988; Harris and others 1992; Lepetit and Culioli 1992; Shackelford and others 1994; Wheeler and others 1994; Shackelford and others 1995; Dikeman 1996).

Due to the importance of tenderness and its relationship to consumer acceptance, more attention has focused on developing and correlating instrumental measures with sensory methods of texture evaluation (Szczesniak 1972). Refinements in instrument design and control of sample size and test conditions contribute to correlation improvement. Tenderness is not due to one factor but to a spectrum of physical variables that can be related directly or indirectly to organoleptically sensed textural attributes.

Most mechanical texture measurements are destructive, time consuming and require cooking of the sample, which prohibits making several tests on the same sample. New, objective techniques that are more cost effective, accurate, rapid and non-destructive are needed to enhance the USDA grading system, assess improvements in beef carcass merit and ensure consumer acceptance. Also, more accurate methodologies for measuring tenderness and other textural parameters would provide scientists with a unique opportunity to make unparalleled and in-depth comparisons of data taken from experimental animals at minimal cost. This could be applied to projects mapping the bovine genome and could allow identification of economically viable traits and allow for genetic selection of breeding populations that are inherently more tender. This would in turn provide greater economic returns to producers and processors alike, and provide consumers with a more desirable product.

Non-destructive methods to assess tenderness have been considered previously, but they pose specific problems in correlating non-destructive tests with sensory testing, which is destructive by nature. Two typical groups of tests that are recognized for a being non-destructive are resonance and direct force application. By direct application of a sinusoidal force to determine the complex dynamic modulus and energy loss of frankfurters, Webb and others (1975) found significant correlations (r = 0.61 to 0.98) between the energy loss and a number of sensory texture parameters characterized by a trained profile panel.

Spadaro (1996) and Spadaro and others (2002) initially developed a biomechanical technique that characterized the rheological behavior of post rigor bovine *Longissimus dorsi* muscles. The highest correlations with sensory tenderness and linear viscoelastic properties were found using a standard stress-relaxation technique at 3% strain for four minutes. Mechanical measurements were taken on 2.54 cm^3 squares of *Longissimus dorsi* oriented with fibers parallel or perpendicular to the applied strain. Initial and final stiffness and total energy dissipated were then calculated according to Spadaro (1996) and compared to overall sensory tenderness and WBSF. Overall sensory tenderness was highly correlated to final stiffness and energy dissipated in the parallel fiber orientation (r = 0.86 and r = -0.91). This compressive model of using energy dissipated in the parallel fiber orientation exceeded the WBSF correlation to overall sensory tenderness by 53%. Spadaro (1996) and Spadaro and others (2002) then constructed a model that would predict overall tenderness of beef loin steaks using energy dissipated in parallel fiber orientation or final stiffness in parallel fiber

orientation, which correlated highly to overall sensory tenderness (r = -0.95 and r = 0.95, respectively). WBSF values on the same set of samples were correlated to overall panel tenderness, but yielded a much lower correlation (r = 0.55). The obvious advantage to this objective technique was that overall tenderness of cooked meat could be predicted on raw samples, thus eliminating the need for cooking and subsequent sensory panel testing.

Marburger (1999) applied the technique and mathematical models developed by Spadaro (1996) and Spadaro and others (2002) to predict muscle tenderness of *Longissimus dorsi* steak samples that varied in tenderness and degree of aging. Energy dissipated-parallel (EDPL) and initial stiffness-perpendicular (ISTFPP) (r = -0.86 and r = 0.85, respectively) were effective predictors of sensory tenderness. WBSF was less effective for predicting tenderness (r = -0.79) than the biomechanical parameters. Marburger (1999) confirmed that the application of an objective, biomechanical strain to raw steaks could effectively predict overall sensory tenderness of cooked steaks more effectively than WBSF. Energy dissipated from samples in a parallel fiber orientation alone accounted for 73.3% of the variation in tenderness and was a more accurate assessment of tenderness than WBSF (61.9%). Regardless of degree of aging, each biomechanical property measurement accounted for more variation in the sample than did WBSF, and did so more effectively. Because this technique accounts for more variation in tenderness than WBSF and provides for a more accurate, rapid, less costly, and predictable method of measuring beef loin tenderness, further development of this technique could provide an on-line tenderness assessment test for segregation of beef

cuts. However, additional work is needed to enable measurements of intact muscle (regardless of muscle fiber orientation), determine the effect of sample temperature at measurement and potentially reduce compression time of the sample.

The current study was conducted to develop a non-destructive, more rapid and accurate tenderness assessment method using the biomechanical technique and mathematical models developed by Spadaro (1996) and Spadaro and others (2000), and verified by Marburger (1999). These studies demonstrated that biomechanical properties can more accurately assess overall tenderness than WBSF values but required excision of a raw muscle sample. The development of a non-destruction technique could give meat scientists a valuable research tool as well as allow wholesale beef loins to be segregated on the basis of tenderness, yet be compatible with the USDA quality grading system.

OBJECTIVES

The objectives of this research were to:

1. Evaluate the influence of muscle fiber orientation and sample temperature for predicting beef tenderness using the compressive method of Spadaro (1996);
2. Correlate raw compression values for tenderness with sensory panel profile data and Warner-Bratzler shear force measurements;
3. Correlate factors affecting palatability (USDA quality grade, calpastatin activity, collagen solubility, protein fractions, pH and others) with corresponding tenderness values;
4. Improve the technique and mathematical model of Spadaro (1996) to assess biomechanical properties of intact samples; and
5. Evaluate sample temperature and compression time for predicting beef tenderness of intact samples using the revised methodology.

REVIEW OF LITERATURE

Factors Influencing Meat Tenderness

Meat tenderness is due to a complex of subtle interactions among many textural factors. Correlating physical properties with subjective sensory evaluations could be beneficial in the development of a method that decreases the number of variables to predict tenderness or pinpointing a single variable that best predicts meat tenderness (Stanley and others 1971).

Lepetit and Culioli (1992) define tenderness as the ease, perceived by the consumer, with which meat structure is disorganized during mastication. Although tenderness cannot be defined strictly in physical terms, it involves the ability of meat to be sheared, compressed and ground during consumption and therefore depends directly on the structural characteristics and mechanical properties of the muscles.

The primary factor that produces texture is molecular structure of food. Interactions between perceived texture and physical structure are complex. Meat structure consists of muscle fiber bundles that are lying parallel to one another in an elastic-like matrix of connective tissue and associated structures (blood vessels, nerves, adipocytes, etc.) (Jack and others 1995). The myofibrillar, sarcoplasmic, and connective tissue proteins, and their interactions have major effects on texture. The subsequent structural and textural changes that result after cooking are the major determinants of meat tenderness.

Meat structure is defined as a collection of parallel myofibrillar fibers bound together by a connective tissue network of collagen fibers (Bouton and others 1975). By

the application of a deforming force to meat, one can shear through myofibrillar and connective tissue until one or the other breaks. Myofibrillar fiber physical properties can be affected by: (1) post-mortem enzymatic degradation (aging), which weakens fibers and produces small changes in connective tissue; (2) loss of moisture and other changes through cooking; and (3) increased myofibrillar contraction that increases muscle fiber diameter (Bouton and others 1975). Connective tissue is affected by (1) changes in spatial orientation of collagen fibers in the connective tissue network associated with myofibrillar contraction state and (2) chemical changes in the collagen produced by aging and cooking (gelatinization). Collagen properties change from being relatively inextensible in raw meat to elastic in cooked meat.

Changes in meat tenderness that occur during heating are related to the structural components of muscle tissue, the muscle fibers and the connective tissue fibers (Moller, 1981). The nature and extent of changes in these two components present opposing effects on tenderness. Heat induced changes of fibrous connective tissue to a granular and more soluble fraction has a tenderizing effect, whereas the denaturation of the myofibrillar proteins has a toughening effect.

The mechanical properties of meat are closely related to its structural remodification due to such things as the extent of enzymatic degradation (aging), sarcomere length, pH and water retention in the myofibrillar structure, collagen amount, degree of collagen cross-linking and thermostability of collagen, and spatial distribution of connective tissue (Lepetit and Culioli 1992). Muscle is a collection of cylindrical muscle fibers, representing about 85% of the muscle volume, joined together by

connective tissue, whose mechanical resistance is provided by collagen and elastin fibers. Endomysium, which encloses each muscle fiber, is a dense network of fibrils with no clear overall directional pattern, but when observed under stress, can become orientated either perpendicular or parallel to the muscle fibers. Intramuscular lipid (marbling), through its rheological properties and diluting effect on the collagen network, has a beneficial influence on tenderness. The complex nature of meat structure makes it difficult to analyze its behavior. However, the inherent structural features of meat have been used to devise mechanical stress tests to characterize a given structure. Another difficulty in analyzing meat is that local variations in connective tissue distribution and sarcomere length exist within each muscle and induce large variation in its mechanical properties (Segars and others 1974). Numerous factors play a role in mechanical testing such as dimension of the sample analyzed and the rate of strain applied, each of which can substantially influence specimen measurements.

Bouton and others (1975) studied the effects of contraction state, aging and prolonged cooking at different temperatures on connective tissue and myofibrillar structure of the *Longissimus dorsi* muscle from very young and old beef animals. Warner-Bratzler shear force values increased with cooking temperatures > 60° C and decreased with refrigerated aging. This indicated that a decrease in load-bearing capacity or weakening of the aged myofibrillar structure had occurred. Shear force and cooking loss values increased as cooking temperature increased. As cooking loss increased and sarcomere length decreased in the cooked samples, rigidity of the myofibrillar structure increased. Prolonged cooking reduced initial yield force and peak force values

regardless of contraction state, although Warner-Bratzler shear force values obtained for contracted muscles were still very high after 16 hr of cooking. Peak force values decreased more than initial yield force values for samples cooked < 4 hr. Individual fiber bundles of samples cooked for > 4 hr could be easily separated, suggesting that substantial connective tissue weakening had occurred.

Bouton and others (1975) concluded that the force-at-initial yield represented the Warner-Bratzler shear force required to compress and shear through the myofibrillar structure, and was primarily dependent on myofibrillar strength. Also, the difference between initial yield force and peak force could be an indication of the connective tissue strength. Initial yield force values for meat that had not been cold-shortened increased with cooking temperatures over 60° C, decreased with refrigerated aging, were not affected by animal age, and were reduced by cooking time at 90° C. Samples cooked for up to 16 hr at 90° C suggested that the increase in initial yield force values with increased myofibrillar contraction was mainly due to the myofibrillar structure rather than connective tissue.

Dikeman (1996) suggested that some tenderness differences may be due to the insulatory value of subcutaneous fat and possibly of intramuscular marbling. Marbling accounts for 5-10% of the variability in beef palatability (Shackelford and others, 1994). Intramuscular marbling has many roles in affecting palatability: 1) lubrication effect, 2) bulk density effect, 3) insurance theory, and 4) strain theory (Savell and Cross). The lubrication effect refers to the intramuscular fats that are in and around the muscle fibers,

which will lubricate the fibers and fibrils, making for a more tender and juicer product, giving the perception of tenderness. The bulk density effect states that within a bite size portion of cooked meat, the occurrence of marbling decreases the mass per unit volume. This lowers the bulk density by replacing the protein with lipid. Since fat is much less resistant to shear force than coagulated protein, this decrease in bulk density is accompanied by an increase in tenderness. Insurance theory is related to cooking. Fat conducts heat slower than muscle and the presence of greater amounts of marbling, allows the use of high temperature, dry-heat methods of cooking and/or cooking to a greater degree of doneness without adversely affecting the palatability of the meat. Marbling protects the proteins during heating by providing some insurance that if the meat is cooked too long, too rapidly or incorrectly, it will still be palatable. The strain theory refers to the weakening of connective tissue by marbling. As marbling is deposited inside the cell walls of the perimysium or endomysium, both are connective tissues, the connective tissue walls on either side of the fat deposit are thinned, thus decreasing their width, thickness and strength.

Other differences may be due to the degree of maturation of collagen because of differences in protein turnover or the dilution effect of high marbling on collagen amount. Other reasons for variations in tenderness include differences in activity of the calpain enzyme system and/or the activity of calpastatin (Koohmaraie and others 1988) and the effects of high marbling on heat transfer during cooking and increased cooking yield. A large amount of variation in beef tenderness is due in part to cattle being physiologically older at slaughter, and their tissues, especially collagen, may be more

mature (cross-linked). Shackelford and others (1994) showed that Warner-Bratzler shear force decreased and trained sensory panel tenderness values increased with each successive increase in degree of marbling from < Traces, to Slight, Small and > Modest. This study demonstrated that marbling was related significantly to sensory panel tenderness. Dikeman and others (1972) reported that marbling score correlated significantly with tenderness factors, but the percentage of the tenderness variation that was accounted for was small. Huffman (1974) plotted sensory tenderness scores, used as the standard, against marbling scores and found that 64% of the marbling scores were correct for predicting sensory tenderness. Other studies indicated that marbling accounts for 5 to 15% of tenderness (Campion and others 1975; Carpenter 1974). Wheeler and others (1994) evaluating the tenderness of the *Longissimus dorsi* found Warner-Bratzler shear force values to decrease as marbling increased from Traces to Slight to Small.

Harris and others (1992) evaluated tenderness of 2.54 cm thick beef top sirloin steaks, top sirloin butts and strip loins from both sides of 20 USDA Choice beef carcasses. Six steaks each were assigned randomly to 0, 7, 14, 21, 28, or 35 days of aging in vacuum pouches. Top sirloin steaks were less tender and had more variation in tenderness than top loin steaks. This difference in tenderness appeared due to higher amounts of collagen in the top sirloin steaks, lower collagen solubility, shorter sarcomere lengths and a higher (less tender) myofibrillar fragmentation index.

Many factors have been shown to be related to beef tenderness. Muscles having shorter sarcomeres tend to be less tender than those with longer sarcomeres (Locker and Hagyard 1963; Marsh and Leet 1966; Herring and others 1965; Harris and others 1992).

Fragmentation indices, the relative measure or ease with which beef muscle fibers break apart, also have been used as predictors of cooked beef tenderness (Davey and Gilbert 1969; Olson and others 1976; Culler and others 1978; Parrish and others 1979; Harris and others 1992). A lower fragmentation index predicts a more tender sample because the muscle fibers can easily be broken apart.

Connective tissue, specifically collagen, is one of the most widely studied tenderness-related components. As physiological and chronological age increases, decreases in tenderness can be accounted for by a greater amount of heat-stable collagen present, and its relative solubility. Others (Cover and others 1962; Field and others 1970; Harris and others 1992) have found differences in collagen concentrations between different muscles within a carcass, and demonstrated that muscles with more collagen were less tender than those with less collagen.

Postmortem storage (aging) of carcasses at refrigeration temperatures (-0.8 to 2.0° C) improves meat tenderness and is an important procedure for producing tender meat (Bouton and Harris 1972b,c; Bouton and others 1975; Harris and others 1992; Koohmaraie and others 1988; Shackelford and others 1995). Although improvement in meat tenderness is measurable subjectively and objectively, the exact mechanism of improving tenderness due to postmortem storage remains unclear. There appears to be general agreement that proteolysis of myofibrillar proteins by calcium-dependent proteases and lysosomal enzymes are the major contributor to meat tenderization during postmortem storage (Koohmaraie and others 1988). Koohmaraie and others (1988) studied the factors that were associated with the tenderness of three bovine muscles,

Longissimus dorsi, *Biceps femoris* and *Psoas major*, stored at 1.2° C. At day 1 postmortem, the *Psoas major* was the most tender muscle followed by the *Biceps femoris* and *Longissimus dorsi*. The *Psoas major* muscle had the smallest fiber diameters and longest sarcomeres followed by the *Biceps femoris* and *Longissimus dorsi*. Shear force values decreased to a greater degree for the *Longissimus dorsi* than for the *Psoas major*, which declined only slightly after 24 hr postmortem storage. There were no discernible differences in the activities of cathespsins, B, H, and L for any of the muscles, however, *Longissimus dorsi* had the highest Ca^{++}-dependent protease activity.

Purchas (1973) proposed that one explanation for the poor relationship between raw and cooked meat tenderness might be that tenderness determinants, which exert their influence prior to cooking, interact with cooking to influence tenderness. Relationships between biting instrument values and Warner-Bratzler shear values should be closer for cooked meat than biting instrument values on raw and cooked meat samples. Poor relationships were observed between raw meat tenderness and cooked meat tenderness if factors affecting tenderness of meat interacted some time prior to cooking.

Two raw product factors that affect tenderness are cold-shortening (massive sarcomere shortening induced by rapid chilling) and post-rigor aging at refrigeration temperatures. Cold-shortened and non-cold-shortened meat cooked to < 50° C did not differ in tenderness when raw or cooked (Purchas 1973). However, major tenderness changes took place at temperatures > 50° C, in which cold shortened meat was much tougher. The tenderness pattern was similar between Warner-Bratzler shear and biting

instrument values. When tenderness of aged and unaged *Longissimus* samples were compared after cooking to different endpoint temperatures, similar results were obtained. In this case, cooking for 1 hr at 50° C was sufficient to produce the same effects as aging on tenderness. Again, change in shear patterns for samples cooked 1 hr at 50° C were similar for Warner-Bratzler shear values and for biting instrument values. Thus, the effects of cold-shortening (toughening) and aging (tenderization) were very apparent on meat tenderness cooked at 70° C, but undetectable in raw meat. Pre-cooking treatment (cold-shortening or aging) and cooking treatment (raw or cooked at 70° C) interactions were highly significant. This study concluded that there was little point in classifying beef according to its raw meat tenderness if it had been subjected to varying degrees of cold shortening or aging.

Animal age, a determinant of meat tenderness, appears to interact strongly with cooking time and temperature. Bouton and Harris (1972c) showed that Warner-Bratzler shear values of the raw deep pectoral muscle of calves (0-2 mo) was greater than shear values on muscles from 5-7 year-old cows. After cooking samples from each age group to 75° C, the shear value of the cow muscle was more than twice that of the calf muscle. They suggested that this difference in tenderness was due to connective tissue changes due to heat solubilization.

Bouton and Harris (1972a) stated that devices other than the Warner-Bratzler shear device and the Kramer shear have been used to measure meat tenderness. The sensitivity of these mechanical devices to changes in tenderness could depend upon

whether such changes were the result of differences either in the properties of muscle fibers or connective tissue. Bouton and Harris (1972b) showed that degradative changes in the myofibrillar structure caused by aging resulted in large decreases in fiber tensile strength without significantly affecting adhesion between the fibers. The influence of post-slaughter treatments such as aging, contraction state and cooking method on shear and compression measurements were compared. Aging and temperature-time treatments have been used to produce meat samples that were either representative of large changes in fiber tensile strength or of large changes in adhesion between the fibers. Samples from aging experiments were used to determine if the Instron compression method (Bouton and others 1971), which uses a two-cycle compression, and the Warner-Bratzler shear device were measuring the same structural property of meat. Bouton and Harris (1972a) demonstrated that both the Instron Universal Testing Machine and Warner-Bratzler shear device gave high correlations with taste panel tenderness (Bouton and others 1971), which indicates that both were monitoring changes in mechanical properties that could be observed subjectively. Thus, the Instron compression method and Warner-Bratzler shear device each demonstrated highly significant changes in tenderness with aging. The magnitude of this response to the aging treatment was different because shear force values were reduced by nearly 50%, whereas compression values were reduced by 20%. Warner-Bratzler shear force and compression values of *Semimebranosus* (SM), *Semitendinosus* (ST), *Longissimus dorsi* (LD), and *Gluteus medius* (GM) muscles from older animals were greater for all muscles than for younger animals. Data indicated that compression measurements were more strongly influenced

by connective tissue since the SM and ST muscles, which have higher connective tissue amounts than the LD and GM muscles, produced higher values than the LD and GM.

Warner-Bratzler shear force values are influenced by fiber tensile strength. Fiber tensile strength values for the stretched LD muscle were found to be highly correlated (r = 0.86) with Warner-Bratzler shear force values (Bouton and Harris, 1972a). These results demonstrated a strong relationship between Instron compression and adhesion measurements (r = 0.90) and between Warner-Bratzler shear and fiber tensile strength measurements (r = 0.85). It was evident that Instron compression values were more strongly influenced by the strength of the connective tissue holding the meat fibers together than by the strength of the fibers themselves. The sensitivities of either method to treatment effects would depend upon which structural meat component was most affected by the treatment.

Importance of Sensory Testing

The perception of tenderness, a component of texture, is a complicated process since it involves cutting, grinding, squeezing, shearing, and tearing of a meat sample (Pearson 1963). It is very difficult to measure tenderness due to the complexity of the chewing motions and the impression of tenderness that is conveyed to the brain. Texture should always be measured under conditions that closely mimic actual consumption situations (Jack and others 1995). Texture cannot be measured directly, but is measured through behavioral responses such as scores for attribute descriptions (Jack and others 1995). Responses will also depend upon test conditions, temperature influence on food's

physical properties, perception of hardness and chewiness and portion size (Cardello and Segars 1989, Jack and others 1995). The best way to record these textural attributes is through sensory evaluation (Tornberg and others 1985). In sensory evaluation, researchers look to two types of sensory panels: trained analytical descriptive sensory panels and consumer panels.

Trained analytical descriptive sensory panels are useful in pinpointing differences between treatments, monitoring changes in processing, defining mouthfeels and aromatics, monitoring quality control, and defining overall sensory properties of the sample (Pearson 1963; Bett 1993). Descriptive sensory panels can offer a measurement close to an actual measurement of tenderness, but more quantifiable than the tenderness perception that a consumer would experience. This can be attributed to the fact that only the human oral factory sensory network in the mouth can incorporate the spectrum of variables that translate to perceived impact tenderness, flavor and palatability, and relate these sensations to a sensory acceptance score (Szczesniak 1963; Szczesniak and others 1963).

Trained sensory panels consist of no less than five members who have undergone extensive training for different attributes and are always refreshed prior to starting a new project. Texture profile analysis requires a panel of judges with prior knowledge of the texture classification system, use of standardized rating scales, and proper panel procedures with regard to the mechanics of testing and sample control. Development of a comprehensive sensory method for food texture evaluation is dependent upon a rational and well-defined system for texture classification. The body of literature on sensory

methods of texture evaluation contains a variety of definitions for texture, panel techniques, standardization of testing conditions, and correlation with instrumental measurements (Brandt and other 1963; Meilgaard and others 1987). A well-trained, calibrated sensory panel can evaluate sensory properties with accuracy and precision.

Texture analysis of meat occurs over five sequential stages, with properties in each stage varying among species (Bett 1993). Many flavor descriptors are the same from species to species, while others are species specific. Likewise, some texture characteristics are consistent from species to species with many of the same attributes being applied to all meat species. Processed meat products and intact muscles products share many of the same descriptive texture attributes.

The five stages of texture analysis are surface evaluation, partial compression, first bite, mastication and residual texture stage. Surface evaluation includes properties such as smoothness, particle amount, surface coating, surface fat and degree of fat present on the surface. The partial compression stage relates to the degree to which the sample returns to its original form, which can relate to springiness and elasticity. Hardness, cohesiveness, coarseness, uniformity, denseness and moisture retention are evaluated during the first bite stage, which consists of the first three to five bites. The number of chews required to prepare the sample for swallowing, cohesiveness, saliva absorption and/or production, fibrousness or connective tissue, denseness, bolus formation and breakdown are all involved in mastication. Finally, the residual texture stage evaluates the ease of swallowing, how much and what is remaining in the mouth

after swallowing, remaining particle description, amount of material packed into teeth, and the mouth's residual coating.

Sensory measurements offer their share of disadvantages. The primary disadvantage is that a sensory panel is a subjective method of assessing tenderness, therefore, it may be difficult to compare results between sensory testing facilities and these facilities' sensory panels. However, sensory testing calibration helps to alleviate the variation between panels and facilities. The scorecard, questions asked on card, order of presentation, and sample preparation must be carefully considered prior to the start of testing. Training for a sensory panel can be time consuming, thereby delaying specimen testing until training is accomplished (Tornberg and others 1985). Trained panels are also costly (Tornberg and others 1985). Panelists are most often compensated for their time devoted to being on a sensory panel. Sessions can last two hours and be expensive due to panelist salary.

Consumer panels are another type of subjective assessment. This type of panel offers insight into the overall acceptability of the product, its flavor, tenderness, and palatability. Consumer response to texture is of primary concern during product development (Jack and others 1995). The manner in which the consumer perceives texture is due to an array of sensory inputs arising before and during consumption. The relationship between the sensory input measured in individuals during consumption and perceived texture can provide a simple and rapid indices of texture, and can be used as a routine monitoring tool in product development applications (Jack and others 1995). It is often a less costly approach to sensory testing, more convenient, and allows for

collecting a large volume of data (Pearson 1963). But like the trained descriptive panel, consumer panels are criticized for being subjective, and not having the training sessions offered to the descriptive sensory panels. Consumers are sensitive to texture, which is an important constituent of a food's acceptance (Szczesniak 1977). Therefore, consumer sensory evaluation of a product can be just as important as that of a trained sensory panel, for it can help predict the success of the product in the marketplace.

Correlating Instruments to Sensory Evaluation

Because of the importance of texture to consumer acceptance, more attention has focused on correlating instrumental measures with sensory methods of texture evaluation (Szczesniak 1972). Texture is not due to one factor but to a spectrum of variables. The current texture measurement devices detect only a portion of the variables to varying degrees. Only the human mouth and senses can perceive, analyze, integrate, and interpret the entire spectrum of textural characteristics in a single evaluation. The concept of texture is significant only when viewed as an interaction between the human mouth and the material's mechanical properties (Szczesniak 1972). Instruments are limited in their ability to measure complex sensory properties, but can quantitatively measure physical properties that can be correlated directly or indirectly to organoleptically sensed textural attributes. Limitations of such measurements must be taken into consideration when interpreting the data (Bett 1993).

Textural sensory evaluation faces methodological, psychological and physiological problems, and is time-consuming and costly. Sensory evaluation is

considered subjective, whereas instrumental measurements are regarded as objective but with some limitations. Speed, reproducibility, potential for easy standardization and freedom from problems indigenous to sensory assessment have prompted the development of instrumental methods for texture evaluation to overcome such disadvantages (Tornberg and others 1985).

However, instrumental methods endure their own limitations. Objective methods can be costly. Purchase price of an instrument, maintenance and software updates can be high, particularly if frequency of instrument usage does not support these high costs. Due to time and financial support, the researcher is often faced with the need to be very efficient in obtaining textural data. Instrumental approaches often meet this need more fully than sensory approaches. However, many studies with meat products have failed to show a sufficient degree of accuracy that would allow complete substitution of an instrumental measure of tenderness for a sensory method. In addition to insufficient accuracy and cost, instrumental methods are destructive to the sample.

A variety of approaches to instrumental assessment of tenderness have been studied. Compression tests, tensile tests and shearing tests have presented promise and disappointment. One must understand what is structurally occurring within the tissue to ascertain what effect the method has and how to interpret the data. Lewis and Purslow (1990) reported that when a cooked meat sample was stretched perpendicular to the muscle fibers, breaking stress increased with sample thickness in the direction perpendicular to the muscle fibers. When deformations are applied parallel to the myofiber axis in a tensile test, resulting stresses can be transmitted by the sole internal

components of the myofibers without the participation either of their membranes or of the connective tissue. Therefore, tensile tests have been widely used to study the mechanical properties of muscle fibers. These properties can be determined either by following the stress or strain developed in isometric and isotonic tests or by analyzing the relations between stress and strain in tests in which these two factors vary simultaneously. The first studies on meat behavior in compression tests were made with devices having non-flat compression surfaces which made the strain pattern complex. These tests, usually called bite tests or tenderometer, have been used to study myofiber strength in cooked meat.

As in tensile and compression tests, orientation of strains imposed in relation to the myofibers influence shear force values (Murray and others 1983). The most commonly used configuration is that the shearing plane is perpendicular to the muscle fibers. For some time, research on mechanical properties of meat focused mainly on the development of devices for texture evaluation of cooked meat. As they generally gave a force value determined under various deformation conditions, no universal method for assessing texture was established. About 20 years ago, studies began to concentrate on a critical analysis of current methods advocating a more fundamental approach to determine which structures are stressed during mechanical testing and under what conditions. Much remains to be understood before cooked meat texture can be predicted for the intact muscle. Non-destructive methods will require determining both the influence of collagen and myofiber relationships to overall tenderness. Research efforts

should be devoted to providing the meat industry with a method capable of assessing tenderness from raw materials.

The most common objective tenderness measurement device is the Warner-Bratzler shear apparatus (Bratzler 1932; Bouton and Harris 1972a; Voisey and Larmond 1974), which measures the maximum shear force exerted during complete severance of a cored muscle sample. It is widely used but research indicates that correlations between Warner-Bratzler shear force (WBSF) readings and sensory tenderness range from highly significant to non-significant and are related, in varying degrees, to readings from other mechanical instruments that test meat texture or measure other biomechanical properties (Pearson 1963; Szczesniak 1963, 1966, 1968, 1969, 1972; Szczesniak and Torgeson 1965; Szczesniak and others 1963; Pool and Klose 1969; Rhodes and others 1972; Purchas 1973; Voisey and Larmond 1974; Voisey 1976; Moller 1981; Berry 1983; Tornberg and others 1985; Whipple an others 1990; Beilken and others 1991; Shackelford and others 1991a, b; Lepetit and Culioli 1992; Bett 1993; Shackelford and others 1995). Correlation coefficients between WBSF and sensory evaluation range from –0.0001 to –0.942 (Szczesniak and Torgeson 1965; Tornberg and other 1985). Variation in correlation could be influenced by muscle fiber, muscle connective tissue properties, aging of sample, animal age, cooking method, and myofibrillar contraction (Moller, 1981).

Another limitation of Warner-Bratzler shear force is that is does not accurately reflect tenderness differences among muscles (Harris and Shorthose 1988; Shackelford and others 1995). Shackelford and others (1995) evaluated the relationship between

Warner-Bratzler shear force and trained sensory panel tenderness ratings of 10 major muscles from *Bos indicus* and *Bos taurus* cattle. Warner-Bratzler shear force and trained sensory panel tenderness were determined for *Psoas major* (PM) , *Infraspinatus* (IS), *Triceps brachii* (TB), *Longissimus dorsi* (LD), *Semitendinosus* (ST) *Gluteus medius* (GM), *Supraspinatus* (SS), *Biceps femoris* (BF), *Semimemranosus* (SM), and *Quadriceps femoris* (QF) muscles from grain-fed steer carcasses. Shear force of the LD was not highly correlated with shear force of other muscles. Thus, Warner-Bratzler shear values that accurately predict LD tenderness will do little to accurately predict the tenderness of other muscles. Individual Warner-Bratzler shear force values differed little among beef muscles, but muscles differed greatly in overall tenderness ratings (PM = IS > TB = LD > ST = GM = SS > BF = SM = QF) (Shackelford and others 1995). A single equation to predict overall tenderness ratings of 160 beef muscle samples from shear force (peak load) alone explained only 50% of the variation. When peak load and other parameters of the shear force profile were used to develop a multiple regression equation, 66% of the total variation in overall sensory tenderness could be explained. Thus, explanation of the differences in overall sensory tenderness among muscles is limited with the use of Warner-Bratzler shear force. The relationship between peak load and overall tenderness within each muscle ranged from very weak for GM to strong for LD. This study suggested that the meat industry should review the validity of using *Longissimus* tenderness as an index of carcass tenderness because although the *Longissimus* constitutes a high proportion of carcass value, it does not always reflect the true tenderness of the entire carcass.

Even though a correlation exists between sensory panel tenderness and Warner-Bratzler shear, and the shear is used as the primary instrumental method of predicting tenderness, then why not use the Warner-Bratzler shear as a measure of overall tenderness? One problem with substituting Warner-Bratzler shear for sensory evaluation is not knowing whether the instrumental shear is actually measuring the same textural components as sensory panel tenderness. The mechanical approach is often quicker, easier and potentially less costly than sensory evaluation, but it may also incorporate compression and tensile factors as well as shear. When differences exist between samples, Warner-Bratzler shear cannot determine which textural property caused the difference.

Although the Warner-Bratzler shear force test remains the preferred instrumental method for assessing meat tenderness, it is a destructive test that must be performed on a cooked meat sample. In many cases, it is used in combination with sensory and consumer panels to establish tenderness acceptability thresholds for meat (Shackelford and others 1991a).

Alternative objective methods have been employed to predict tenderness and compared to the accuracy of Warner-Bratzler shear force values. In a study by Caine and others (2003), texture profile analysis (TPA) that incorporated compression and penetration of the sample was utilized to predict sample tenderness and compared with the Warner-Bratzler shear. Cyclical TPA parameters were obtained using a star-shaped probe and a two cycle penetration at 80% depth into the sample. Both TPA and Warner-Bratzler shear force were then compared as predictors of objective tenderness and

compared to sensory tenderness. TPA hardness, cohesiveness and chewiness and Warner Bratzler shear were negatively correlated to sensory overall tenderness (r = -0.68, -0.39, -0.64, and -0.60, respectively), and the amount of connective tissue (r = -0.57, -0.27, -0.55, and -0.49, respectively). Regression analysis showed that the TPA parameters of hardness and adhesiveness accounted for 51% and 38% of variation in overall tenderness and overall palatability whereas Warner Bratzler accounted for only 36% and 31% of the same parameters.

Perry and others (2001) studied the relationship between sensory tenderness, Warner-Bratzler shear force and compression values. Warner-Bratzler shear force showed low predictability for sensory tenderness (R^2 = 0.55 to 0.64) and regression equations for compression and sensory tenderness were even less promising (R^2 = 0.34 to 0.62). When additional values such as cook loss, aging treatment effect and application of electrical stimulation are incorporated into the equation with Warner-Bratzler shear force and compression values, a greater accountability of variation was possible (R^2 = 0.78).

Jeremiah and Phillips (2000) evaluated the ability of the Meat Industry Research Institute of New Zealand (MIRINZ) tenderness probe to accurately assess tenderness on raw beef samples. The instrument consists of two sets of pins, an outer row that are stationary and an inner row that rotates. The pins are impaled into the sample and tension is applied to the muscle fibers by one set of pins which rotate relative to the static set of pins. The torque required to rotate the inner (rotating) pins were measured and values for peak torque value (peak), maximum slope before peak (slope), torque at 50º of

rotation (D50), area under the trace before the peak (area 1), area under the trace before 50º or rotation (area 2), and area under the whole trace (area 3) were obtained. Correlation coefficients between probe values of peak, D50, slope, area 1, area 2 and area 3 and Warner-Bratzler shear on *Longissimus lumborum* steaks were low (r = 0.07. 0.19, 0.13, 0.13, 0.05, 0.11, respectively). Correlation to sensory tenderness was not better (r = -0.16, -0.31, -0.25, -0.28, -0.12, -0.21, respectively). When applied to a cooked sample, area 3 proved to have an acceptable coefficient of determination to overall sensory tenderness ($R^2 = 0.73$), which showed this method to be a potential replacement to the Warner-Bratzler shear for assessing cooked beef tenderness.

Correlation coefficients between sensory results and mechanical properties vary greatly, indicating that the sensory panel is not evaluating the same property as the instrument (Deatherage and Gernatz 1952; Brandt and others 1963). Significance of the correlation depends upon the experimental conditions present. Instrumental texture measurements should be performed under conditions simulating those occurring during sensory evaluation. Since most foods are viscoelastic in nature, the rate of deformation and applied force become critical parameters. Shama and Sherman (1973), as reported by Voisey (1976), indicated that both variables must be taken into account, since they vary during sensory evaluation depending on the food's textural characteristics. Inexpensive and accurate instrumentation would be beneficial if it could rapidly assess the tenderness of raw meat cuts without altering the sample.

The major problem impeding the development of a singular test that measures a multi-dimensional sensory characteristic such as tenderness is that a single mechanical

variable (or factor) must be identified and highly correlated to overall tenderness. Furthermore, the mechanism of mastication is complex and governed by parameters of stress and strain rate, which are unknown.

The relationship between mechanical and sensory measurements of texture has its foundation in two inherently different measuring capabilities: 1) the machine is more reproducible than the human sensor but "too simple" to completely describe such a multi-dimensional attribute as texture, and 2) the human being with its immense complexity, perplexity in calibration and tendency to drift, is difficult to fit into an equation (Kapsalis and Moskowitz 1977). By examining this relationship, one should consider: 1) the sample variability or reproducibility as expressed by the standard deviation; and 2) the sensitivity of the machine versus the human sensor, in terms of the smallest difference that can be perceived. The reproducibility of mechanical measurements is much greater than that of sensory measurements. Therefore, small differences between means can be statistically significant. Due to the great scatter or low reproducibility of sensory ratings, differences between means may not be as significant, as compared to differences generated by instrumental means. Improvement in the magnitude of the correlation coefficient can be obtained by: 1) muscle selection; 2) application of a cooking method(s) which will result in minimum temperature differences between the surface and the center of the muscle; 3) proper sampling procedure, corresponding to the particular muscles examined and their expedited variability; and 4) selection of the optimum method for sensory testing. The heterogeneity of the experimental material interferes not only with sampling, but also

with the magnitude of the correlation coefficient, for fundamental psychophysical reasons. Meat tenderness is provided by the myofibrillar portion, or main tenderness, and the connective tissue portion, or background tenderness. Instrumental tests provide an analog response to sample deformation on the basis of the same scale for both components. On the other hand, human subjects may have different sensitivities towards such tenderness. The importance of applying the appropriate mechanical test for the sample type examined cannot be overemphasized. Poor correlations may result if an inappropriate or incomplete test has been utilized, since this measurement type may have missed certain characteristics of the material to which the consumer may be highly sensitive. The most commonly used procedures for the mechanical testing of meat depends upon uniaxial compression, penetration and extension. Meat is an anisotropic material, consisting of meat fibers which run parallel to each other and different types of connective tissue which bind these fibers together crosswise. Important information may be lost if measurements reflect properties in only one dimension. The limits of correlation that can be obtained using mechanical and sensory measurements of textural properties should be considered. Mechanical measurements applied to a number of samples can be replicated within the inherent textural variability of the material. Sensory ratings refer to a material that undergoes continuous change during the chewing process. The biochemical effects of saliva and enzymes at body temperature and the altered structure of the food through successive biting are all constantly integrated by the brain to a final judgement. Therefore, there will always be a limit on the maximum correlation which can be obtained by instrumental and sensory texture measurements.

Most mechanical texture measurements are destructive, because the force applied exceeds the strength of the test food, which disintegrates in the process. This prohibits making several tests on the same sample. As a result, non-destructive methods have recently been considered. This poses specific problems in correlating non-destructive tests with sensory testing, which is destructive by nature.

Because foods are destroyed during sensory testing, there is interest in non-destructive dynamic testing and its correlation with sensory parameters. Non-destructive testing would offer several distinct advantages, including the capability of being able to follow changes during maturation, aging, and storage on the same specimen.

The oldest non-destructive method of predicting beef quality attributes is the USDA Quality Grade in which carcasses are assigned a quality grade and marbling score 24 – 48 hr postmortem by a trained USDA inspector. Marbling score and quality grade have been the easiest method by which the palatability of the cooked meat could be predicted from the raw state without sample adulteration. However, they do not always prove to be a reliable indicator of cooked tenderness. Some studies found that marbling and quality grade only account for a small percentage of the tenderness variation found by trained sensory panels (Palmer and others 1958; Fielder and others 1963) and that marbling score and quality grade are not reliable sources of predicting tenderness (Palmer and others 1958; Batcher and others 1962; Walter and others 1963; Smith and others 1987). However, McBee and Wiles (1967) showed that as marbling increased, so did overall tenderness as determined by sensory panel and shear force, although no significant differences were observed between the increased levels of marbling.

Luchak and others (1998) evaluated the effect of intramuscular and external fat on sensory, chemical and cooking characteristics in beef. Their study found that certain beef cuts (top loin, top sirloin and loin end) grading USDA Choice were significantly higher in palatability than those same cuts grading Select. However, palatability of those beef cuts that typically do not marble well (eye of round roast and steaks) and those cuts higher in fat (blade end rib) were not affected by quality grade. Therefore, marbling and quality grade can have an effect on certain muscle palatability traits while leaving others unaffected, even in samples from the same animal.

Results of studies like these leave scientists still searching for a more accurate, non-destructive method of assessing tenderness and left to develop such methodology. Technologic improvements in hardware and computer software have afforded researchers new instrumental assessments of tenderness.

In attempt to predict raw meat tenderness to cooked meat tenderness, Hinnergardt and Tuomy (1970) evaluated the force required by a modified Allo-Kramer Shear Press to penetrate raw sample. The shear-compression cell and shearing blades were replaced with a plate containing five needles (0.007 in diameter) and the needles compressed into raw and cooked pork loin samples to obtain a maximum force value. Correlations between raw and cooked penetration ranged from 0.56 to 0.75. When raw penetration was correlated with trained sensory panel scores, the range was 0.50 to 0.63. Correlation values varied from 0.63 to 0.87 between cooked penetration and sensory evaluation. Hinnergardt and Tuomy (1970) concluded that the penetrometer had potential for predicting cooked meat tenderness from the raw product without destroying the sample.

Recently, the Tendertec has been studied as an online tenderness grading instrument and its ability to assess beef palatability. Tendertec is an electromechanical penetrometer, armed with a 14 cm piston. The piston penetrates the carcass 8 cm. In George and others (1997), the capability of the Tendertec to predict sensory tenderness was studied and compared to Warner-Bratzler shear force. Area 2, Area 2B, Power 2 and Power 2B values for Tendertec were obtained and correlated to sensory scores. Correlation coefficients between Tendertec and overall tenderness were low with the Area 2 output variable being the highest ($r = -0.13$). Warner-Bratzler shear had a greater coefficient of determination for overall tenderness ($R^2 = 0.55$ to 0.64). It was concluded that at that time, Tendertec showed limited sensory tenderness prediction potential.

Ultrasound has proven to be a resourceful test method in various fields. Its application as a non-invasive tenderness prediction tool has shown to lack accuracy, but exhibits potential with continued research and refinement. Ultrasonic images are a record of sound wavers interacting with physiological properties. It is a relatively low cost method, easy to use and offers inherent safety features. It also possess the potential to estimate both yield and quality traits. Cross and Belk (1994) addressed the use of ultrasonic measurement in predicting beef tenderness and concluded that its advantages included the fact that it may be used in live animals, it may be used on slaughter floors before hide removal, it offers no health hazards, it would allow complete automation grading and remove human error, with development it may accurately predict traits related to palatability, and with further development, it offers great compatibility with intergraded artificial neural networking technology.

Park and others (1994) evaluated ultrasonic spectral feature analysis and compared these features with instrumental texture, chemical data and sensory evaluation. Seven ultrasonic features were evaluated for their predictability of juiciness, muscle fiber tenderness, connective tissue amount, overall tenderness, flavor intensity, percent total collagen and percent soluble collagen. These seven ultrasonic features were lower frequency, upper frequency, central (resonant) frequency, peak frequency, bandwidth, skewness and number of local maxima. The most significant correlations to ultrasonic data were between local maxima and juiciness ($r = 0.49$), connective tissue amount ($r = 0.52$), flavor intensity ($r = 0.39$), percent total collagen ($r = 0.34$) and Warner Bratzler shear force ($r = 0.51$). For sensory muscle fiber tenderness and overall tenderness, central frequency showed to have the highest correlation ($r = 0.45$ and $r = 0.44$, respectively). Through stepwise regression, multivariate models for predicting sensory attributes were developed. The highest prediction using these models was for connective tissue amount ($R^2 = 0.64$). Sensory overall tenderness ($R^2 = 0.43$), muscle fiber tenderness ($R^2 = 0.43$), juiciness ($R^2 = 0.49$) and flavor intensity ($R^2 = 0.49$) did not have as strong of a prediction potential as did connective tissue amount. It was concluded that ultrasonic spectral features may not prove to be an effective tool for predicting tenderness, but potential did exist for a non-destructive sensory measurement.

Ultrasonic elastography has emerged as a potential meat quality predictor. Elastography is a technique for making quantitative cross sectional images of tissue elasticity. Ultrasonic pulses track the internal displacement of small tissue elements in response to the externally applied stress. The displacements are converted into strain

values along the axis of compression and the pre and post compression signals compared. The resulting image is called an elastogram. Elastography combines ultrasonic technology with compression tests resulting in images or elastograms that carry structural and textural information.

A previous method of elastography called Haralick's approach, statistically computed 14 textural features based on gray-tone spatial dependence matrices at the nearest neighbors of each pixel in different angles and distances. When samples were grouped, Haralick's approach produced low R^2 values for meat quality prediction, but when samples were divided by maturity or muscle group, significant improvements in elastography ability to predict tenderness occurred ($R^2 = 0.69$) (Lozano 1995).

In a study by Huang and others (1997), ultrasonic elastography was used for quantitative imaging of strain and elastic modulus distribution in meat samples. Wavelet analysis proved to be advantageous to extraction of textural feature from images. Beef tenderness prediction wavelet features produced significantly higher R^2 values (0.70 to 0.90) in linear models than Haralick's features (0.10 to 0.80). It was concluded that wavelet analysis was a promising alternative for textural feature extraction from meat elastograms. Wavelet beef elastogram features were more informative, consistent, compact, and could be used to produce more acceptable tenderness prediction models.

A study by Swatland and Findlay (1997) assessed the ability of an on-line probe prediction of beef toughness and its relationship to sensory evaluation. The study consisted of muscles of major commercial beef cuts being probed to detect ultraviolet (UV) florescence of connective tissue and a dynamic analysis of electromechanical

signals for overall toughness. Results showed that tough regions of the muscle cuts had a high frequency of narrow fluorescence peaks subtending a small area under the fluorescence signal. Probe measurements were made both along and across the muscle axes and for measurements perpendicular (across) muscles, the area under the signal was correlated ($p<0.01$) with tenderness ($r = 0.57$), chewiness ($r = -0.61$) and residual tissue ($r = -0.58$). Those cuts that were most tender appeared to have lower fluorescence and wider peaks than tough cuts, with stronger relationships observed for measurements taken along the muscle axes and weaker for across axes. Strong prediction models for each measurement direction were derived using stepwise regression. The strongest prediction model of tenderness ($R^2 = 0.81$) was derived from using combined measurements, utilizing the area under the signal from perpendicular measurements, combined with the mean peak width from both perpendicular and longitudinal probing. The conclusion of the study determined that although there exists variation in post-mortem treatment and cooking, muscle toughness may contribute to the overall toughness of the beef cut and that the UV probe may predict sensory tenderness in a non-destructive manner.

Shackelford and others (1998) studied the ability of image analysis to correctly predict carcass cutability, longissimus area, subprimal cut weights and 12^{th} rib cross section tenderness. Carcasses were ribbed between the 12^{th} and 13^{th} rib. USDA quality and yield grades were recorded and lean color scored and the right side of the carcass. The left side was fabricated and the yield of the totally trimmed retail products were determined. A 2.54 dm thick steak was removed from the left side and image analysis

applied to the steak. Values for total lean area, total fat area, total steak area, percentage lean and color data were obtain from the steak. Results of the study showed that image analysis accounted for more variation in the retail product yield (89 vs. 77%) and product weight (95 vs. 90%) than did calculated yield grade. Image analysis also accurately predicted longissimus area ($R^2 = 0.88$). It was concluded that image analysis could potentially be used by industry to more accurately predict subprimal weights and used in combination with tenderness classification to accurately characterize carcasses for cutability and tenderness.

Li and others (1999) developed an image processing technique to predict cooked beef tenderness from fresh beef sample image characteristics. Image processing utilized color, marbling and image texture features to assess tenderness. Color characteristics for the longissimus muscle were obtained, with red, blue and green (R, B, and G) color functions obtained. These functions included the R, B, and G means, standard deviations and third moments which shows an imbalance of colors. Marbling features evaluated included marbling flecks total count, marbling area divided by ribeye area and marbling fleck count divided by ribeye area. Image texture features include properties such as fineness, coarseness, smoothness, granulation, randomness and graininess of an image. Color, marbling and image texture features were obtained for images from a sample population that varied in USDA quality grade and sensory panel tenderness. Image values were related to sensory tenderness scores, resulting in prediction equations for beef tenderness with R^2 values up to 0.70 by using color, marbling and texture image features. Prediction models using only color and marbling produced less desirable R^2

values of 0.30, indicating that textural features are necessary for a stronger prediction model.

Li and others (2001) continued to evaluate the effectiveness of image texture analysis and its ability to classify tender beef cuts. Texture features of fresh beef cut images were obtained and used to classify steaks into either tender or tough groups in terms of cooked beef tenderness. Two short loin steaks were obtained from each carcass in the study, with one assigned to textural imaging and the other to sensory evaluation. Samples were classified into tender or tough categories based on sensory scores. A wavelet based decomposition method was used to obtain texture features of the fresh sample and these features evaluated as to whether the results accurately predicted the tough/tender classification of the sample. The wavelet-based method decomposes an image into textural primitives of different sizes. The degrees of presence of an image's textural primitive were measured by the fractional image area occupied by the textural primitive in number of pixels and were referred to as primitive fraction, in which the primitive fractions can be used to distinguish tough from tender samples. A correct classification rate of 83.3% was obtained in cross validations using classification based on primitive fractions. Li and others (2001) concluded that although texture features alone are not sufficient to segregate beef productions into levels of tenderness, they can be indicators that can lead to adequate tenderness prediction.

Near infrared reflectance (NIR) has emerged as an innovative method to predicting tenderness. Park and others (1998) evaluated the effectiveness of NIR spectra to predict cooked *Longissimus* Warner-Bratzler shear force values. The study employed

partial least squares (PLS) analysis and multiple linear regression (MLR) analysis to predict Warner Bratzler shear (WBSF) values. PLS analysis for tenderness prediction yielded models with R^2 values of 0.63 and 0.67. Validation of PLS using a data set of 39 samples resulted in 48.7, 87.7 and 97.4% of the samples being predicted within 1.0, 2.0, and 3.0 kg of the WBSF value, respectively. MLR analysis yielded a predictive model with a R^2 value of 0.67, and 89% of the samples were correctly classified for WBSF. Park and others (1998) concluded that potential existed for this technology to be implemented into the beef industry, but were unclear as to how accurately NIR could predict tenderness on aged sample.

Byrne and others (1998) evaluated near infrared reflectance spectroscopy between 750 and 1098 nm range. Results from this study show that NIR in this range correlated well with Warner-Bratzler shear (r = 0.73 to 0.82) and slightly lower with sensory tenderness (r = 0.53), texture (r = 0.54), flavor (r = 0.24) and acceptability (r = 0.42). This study suggests that NIR as a non-destructive technique to predicting tenderness potentially exists.

More recently, Rodbotten and others (2000) studied near infrared reflectance spectra as a potential tenderness prediction method. They found that NIR spectra recorded at different post-mortem times yielded tenderness predictive models, but these models had low correlation coefficients with Warner-Bratzler shear (r = 0.47 to 0.55) and sensory tenderness scores (r = 0.34 to 0.51). However, NIR spectra did correlate highly with intramuscular fat content (r = 0.78 to 0.85). It was concluded from this study

that although NIR spectra is a non-destructive objective method, it was not a precise or effective predictor of final tenderness.

Lui and others (2003) evaluated the ability of both visible and near infrared reflectance spectroscopy to predict beef color, texture and sensory characteristics at various days post-mortem. Partial least squares regression was used in predicting color, Warner-Bratzler shear and sensory characteristics of beef carcasses at 2, 4, 8, 14 and 21 d post-mortem from visible/near infrared (visible/NIR) reflectance spectroscopy in the 400-1080 nm range, and soft independent modeling of class analogy (SIMCA) of principal component analysis (PCA) used to classify samples into tender or tough categories. For visible/NIR, R^2 values ranged from 0.78 to 0.90 for Hunter a, b and E*, and from 0.49 to 0.55 for tenderness hunter L, chewiness and juiciness. Coefficient of determination (R^2) range was broader for tenderness (0.22 to 0.72) than other measured attributes. Prediction of Warner-Bratzler shear force by visible/NIR for all aging days was low (R^2 = 0.20 to 0.49), but when separated by aging day, the highest coefficient range was for 4 d post-mortem (R^2 = 0.64 to 0.69). Visible/NIR correctly classified samples as either tough or tender 83% of the time, but SIMCA/PCA did so 96% of the time.

Texture analysis is a technique that relies on image acquisition and computer translation of the image analysis. The acquired image is transformed into a two-dimensional matrix of numbers. Each matrix entry is a picture element, or pixel, with a value called “grey level”. The grey level values are used to characterize an object or image surface. Texture analysis requires the calculation of various textural features.

These features contain information that represents visual textural characteristics, such as coarseness of texture, regularity, presence of direction, and size of representative neighborhood. The quantification of meat quality is of importance to the meat industry and this technology has the potential to assess those muscle tissue characteristics that influence meat tenderness such as connective tissue quantity and distribution and perform as a non destructive method of marbling determination. To evaluate the application of texture image analysis for the classification of beef, Basset and others (2000) utilized meat slices from three different muscles (*Longissimus dorsi, Semitendinosus, triceps brachii*) of animals of different ages (15 mo, 19 mo, 24 mo, > 3yr) and breeds (Limousin, Salers, Aubrac, Charolais). They also evaluated the efficacy of image analysis for quantifying those muscle attributes, lipid content and collagen content, which affect tenderness. Image analysis was conducted with aim for classification according to age of animal, muscle or breed. Only 25.4% of the samples were correctly classified, but 60% of the muscles were correctly classified by utilizing minimal textural feature evaluation. Lipid and collagen content and textural analysis imagery correlation coefficients were not strong ($r = -0.26$ and 0.49, respectively). Although non-destructive of the sample, poor correlation limits textural imaging predication potential.

Based on previous studies relating muscle tissue color to overall tenderness, Wulf and others (1997) studied whether an objective measurement of muscle color could accurately predict tenderness of beef carcasses. Following slaughter, electrical stimulation and 24 hr chill, all carcasses in this study were USDA graded and L*, a*, b*

colorimeter readings were obtained of the exposed longissimus muscles. Warner-Bratzler shear force at 1, 4, 7 14, 21 and 35 d postmortem, sensory evaluation at 14 d postmortem and pH values were obtained and correlated with L*, a* and b* readings. Correlations of L*, a*, b* color measurements with tenderness (r = 0.34, r = 0.21 and r = 0.37, respectively) were higher than correlations of marbling scores with tenderness (r = 0.11). Of the three color measurements, b* showed the greatest potential as a prediction tool by correlating highest with Warner-Bratzler shear force (r = -0.38) and sensory tenderness (r = 0.37). Multiple regression equations were constructed to determine if a multiple variable equation proved to have higher sensory tenderness predictability than a single measurement. An equation incorporating all color measurements lacked acceptable prediction potential ($R^2 = 0.18$). The greatest predictability came from two equations with the first using calpastatin values, L*, a*, b* and marbling scores ($R^2 = 0.28$) and the second using calpastatin values, L*, a*, b*, pH and marbling scores ($R^2 = 0.28$). Although this study failed to produce an accurate tenderness prediction equation, it did show that a relationship between muscle color and tenderness does exist and with continued study may produce a non-destructive objective method for tenderness prediction.

To further evaluate the ability of muscle color to predict tenderness, Wyle and others (2003) studied the effectiveness of the SmartMV prototype BeefCam Video Imaging System on classifying beef carcasses into palatability groups. The study utilized beef carcasses from three USDA quality grades (Top Choice, Low Choice, Select). After chilling, an image of the longissimus muscle was obtained using the BeefCam. Warner-

Bratzler shear force values and consumer panel scores were obtained for the steaks from the same carcasses that underwent imaging. Two regression models were constructed to predict the first principal component of WBSF and consumer scores based on expected palatability, with the first model or Model I using the BeefCam output and the second model or Model II using the BeefCam output and a quality grade coded value. Upon development of prediction models, a second phase of the study was conducted to test the validity of the BeefCam. BeefCam Model I certified 47.3% of the carcasses, (grades Top Choice, Low Choice, Select) in the population, and of those carcasses certified by the Beef Cam Model I, only 1.4% of steaks from these carcasses were tough. BeefCam Model II certified 42.1% of the carcasses and of those carcasses, only 1.6% of steaks were tough.

Preliminary studies of the use of Raman spectroscopy to predict tenderness of beef have been performed by Beattie and others (2004). Raman spectroscopy offers many advantages over current texture measuring methods. It is insensitive to water, which can be valuable since many foods contain more than 75% water. It also does not require any sample preparation. Finally, it is non-destructive. In this study, Raman spectra, Warner-Bratzler shear force and trained sensory scores were correlated to Raman data. Good correlations were observed between Raman data and sensory acceptability of texture ($R^2 = 0.71$), degree of tenderness ($R^2 = 0.65$), juiciness ($R^2 = 0.62$), and overall acceptability ($R^2 = 0.67$). Warner-Bratzler shear did not correlate as highly with tenderness ($R^2 = 0.15$). Beattie and others (2004) concluded that Raman

spectroscopy demonstrated to be a potential method for non-destructive and rapid determination of beef tenderness.

Spadaro (1996) and Spadaro and others (2002) developed a biomechanical technique that characterized the rheological behavior of post rigor bovine *Longissimus dorsi* muscles and evaluated the biomechanical parameters of stiffness and total energy dissipated in the parallel and perpendicular fiber orientation that could be used to predict overall tenderness as evaluated by a trained descriptive sensory panel.

Stiffness and total energy dissipated values were calculated according to Spadaro's (1996) stress relaxation technique at a 3% compression for 4 min on a 2.54 cm^3 *Longissimus dorsi* sample with fibers parallel or perpendicular to the applied strain. The mechanical variables of initial and final stiffness (1.1, designated as 4.45 in Spadaro (1996)) and total energy dissipated (1.2, designated as 4.47 in Spadaro (1996)) were calculated using the following equations:

$$K = \frac{\bar{\sigma}_{22}}{\bar{\varepsilon}_{22}} \qquad (1.1)$$

and

$$E_D = \frac{\bar{\sigma}_{ij}\bar{\sigma}_{kl}}{2a^3}\left[D^r_{ijkl}\frac{0.25^2}{2} + \frac{D^r_{ijkl}}{d^r_{ijkl}}\left(1 - e^{-0.25 d^r_{ijkl}}\right) - 0.25\frac{D^r_{ijkl}}{d^r_{ijkl}}\right] \qquad (1.2)$$

where K = stiffness (Pa).

$\bar{\sigma}_{22}$ = homogenized stress value acting in direction of applied of force (Pa).

$\bar{\varepsilon}_{22}$ = homogenized strain value acting in direction of applied of force (m/m).

E_D = dissipated energy per unit volume (J/m^3)

$\bar{\sigma}_{ij}$ = homogenized stress tensor (Pa)

$\bar{\sigma}_{kl}$ = homogenized stress tensor (Pa)

a = length of one side of meat sample (m)

D^r_{ijkl} = creep compliance moduli (1/Pa)

d^r_{ijkl} = creep rate time constants (1/s)

to evaluate biomechanical parameter relationship with overall sensory tenderness and WBSF. Overall sensory tenderness was highly correlated to final stiffness and energy dissipated in the parallel fiber orientation (r = 0.86 and r = -0.91). This compressive model of using energy dissipated in the parallel fiber orientation exceeded the WBSF correlation to overall sensory tenderness by 53%. Spadaro and others (2002) constructed a model that would predict overall tenderness of beef loin steaks using energy dissipated in parallel fiber orientation or final stiffness in parallel fiber orientation, which correlated highly to overall sensory tenderness evaluation (r = -0.95 and r = 0.95, respectively). Warner-Bratzler shear force values on the same set of samples were correlated to overall panel tenderness, but yielded a much lower correlation (r = 0.55) value. The obvious advantage to this new objective technique was that overall tenderness could be predicted

on raw samples, thus eliminating the need for cooking, and subsequent sensory panel testing.

Marburger (1999) tested the compressive technique and mathematical models developed by Spadaro and others (2002) to predict muscle tenderness of raw *Longissimus dorsi* samples that varied in tenderness and degree of aging. The energy dissipated-parallel (EDPL) and initial stiffness-perpendicular (ISTFPP) to the muscle fibers ($r = -0.86$ and $r = 0.85$, respectively) were effective predictors of sensory tenderness in raw samples, whereas the Warner-Bratzler shear force (WBSF) of cooked samples was less effective (than biomechanical parameters) for predicting tenderness ($r = -0.79$). Energy dissipated from samples (2.54 cm^3) with the strain applied parallel to the fiber orientation accounted for 73.3% of the variation in tenderness and was a more accurate assessment of tenderness than WBSF (61.9%). Regardless of degree of aging, each biomechanical property measurement accounted for more variation in the sample than did WBSF, and did so more effectively.

This study confirmed that the application of an objective, biomechanical strain to raw muscle specimens could effectively predict overall sensory tenderness of cooked steaks more effectively than WBSF. Because the biomechanical technique accounts for more variation in tenderness than WBSF and provides a more accurate, rapid, less costly, and predictable method of measuring beef loin tenderness, further development of this methodology could potentially provide an online tenderness assessment test for segregating beef cuts. It was concluded that optimization of the measurement technique (regardless of muscle fiber orientation) is needed to reduce the sample compression time

to a few seconds, determine an acceptable temperature range for measuring tenderness and to establish the best platen (flat plate that compresses the sample) or probe configuration to compress the sample.

MATERIAL AND METHODS

Phase 1

Twenty pairs of beef *Longissimus dorsi* muscles (IMPS 180-boneless strip loin, quarter inch backfat, one rib mark) from USDA graded carcasses (Choice, Select) were selected on the basis of estimated tenderness. Beef strip loins were collected from steers (< 24 mo of age) slaughtered at Kanes Processing in Corpus Christi, TX. Carcasses were chilled and assigned USDA yield and quality grades and marbling scores. Strip loins were extracted from the carcass 48 h postmortem and vacuum packaged. Steaks, 2.54 cm thick, were cut serially from each loin, except for six steaks, 3.81 cm thick, for compressive testing with a TA.XT2 Texture Analyzer. Each 3.81 cm thick steak specimen was evaluated at one of six temperatures (0, 2, 4, 6, 8 and 10°C). This temperature range was selected due to its representation of the variation of temperature of meat in a packing plant environment. Assignment of steaks for testing were: LOIN 1 = Steak 1 (2.54 cm thick) – Warner-Bratzler Shear Force; Steaks 2, 3, 4, 5, 6, 7 (all 3.81 cm thick, randomly assigned to compression temperatures) - Compressive Tenderness Test with Texture Analyzer. LOIN 2 = Steak 1 (2.54 cm thick) - collagen analysis, color, pH, proximate analysis; Steaks 2, 3, 4, 5, 6, 7 – not used in the study, but utilized in another research study; and Steaks 9, 10 (each 2.54 cm thick) – sensory evaluation.

Phase 2

Forty beef *Longissimus dorsi* muscles (IMPS 180-boneless strip loin, quarter inch backfat, one rib mark) from USDA graded carcasses (Choice, Select) were selected on

the basis of estimated tenderness. Beef strip loins were collected from steers slaughtered at Kanes Processing. Carcasses were chilled and assigned USDA yield and quality grades and marbling scores. Strip loins were extracted from the carcass 48 h postmortem and vacuum packaged. Steaks, 2.54 cm thick, were cut serially from the anterior end of the loin, except for one 5.08 cm steak, which was removed for compressive test using the TA.XT2 Texture Analyzer (TA). Assignment of steaks for testing were: 1 – chemical analysis; 2 – WBSF; 3 – sensory evaluation; 4 – probe compression TA test; 5 (5.08 cm thick) – platen compression TA test. Each 5.08 cm thick steak specimen assigned to platen compression and each 2.54 cm thick steak specimen assigned to probe compression was evaluated at one of three temperatures (-6.6, -4.4 and 10°C). These temperatures were selected so that compressive measurements could be performed on the variation of temperature of meat in a packing plant environment (4.4 and 10°C), in which the water in the sample is at a fluid state. These measurements could then be compared to muscle with water in a solid state (-6.6°C), which served as a control for biomechanical measurements.

Analytical Techniques

Proximate Analysis

Percentages of moisture, fat, and protein were determined according to AOAC (1995) procedures. Moisture and fat content was analyzed using the CEM Smart Trac System (CEM Corp., Matthews, NC). Analysis of the samples from Phase 1 and Phase 2 were performed in duplicate. Crude protein percentage was determined by the Dumas

method using a LECO FP-528 Nitrogen/Protein Analyzer (AOAC #992.15 LECO N_2 Analysis, LECO Corp., St. Joseph, MI). The instrument was standardized using an ethylenediamine tetraacetic acid (EDTA) (Leco Lot # 1030, %N = 9.56 $\pm$ 0.03) standard supplied by LECO Corporation (St. Joseph, MI). The sample was placed in a sample capsule, inserted into the combustion furnace and ignited in the presence of O_2. Combustion gases were swept out to filters, cooled and allowed to fill a ballast for equilibration. Afterward, an aliquot was mixed with He as a carrier gas, and transferred to a heater. The heater reduced NO_x to N_2 and removed H_2O and CO_2. The remaining N_2/He mixture flowed through a thermal conductivity detector cell and the concentration of N_2 converted to an output voltage. The sample gases output voltage with He were compared to He alone and converted into protein values using multiplication factor of 6.25 (%N x 6.25 = % Protein).

pH Determination

The pH of the *Longissimus dorsi* muscle samples was determined using a direct glass probe (spear) electrode attached to a pH meter (HI 9025 microcomputer pH meter, Hanna Instruments, Limena, Italy). The pH probe was calibrated with pH 4 and 7 standard buffer solutions before inserting the glass tip into the sample (~ 1.0 cm). Care was taken to ensure that the glass tip would be completely inserted into the muscle. The probe was allowed to equilibrate for 30 to 60 sec and individual pH readings at two muscle locations were reported. pH determination was performed on samples in both Phase 1 and 2.

Color Space Values (L*, a*, b*)

Color space values (L*, a*, b*) of the *Longissimus dorsi* muscle were obtained approximately 1 hr after fabrication by reflectance using a Minolta Colorimeter (CR-200, Minolta Co., Ramsey, NJ). Positive L* values indicated the degree of lightness while negative L* values indicated darkness. Positive a* values quantified the degree of redness whereas negative a* indicated greenness. Positive b* values indicated yellowness whereas negative b* values indicated blueness. The porthole of a Minolta Colorimeter was covered with clear Saran Wrap® and random readings were taken at six locations on each steak surface. The colorimeter was calibrated to a standard white tile surface (L* = 96.66, a* = -0.03, b* = 1.61) at channel 00. Color measurements were performed on samples in both Phase 1 and 2.

Calpastatin Activity

Calpastatin stabilization was determined using the procedures outlined by Wheeler and Koohmaraie (1991) and heated column calpastatin activity was determined using the procedures outlined by Koohmaraie and others (1995). Calpastatin activity per gram tissue was determined only for samples evaluated in Phase 2. Approximately 10 grams of *Longissimus dorsi* muscle tissue, taken from the center of the muscle, was placed into 30 ml of chilled (5°C) extraction buffer. The extraction buffer consisted of 100 mM Tris, 5 mM EDTA, and 10 mM beta-mercaptoethanol. Samples were homogenized in a chilled Waring Blender (model 31BL92, Waring Products Division, New Hartford, CT) three times for 30 seconds each with a 30 second lag time between

homogenizations (blender cups were not be allowed to warm). Samples were kept cool and centrifuged at 15,000 rpm for 60 minutes. Supernate was transferred equally into five 13 x 100 borosilicate tubes and placed into a 95°C water bath for 15 minutes. The tubes then were placed on ice to chill for approximately 15 minutes. The coagulated protein in each tube was scrambled with glass rods to separate pellet and supernate. The samples were transferred to centrifuge tubes and centrifuged as before for 30 minutes. The supernate was filtered through a glass wool plug into a sterile 50-ml conical tube. The volume of supernate was measured and recorded for calculation of calpastatin activity. Samples were assayed by adding the sample, elution buffer, purified calpain, and calcium to a tube. Heating, spinning, and then reading the sample at 278 nm on a spectrophotometer (Wheeler and Koohmaraie, 1991) followed. Data were reported in terms of calpastatin activity per gram of fresh tissue.

Collagen (Connective Tissue)

Collagen characteristics were determined by isolating hydroxyproline from homogenized steaks according to the method of Hill (1966). Hydroxyproline concentration was determined using the color reaction outlined by Kolar (1990). Percent soluble and total collagen was derived according to the method of Cross and others (1973). Sample analysis was performed in duplicate on samples from both experimental phases. Eight grams of each sample were placed in two centrifuge tubes (4 g/tube) and 12 ml of 25% strength Ringer solution (full strength Ringer solution = 7.0 g NaCl, 0.026 $CaCl_2$, 0.35 g KCl per 1 L distilled water) was added to each tube. Each tube was

assigned a glass rod and stirred 20 revolutions. The tubes were placed in a 78°C water bath and stirred 15 revolutions every 5 min for 60 min. The tubes were cooled for 15 min, placed in a Beckman J-21B centrifuge fitted with a JA-17 head and centrifuged at 15,000 rpm for 10 min. The tubes were removed and the liquid portion decanted into individual supernatant jars, being careful to leave all the meat pellet in the tube. Eight milliliters of 25% strength Ringer solution were added to each meat pellet, the solution mixed with a glass rod for 15 revolutions, and the tubes centrifuged for 10 min as above. The supernate was decanted into respective sample jars, 5 ml of distilled H_2O added to each tube, the mixture stirred with a glass rod 15 times, and the liquid poured into jars labeled residue. Each tube was rinsed with 5 ml of distilled H_2O and poured into individual sample jars. Thirty milliliters of 7 N sulfuric acid were added to each supernatant jar and 20 ml added to each residue jar. The jars were tightly capped and heated to 105°C in an oven for 16 hr. Afterward, the jars were removed from the oven, the lids removed and the jars allowed to cool under a vented hood. The hydrolyzed supernate and residue were transferred into 200 ml and 500 ml volumetric flasks, respectively, and diluted to volume with distilled water. The liquid fractions were filtered through one Whatman #1 (cat no. 1001 150) filter paper, collected into 50 ml centrifuge tubes and capped. A two ml aliquot of the final filtrate was pipetted into glass test tubes (VWR), in duplicate. A blank was prepared using 2 ml of distilled water and a standard curve constructed by preparing 0, 2, 4, 6, 8, and 10 g/ml hydroxyproline standard solutions. Two milliliters of each standard were pipetted into duplicate glass test tubes. Each tube received 1 ml of oxidant solution, was vortexed for 5 sec and the

tubes allowed to set for 20 min at room temperature. Tubes received 1 ml color reagent, were vortexed for 5 sec, covered with aluminum foil, and placed in a water bath for 15 min at 60°C to develop color. Tubes were removed, cooled to room temperature, and sample fractions read at 558 nm using a Beckman DU-7 spectrophotometer (Beckman Instruments, Inc., Fullerton, CA). Percent soluble collagen and total collagen values were computed using the following formulas:

$$\text{Supernate mg} = \frac{(\text{Abs.} + \text{y-intercept})}{\text{slope}} \qquad \text{Residue mg} = \frac{(\text{Abs.} + \text{y-intercept})}{\text{slope}}$$

$$\text{Supernate} = \frac{(\text{Supernatant mg} \times \text{ml diluted})}{\text{sample wt.}} \qquad \text{Residue} = \frac{(\text{Residue mg} \times \text{ml diluted})}{\text{sample wt.}}$$

Super. Collagen = Supernatant x 7.52 Residue Collagen = Residue x 7.25

Super. mg/g = Super. Coll./1000 Residue mg/g = Residue Coll./1000

TOTAL COLLAGEN = SUPERNATE mg/g + RESIDUE mg/g

% SOLUBLE COLLAGEN = ((SUPERNATE mg/g)/TOTAL)*100

Warner-Bratzler Shear

Raw steak weights were recorded, type-T copper/constantan thermocouples inserted into the geometric center of each steak, and internal temperatures monitored using an Omega HH21 microprocessor thermometer (Omega Engineering Inc., Samford, CT). Steaks were placed on a Faberware Open Hearth grills (model 450N, Kidde, Inc., Bronx, NY) and the initial temperature and time recorded. Steaks were turned at 35°C and cooked to an internal end point of 70°C. Time elapsed at the completion of cooking

and final cooked weights were recorded. Steaks were wrapped in Saran Wrap® and placed in a cooler maintained at 4°C for 4 hr. Steak sample cores (2.54 cm) were extracted from six locations within the *Longissimus dorsi* muscle, avoiding fat pockets and connective tissue. Cores were then sheared using the Warner-Bratzler shearing device attachment on the Instron Universal Testing Machine (Model 1011, Instron Corporation, Houston, TX) and the maximum force recorded in kg for Phase 1 and 2 samples.

Compression Tenderness Test with a Platen and Texture Analyzer (TA)

Phase 1 – Assessment of platen specimen temperature on compressive strain measurements.

A compressive test as described by Spadaro (1996) was performed on cubed portions of the *Longissimus dorsi* samples. Compressive measurements were performed perpendicular and parallel to the muscle fiber orientation at 0, 2, 4, 6, 8 and 10°C using a TA.XT2 Texture Analyzer (Texture Technologies Corp., Scarsdale, NY/Stable Micro Systems, Godalming, Surrey, UK). Prior to sample preparation, water baths were set up and temperature dials set to one of the assigned testing temperatures (0, 2, 4, 6, 8 or 10°C). Ice, salt and a self constructed circulating water bath system was utilized to maintain the water baths at the appropriate temperature (Figure 1).

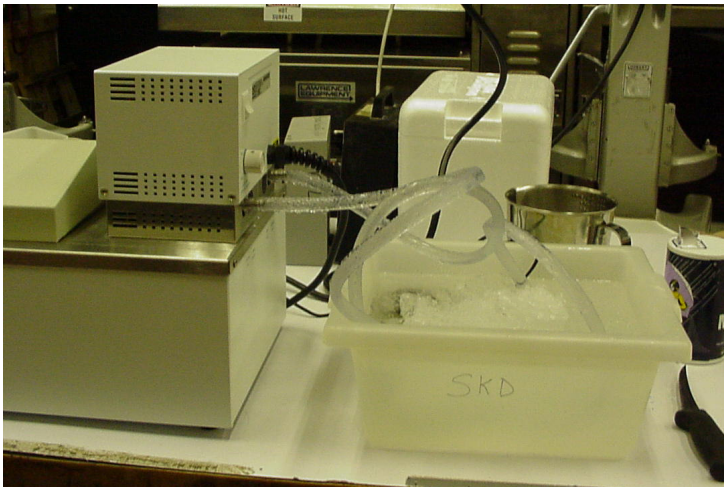

(a)

(b)

Figure 1. (a) Ice, salt and water are contained in a plastic tub with tubing to a circulating water bath system, and (b) cubed samples of *Longissimus dorsi* muscle submerged in a water impermeable resealable plastic pouch (Ziploc®), submerged in a circulating water bath.

For sample preparation, specimens from the top portion of each steak (3.81 cm) were removed to observe fiber orientation, and the *Longissimus dorsi* was cut to obtain two

2.54 cm^3 cubes with fibers in a parallel (PL) and perpendicular (PP) orientation, respectively, for compression testing (Figure 2).

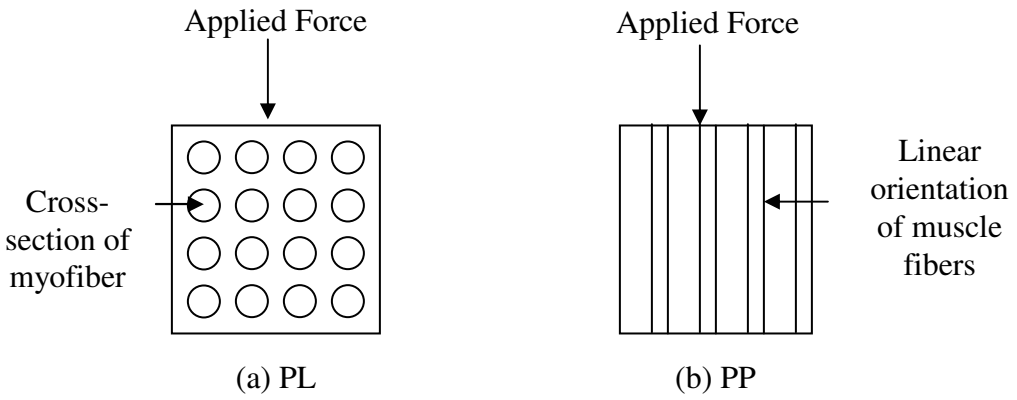

Figure 2. Force applied (a) parallel (PL) or (b) perpendicular (PP) to the myofiber orientation.

Cubed samples for each fiber orientation of *Longissimus dorsi* muscle were placed in a water impermeable bags (Ziploc®), submerged in a water bath set to one of six test temperatures (0, 2, 4, 6, 8 or 10°C) and the samples allowed to equilibrate to that temperature for 2 h. Samples were then placed on the TA platform and compressed for 240 sec at a 3% compression of sample height. Acquisition rate was set at 50 pps and an auto trigger set at a force of 0.05 N. Calibration of the compression platen (10 cm diameter x 7 mm tall aluminum cylinder, 30 mm tall adapter) and net force were set with a 5 kg weight (Figure 3).

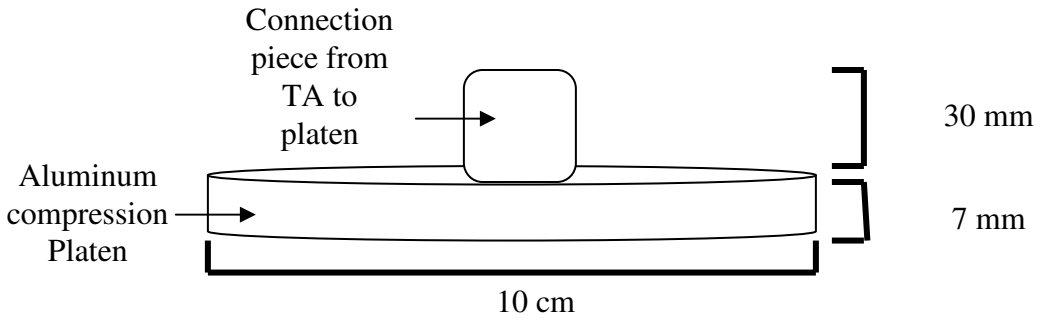

Figure 3. Aluminum platen utilized in platen compressive measurements.

Data were processed and saved as a comma delimited file for further analysis using the Matlab v4.2c1 (The MathWorks, Inc., Natick, MA) software package. Data were fitted to a non-linear curve over equation (1.3, designated at 4.14 in Spadaro (1996)):

$$E(t) = \sum_{i=1}^{n} E_i e^{-(E_i t/\eta_i)} + E_\infty \qquad (1.3)$$

$E(t)$ = stress relaxation modulus (Pa)

E_i = elastic moduli for individual spring elements (Pa)

η_i = viscous damping parameters for individual dashpot elements (Pa-s)

n = total number of spring/dashpot groupings (--)

t = time (s)

E_∞ = long-time equilibrium modulus (Pa)

with a three-term prony series plus an infinite equilibrium term function (1.4, designated as 6.2 in Spadaro (1996)), which being:

$$E(t) = c_1 e^{-c_2 t} + c_3 e^{-c_4 t} + c_5 e^{-c_6 t} + c_7 \qquad (1.4)$$

where $E(t)$ = stress relaxation modulus (Pa)

c_1, c_3, c_5 = relaxation moduli (1/Pa)

c_2, c_4, c_6 = relaxation rate time constants (1/s)

c_7 = long-time equilibrium modulus (Pa)

After relaxation model functions were obtained, calculation of creep compliance functions was performed by application of relationship of equation (1.5, designated as 4.18 in Spadaro (1996)):

$$1 = \tilde{E}\tilde{D} \qquad (1.5)$$

E = stress relaxation modulus (Pa)

D = creep compliance (1/Pa)

which resulted in equation 1.6 (designated as 6.3 in Spadaro (1996):

$$D(t) = D_0 + D_1\left(1 - e^{-d_1 t}\right) + D_2\left(1 - e^{-d_2 t}\right) + D_3\left(1 - e^{-d_3 t}\right) \qquad (1.6)$$

where $D(t)$ = creep compliance (1/Pa)

D_0 = initial creep compliance (1/Pa)

D_1, D_2, D_3 = creep compliance moduli (1/Pa)

d_1, d_2, d_3 = creep rate time constants (1/s)

Energy dissipated from parallel (EDPL) and perpendicular (EDPP) fiber orientation, initial stiffness of parallel (ISTFPL) and perpendicular (ISTFPP) fiber orientation, and final stiffness of parallel (FSTFPL) and perpendicular (FSTFPP) fiber orientation were calculated according to equations (1.1) and (1.2) to evaluate the performance of biomechanical variables with respect to overall sensory tenderness evaluation and WBSF.

Compression Tenderness Test with a Probe and Texture Analyzer (TA)

Phase 2 – Assessment of biomechanical properties of intact raw muscle sample with a probe.

USDA Choice and Select grade samples were randomly distributed among measurement temperatures of -6.6º (n=14), 4.4º (n=13) and 10ºC (n=13). Due to limited sample numbers, not all loins were treated to every testing temperature. Samples were separated based on USDA grade and then samples from each grade were randomly assigned to one of three measurement temperatures. This helped ensure that equal

number of samples from each USDA grade were equally represented in each measurement temperature.

The compressive test as described by Spadaro (1996) was performed on 2.54 cm cubed portions of raw *Longissimus dorsi* samples at either -6.6º, 4.4º or 10ºC. Compressive measurements were performed perpendicular and parallel to the muscle fiber orientation at one of three temperatures using a TA.XT2 Texture Analyzer (Texture Technologies Corp., Scarsdale, NY/Stable Micro Systems, Godalming, Surrey, UK). Prior to sample preparation, refrigerated units were set up and refrigerated unit temperature allowed to stabilize to one of the assigned test temperatures (-6.6, 4.4 or 10°C). Vacuum packaged steaks were place in their respective holding unit and the sample temperature allowed to equilibrate to that specific temperature for 2 h. For sample preparation, the top portion of each steak (5.08 cm) was removed to observe fiber orientation and the *Longissimus dorsi* was cut to obtain two 2.54 cm^3 cubes with fibers in a perpendicular and parallel orientation, respectively, for compression testing. Samples were excised just prior to the compression test, placed on the TA platform and compressed at a 3% of the sample height for 240 sec (Figure 4).

Figure 4. Platen compressive measurement using aluminum platen.

Acquisition rate was set at 50 pps and an auto trigger set at a force of 0.05 N. Calibration of the compression platen and net force was set with a 5 kg weight. Data were saved as a comma delimited file for further analysis using the software package Matlab v4.2c1 (The MathWorks, Inc., Natick, MA) and processed in the same manner as samples for Phase 1. Data values obtained for Phase 2 cubed samples were initial stiffness of parallel (ISTFPLC) and perpendicular (ISTFPPC) fiber orientation, and final stiffness of parallel (FSTFPLC) and perpendicular (FSTFPPC) fiber orientation and energy dissipated from parallel (EDPLC) and perpendicular (EDPPC) fiber orientation.

A separate modified compressive test with a stainless steel probe was performed on intact *Longissimus dorsi* steaks (2.54 cm) equilibrated to either -6.6º, 4.4º or 10ºC. Prior to testing, vacuum packaged steaks were equilibrated to the same temperatures as described above for the 5.08 cm thick sample that came from the same loin.

Compressive measurements were performed with a TA.XT2 Texture Analyzer (Texture Technologies Corp., Scarsdale, NY/Stable Micro Systems, Godalming, Surrey, UK) equipped with a 2 mm diameter stainless steel probe (Figure 5).

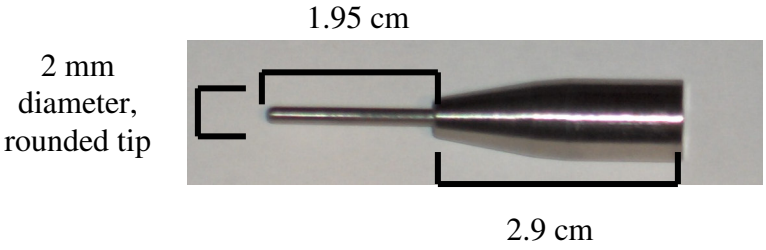

Figure 5. Stainless steel compression probe unit utilized in Phase 2.

Each intact steak was placed on the TA platform and the probe compressed 0.635 cm into the sample and held for 0.25 s, with four compressions of the same duration obtained at different locations on the surface of each steak (Figures 6, 7).

Figure 6. Probe compressive measurements using stainless steel compression probe.

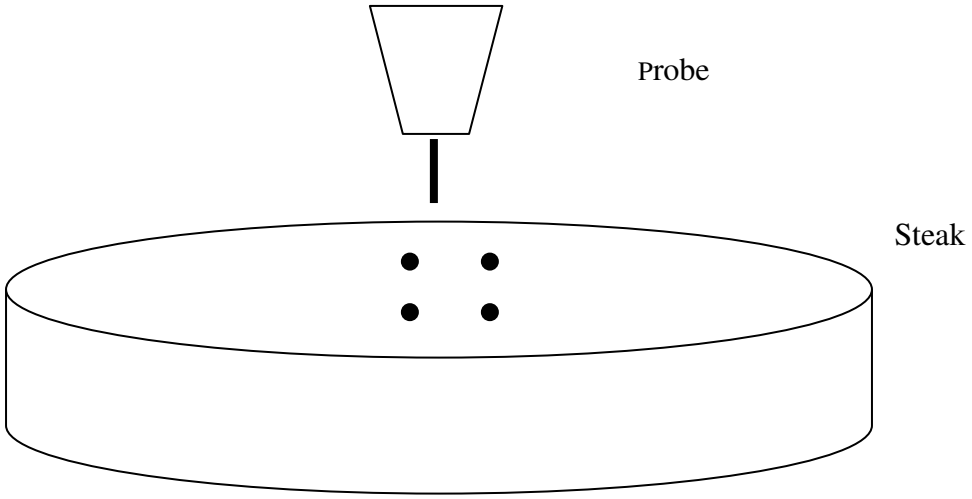

Figure 7. Four measurement locations taken on muscle surface.

This technique could subsequently be adapted to probe an intact loin on a wholesale carcass and was designed with that concept in mind. Acquisition rate was set at 50 pps and an auto trigger set at a force of 0.05 N. Calibration of the compression probe and net force was set with a 5 kg weight. Data were saved as a comma delimited file for further analysis using the Matlab v4.2c1 (The MathWorks, Inc., Natick, MA) software package. Revised mathematical models were developed from the initial Spadaro (1996) and Spadaro and others (2000) models to calculate Phase 2 probe values for initial stiffness (ISTFPR), final stiffness (FSTFPR) and energy dissipated (EDPR) for each compressive reading.

Sensory Evaluation

Companion steaks were evaluated by a trained descriptive attribute sensory panel at the Texas A&M Sensory Testing Facility for correlation to biomechanical measurements. Panelists were selected and trained according to the procedures outlined by AMSA (1995) and Meilgaard and others (1991). Training prior to testing was conducted by presenting reference samples to the panel to characterize the basic tenderness attributes to be scored on these beef samples. Raw weights of each steak were recorded and copper constantan thermocouples were inserted into the geometric center of each steak. Temperatures were monitored using an Omega HH21 microprocessor thermometer (Omega Engineering Inc., Samford, CT). An initial temperature and time were recorded and the steaks were broiled on a Faberware Open Hearth grill (model 450N, Kidde, Inc., Bronx, NY) to an internal temperature of 35°C, turned, and removed at 70°C. Cooked weight and time off the grill were recorded. Panelists were seated in isolated booths to avoid communication during the evaluation and the samples were presented to panelists through stainless steel breadbox servers adjacent to the preparation area. Each segregated booth was equipped with red incandescent lighting to mask sample color. Panelists were provided distilled water and unsalted crackers to cleanse their mouths. Warm, 13 mm-cubed samples were served to a five-to-seven member trained sensory panel. The order of the samples was randomized and a warm-up was presented to panelists before sample evaluation to ensure they had identified the attributes to be tested. Each panelist received at least two cubes of each sample, presented in coded cups with three digit codes. Ten samples were served each

day for both Phase 1 and 2 sensory evaluation, with samples being served 5 minutes apart each day. Each sample was evaluated on an 8-point scale for juiciness (8=Extremely juicy, 1=extremely dry); muscle fiber tenderness (8=extremely tender, 1=extremely tough); overall tenderness (8=extremely tender, 1=extremely tough); and connective tissue amount (8=none, 1=abundant) using eight-point scales.

Statistical Analysis

All statistical analyses was performed using the SAS v8.1 (SAS Institute, Cary, NC) software package with a significance level set at $P<0.05$.

Phase 1 - Assessment of cubed specimen temperature on compressive strain measurements.

To determine if fiber orientation, sample temperature or their interaction had an effect on platen compression values for initial stiffness, final stiffness and energy dissipated, an analysis of variance (ANOVA) was ran under the PROC MIXED procedure as described by the Statistical Analysis System (SAS, 1985), using the variable LOIN as a random variable to more effectively partition out the error associated with LOIN. Least squares means were calculated and means separated using the STDERR PDIFF procedure of SAS (1985).

To determine if prediction equations could be computed using biomechanical properties, TA values were evaluated to identify the strength of their mathematical relationship to become predictors of overall tenderness. Compression data from initial

stiffness (ISTF), final stiffness (FSTF) and energy dissipated (ED) were extended to include squared values (ISTF2, FSTF2, ED2) and platen values (ISTF3, FSTF3, ED3. This data manipulation was performed to evaluate their contributions to correlations between compression tests, sensory evaluations and Warner-Bratzler shear force values. All variables were run under PROC CORR to determine correlation coefficients between variables prior to regression analysis.

Prior to regression analysis, data were sorted based on fiber orientation and temperature at time of compression. Data analysis was run under the PROC REG procedure with a selection option of RSQUARE. This helped to distinguish which variables contributed to the prediction equations with higher R-square values. Once the most favorable prediction equations were selected, the model was ran under PROC REG to derive the appropriate β-values. Prediction equations using biomechanical measurements were developed that would predict sensory panel profile data and Warner-Bratzler shear force (WBSF) measurements.

Sensory evaluations were analyzed as a split-plot design where the main effects of temperature and fiber orientation and their interaction were included in the whole-plot. Loin was used as the whole-plot error term and sensory day was included as a block in the whole-plot. Panelist and panelist by main effect interactions were included in the split-plot. The residual error was used as the error term for the split-plot. Least squares means were calculated and means were separated using the STDERR PDIFF procedure of SAS (1985).

Phase 2 - Assessment of biomechanical properties of intact raw muscle sample with a probe.

An ANOVA was performed using the PROC MIXED procedure (SAS, 1985) to assess if sample temperature during compression had an effect on biomechanical properties. Data were then separated on the basis of compression temperature. All data variables were run under PROC CORR to determine correlation coefficients between variables prior to regression analysis. Regression models to predict overall sensory tenderness from biomechanical measurements were derived for each temperature using the PROC REG procedure. PROC REG was run with a selection option of STEPWISE and RSQUARE to help distinguish which variables contributed to prediction equations with higher R-square values. Once the most favorable prediction equations were selected, the model was run under PROC REG to derive the appropriate β-values. Prediction equations for overall sensory tenderness using WBSF values were obtained and compared to biomechanical measurements to determine which was a more effective predictor of overall sensory tenderness. Sensory data was averaged across panelists and analyzed as defined for other variables.

RESULTS AND DISCUSSION

Phase 1 - Assessment of Cubed Specimen Temperature on Compressive Strain Measurements.

The objective of Phase 1 was to determine if the compressive biomechanical measuring technique developed by Spadaro (1996) could effectively predict overall sensory tenderness of cooked steaks by assessing total initial and final stiffness values and the total energy dissipated by raw muscle fibers oriented in a parallel or perpendicular fashion at different refrigerated sample temperatures. It was also critical to determine what effects fiber orientation and sample temperature had on biomechanical measurements. Samples were tempered to 0, 2, 4, 6, 8 or 10°C in a temperature controlled water bath prior to compressive testing. This temperature range was selected to represent the temperature variation of beef carcasses in a packing plant environment. Incremental evaluation of specific temperatures should enable better assessment of Spadaro's (1996) measurement technique in relation to actual processing plant temperatures. Spadaro's platen compression method was also compared to values derived from the Warner-Bratzler shear device. Two null hypotheses were addressed, with the first being that fiber orientation does not effect biomechanical values and prediction potential of biomechanical properties to predict sensory traits, and the second being that sample temperature does not effect biomechanical values and prediction potential of biomechanical properties to predict sensory traits.

The effects of fiber orientation and sample temperature as they influenced platen compression values for initial stiffness (ISTF), final stiffness (FSTF) and energy dissipated (ED) are shown in Tables 1, 2 and Figures 8, 9, and 10. ISTF refers to the initial resistance of the muscle fibers against the compression plate under 3% compression strain. FSTF was determined after 4 min of 3% compression. The ED represents the amount of energy that is exerted against the compression plate by the sample under a constant compression (strain) of 3%. Both fiber orientation (Table 1) and sample temperature (Table 2) had a significant effect on ISTF and FSTF values as well as ED, but the interaction of the two treatments was not significant for either stiffness or energy dissipated values.

Fiber orientation had a significant effect on all three compression values (Table 1) at various holding temperatures. Fibers orientated in a parallel (PL) direction had lower stiffness (ISTF, FSTF) values and greater ED ($P<0.05$) than perpendicular (PP) fiber values. Stiffness (ISTF, FSTF) values were observed to be inversely proportional to ED values for PL and PP fiber orientations. The more stiff the muscle fiber, the less energy that can be absorbed by the fiber, and conversely, the less stiff the specimen, the more energy that can be radiated throughout the sample. The effect of fiber orientation on compression values can be due to connective tissue distribution in the muscle. Measurements parallel to fibers detected the resistance of fiber bundles, while those against fibers detected the resistance of the connective tissue (Szczesniak, 1977). Similar results were previously demonstrated by Spadaro (1996), Spadaro and others (2002) and Marburger (1999) who noted that the stiffer the sample, the less energy

dissipated. Similar fiber orientation effects during platen compression were seen by Spadaro (1996), Spadaro and others (2002) and Marburger (1999) as well as this study. Fiber orientation also had a significant effect on the predictive effectiveness of models in the previous studies. In these studies, stiffness or energy dissipated in different fiber orientations (PL or PP) were better predictors of sensory tenderness than other combinations of compression values and fiber orientations. Spadaro (1996) and Spadaro and others (2002) observed ISTF, FSTF and ED in both PL and PP orientations to be highly correlated to overall tenderness (r = 0.80 to -0.95) with EDPP having the highest correlation. One predictive model using FSTFPL and another model using EDPL to predict tenderness were highly correlated to sensory tenderness (R^2 = 0.90 and R^2 = 0.83, respectively). Marburger (1999) observed EDPL and ISTFPP (R^2 = 0.73 and R^2 = 0.73, respectively) to be effective predictors of sensory tenderness.

The sample temperature at compression had a significant effect on all compression values (Table 2). ISTF and FSTF at 0, 2, and 6ºC were higher ($P<0.05$) or stiffer than those at 8 and 10ºC. Both ISTF and FSTF at 4ºC were not different ($P>0.05$) from the other samples at 0, 2, 6, 8 or 10ºC. Less energy was dissipated ($P<0.05$) for samples at 2 and 6ºC than those compressed at 8 and 10ºC. As with stiffness values, ED at 0 and 4°C were intermediate between 2 and 6°C and 8 and 10°C. As the sample temperature increased, ISTF and FSTF decreased while ED increased, especially at 8 and 10°C.

The results in Table 2 provide valuable information for the potential use of biomechanical measurements in the beef processing industry. USDA regulations require

that processing facilities keep environment temperatures at 6°C or below. Since samples compressed at 0 to 6°C were not significantly different, this indicates that biomechanical properties can be assessed at any temperature within this range. Should these or similar biomechanical values obtained in this temperature range be incorporated into prediction equations they would not lose their prediction potential as a consequence of cooler temperatures.

The interaction between sample temperature and fiber orientation was not significant for biomechanical properties (ISTF, P=0.32; FSTF, P=0.31; ED, P=0.70). However, for ISTF (Figure 8) and FSTF (Figure 9), samples compressed in the perpendicular (PP) orientation tended to have higher values than those samples compressed in the PL fiber orientation, with stiffness values for samples at 2ºC in the PP orientation being highest. In general, PP stiffness values were higher for compression values taken at 0 and 2°C when compared to PL values at the same temperature, otherwise the values were not different. Figure 10 showed that ED with fiber in the PP orientation were lower only for 2°C when compared to all temperatures for PL orientation. In summary, samples in perpendicular orientation exhibited greater stiffness values and less energy dissipated than samples in a parallel orientation, however, no obvious trend in compression temperature and fiber orientation interaction was identified.

Regression analysis allows one to determine if there is a mathematical relationship between variables and to study the scope and strength of that relationship. Prediction equations derived from regression analysis are useful in determining how

changes in the independent variable affect changes in the dependent variable. Prediction equations with high R-square values are optimal, with R-square value of 0.70 or greater considered a high value, and prediction equations with high R-square values provide better prediction potential since a high R-square value accounts for more of the variation in the sample population. In an effort to identify the strength of their prediction potential for sensory attributes, prediction equations were computed for all compression variables (Tables 3, 4, 5, 6, and 7) in a parallel or perpendicular orientation. Predictive R-square values for sensory attributes such as juiciness, connective tissue amount, muscle fiber tenderness and overall sensory tenderness and Warner-Bratzler shear values (WBSF) from platen compression values of raw *Longissimus dorsi* samples are shown in Tables 3, 4, 5, and 6. Segregation by fiber orientation and compression temperatures are also presented. Regression formulas were derived using the ISTF, FSTF and ED values, as well as the squared (ISTF2, FSTF2, ED2) and platen values (ISTF3, FSTF3, ED3) of each compression variable. The R-square values for each combination of fiber orientation and temperature are listed in the respective tables for that sensory attribute. Although not all R-square values for each equation are listed, the equations with the highest R-square value and those equations with an R-square value closest to the highest are included. Equations with the best predictive R-square values included all nine variables (ISTF, ISTF2, ISTF3, FSTF, FSTF2, FSTF3, ED, ED2, ED3), while equations of similar effectiveness may have included six to eight variables.

Regression models are useful approximations for determining if an independent variable has a predictive effect on the dependent variable and is the easiest method of

interpreting if an equation is a good predictor. Choosing a model based solely on R-square values may not be practical since the variables may not be easily obtained or measured. Requiring more than just the R-square value needs to be taken into consideration when considering an equation's prediction potential. Whether a R-square value is considered large or small can depend up on the context of the study. It is best to consider the root means squared error (RMSE) and Mallow's Cp for the equation in conjunction with the R–square value. RMSE is the statistic whose value is minimized during the parameter estimation process, and determines the width of the confidence intervals for predictions. It is measured in the same units as the data, rather than squared units, and is representative of the size of a typical error. It is important to remember that the width of the confidence intervals is proportional to the RMSE and how much of a relative decrease in the width of the confidence intervals would be noticeable on a plot. RMSE is a measure of the lack of fit while Mallow's Cp is the total square errors. There is no set criteria for an acceptable RMSE and Cp value. Thus, the higher the R-square is, the better the model is. The lower the RMSE and Cp are, the better the model is.

It is also necessary to consider the degree of increase in predictability by adding additional variables to the equation. For example, is a 3% increase in prediction worth adding another independent variable to a regression model to decrease the RMSE and Cp? By adding an additional variable, one may run the risk of the data collector not obtaining an adequate measurement or not obtaining valid data.

Prediction equations for juiciness with the highest R-square values are shown in Table 3. In general, samples compressed perpendicularly at 0, 2, 6, 8 and 10°C had

greater prediction potential than those samples of PL fiber orientation. The best predictive equation for cooked beef juiciness from a raw sample was using an eight variable equation of ISTF, ISTF2, ISTF3, FSTF, FSTF2, ED, ED2, ED3 (R^2 = 0.75, RMSE = 0.42) at 2°C PP. Although at 2ºC in the PP orientation, similar predictability occurs (R^2 = 0.76, RMSE = 0.44) with another equation, however, the former equation is better since it incorporates fewer variables and the R-square and RMSE are acceptable. The complete prediction equation can be found in Table 8. Prediction equations at 8ºC with a PP orientation (R^2 = 0.73 or R^2 = 0.73 or R^2 = 0.73) and 0ºC, PP orientation (R^2 = 0.72 or R^2 = 0.71) also showed prediction potential.

An equation with similar predictability for connective tissue was observed at 2ºC, PP orientation (R^2 = 0.79, RMSE = 0.44) (Table 4). Table 8 outlines the complete prediction equation, with β values for each variable. Two other prediction equations with R-square values of 0.72 were generated from measurements at 4°C using either eight or nine variables, but had higher RMSE values (0.70 or 0.75, respectively) than 2°C PP.

Prediction equations with the highest R-square values for muscle fiber tenderness are given in Table 5. As observed with juiciness and connective tissue amount, the PP fiber orientation had the greatest predictive potential for muscle fiber tenderness as compared to the PL orientation. The equation that best predicted muscle fiber tenderness was at 4ºC, PP orientation (R^2 = 0.73, RMSE = 0.45) and utilized ISTF2, ISTF3, FSTF2, FSTF3, ED2, ED3. The complete prediction equation is given in Table 8. Reducing the

number of compression variables from nine to six, provided favorable predictability with R-squares of 0.73, 0.73, and 0.73, respectively. However, RMSE values decreased as number of variables decreased. R-square values were comparable, but distinction of which equation was best is decided by the lower RMSE value. A nine variable prediction equation (R^2 = 0.73, RMSE = 0.49) at 2ºC yielded similar prediction potential.

Prediction equations for overall sensory tenderness are presented in Table 6 and the equation with highest R-square value is given in Table 8. PP samples compressed at 2ºC yielded the highest R-square value (R^2 = 0.77), as well as the lowest RMSE (RMSE = 0.44) of the other high R-square valued equations using 0°C (R^2 = 0.71 to 0.74, RMSE 0.45 to 0.46), 2°C (R^2 = 0.66, RMSE 0.53 to 0.59) and 4°C (R^2 = 0.65, RMSE 0.55 to 0.60) for PL or 4°C PP (R^2 = 0.70, RMSE 0.50 to 0.56). Aside from 2°C PP, PL samples at 0°C for nine or eight variables (R^2 = 0.74 and R^2 = 0.72, respectively) yielded acceptable prediction equations.

Based on this evidence, both of the null hypotheses were rejected. Fiber orientation and sample temperature during compression did have a significant effect on biomechanical values. This study is of significance to the beef industry since the results show the potential of raw compressive measurements to predict cooked sensory tenderness. It also validates that biomechanical values obtained at any temperature between 0 and 6°C are better predictors of sensory traits than at 8 or 10°C, with 2°C producing the best prediction equation. Since processing facilities maintain an environment temperature of 0 to 6°C, this compressive technique allows for online

tenderness assessment without temperature adjustment. Identifying which fiber orientation produced the highest R-square value will alleviate multiple cubed sample excision. Based on these results, one 2.54 cm^3 cube of raw *Longissimus dorsi* sample needs to be removed for compression in the perpendicular fiber orientation to obtain the best prediction equation. Results showed that compressing parallel to the fiber orientation at 0 to 4°C yielded overall tenderness prediction equations with R-square values ranging from 0.65 to 0.74 (Table 6). Compression in the perpendicular fiber orientation at 2 to 4°C yielded overall tenderness prediction equations with R-square values ranging from 0.70 to 0.77 (Table 6), with data collected at 2°C PP producing the best prediction equation for overall tenderness (Table 8).

The ability for compression testing to predict Warner-Bratzler shear force values (WBSF) is shown in Table 7. WBSF values were obtained on cooked products but since compression testing occurred over a range of temperatures and differing fiber orientations, the data were sorted by temperature and fiber orientation prior to regression analysis. Samples at 8ºC compressed perpendicularly had the highest R-square value (R^2 = 0.88, RMSE = 0.61). With most of the sensory attributes, samples measured at 2ºC and oriented perpendicularly had the best prediction potential, as demonstrated by their R-square value to predict WBSF (R^2 = 0.80, RMSE = 0.58). RMSE values did not differ much between 8°C and 2°C, but the R-square for 8°C PP was 7% higher than that of 2°C PP. Samples compressed at 4 and 10ºC, perpendicularly had high predictability of WBSF values (R^2 = 0.73, RMSE = 0.68 and R^2 = 0.70, RMSE = 0.69, respectively). Although R-square values derived from WBSF values for sensory evaluation scores vary,

the Warner-Bratzler shear apparatus remains the standard objective method for predicting cooked meat tenderness. However, it is time consuming and requires destruction of a complete steak sample. By determining the ability of biomechanical properties to predict WBSF values, time and destruction factors may be alleviated as well as provide for another research tool.

The last null hypothesis that was addressed in Phase 1 was that biomechanical platen values account for or are related to biological components of meat that impact cooked meat tenderness and sensory attributes. Table 8 shows the equations that had the highest predictability (R^2 values) for all sensory attributes (juiciness, connective tissue, muscle fiber tenderness and overall tenderness) derived using a 3% compression (strain) with a platen and the muscle fibers oriented in the PP direction. It is noteworthy that the best predictions for juiciness, connective tissue and overall tenderness come from samples compressed at 2ºC. The exception to this is muscle fiber tenderness, which derived its highest R-square value at 4ºC PP orientation, but as shown in Table 5, samples compressed PP at 2ºC had an R-square of 0.73. In summary, it appears that the most effective predictor of overall cooked beef tenderness derived from a raw sample using a platen to compress excised cubed samples comes from perpendicularly orientated fibers at 2ºC.

A comparison of prediction equations in Table 8 indicates that the TA generated biomechanical values are better predictors of sensory juiciness, connective tissue amount, muscle fiber tenderness and overall tenderness than WBSF values. TA biomechanical values proved to have higher ($P<0.05$) R-square values for all sensory

attributes over that of the Warner-Bratzler shear. The most critical sensory measurement related to eating quality of beef is that of overall tenderness, and the compression values were more effective for predicting tenderness than WBSF. These data indicate that the Texture Analyzer compression values generated from raw loin steaks can be used effectively to predict cooked sensory tenderness more consistently than WBSF values of cooked steaks. Thus, this confirms the Spadaro (1996) predictive equations using 3% compression with a TA platen to predict sensory tenderness of raw steak samples from USDA Choice steers.

Spadaro (1996) evaluated *Longissimus dorsi* steaks from older cattle (48 mo, USDA Utility) and younger Angus steers (18 mo, USDA Choice) using the 3% compressive (strain) platen technique and derived equations. She found that samples from older cattle, 24 hr postmortem, were always less tender, had more connective tissue, and gave higher WBSF values than younger, aged steaks. Warner-Bratzler shear force values also correlated poorly with overall sensory tenderness ($r = -0.55$), muscle fiber tenderness ($r = -0.55$), and connective tissue amount ($r = -0.54$) (Spadaro, 1996). Our study also showed poor prediction potential for WBSF to determine overall sensory tenderness, connective tissue amount and muscle fiber tenderness, and established biomechanical testing as a better predictor of sensory attributes. As was observed in this study, Spadaro (1996) also noted an inverse relationship between stiffness values and energy dissipated, concluding that the more tender a sample, less energy was dissipated and the sample became stiffer. She also concluded that biomechanical measurements obtained from the compression test explained more of the variation in beef loin steak

tenderness than did WBSF values, and that biomechanical measurements would be better predictors of overall sensory tenderness than WBSF values.

Marburger (1999) evaluated the mathematical models developed by Spadaro (1996) and replicated the study in an attempt to validate prediction of their tenderness for *Longissimus dorsi* steak samples that varied in tenderness and degree of aging. EDPL ($r = -0.86$) and PP stiffness (ISTF, FSTF) values ($r = 0.85$) measured at a range of 4.4 to 10°C were highly correlated to sensory tenderness. Warner-Bratzler shear force was less effective ($r = -0.79$) for predicting tenderness than compression measurements. EDPL alone accounted for more variation in overall tenderness ($R^2 = 0.73$) and more accurately assessed tenderness than WBSF values ($R^2 = 0.62$). Marburger (1999) confirmed that an objective, biomechanical strain applied to raw steaks could effectively predict overall sensory tenderness of cooked steaks more effectively than WBSF.

Results from the current study support the findings of Spadaro (1996), Spadaro and others (2002) and Marburger (1999) and concluded that biomechanical values obtained using a compressive technique and the mathematical models developed by Spadaro (1996) were effective predictors of overall sensory tenderness.

All compression values had higher correlation coefficients with overall sensory tenderness than did WBSF, indicating the predictive effectiveness of these values over that of WBSF. Of these prediction equations, it was concluded that samples compressed perpendicularly at 2ºC were better predictors of overall sensory tenderness ($R^2 = 0.77$) than WBSF ($R^2 = 0.11$). Compression values were also better predictors of juiciness ($R^2 = 0.76$), connective tissue amount ($R^2 = 0.79$) and muscle fiber tenderness ($R^2 = 0.73$)

over that of WBSF (R^2 = 0.03, 0.03, 0.10, respectively). Spadaro (1996) likewise observed that all TA compression measurements for both fiber directions (EDPL, EDPP, ISTFPL, FSTFPL, ISTFPP and FSTFPP) (r = -0.91, -0.89, 0.80, 0.86, 0.83, and 0.84, respectively) were more highly correlated (r = -0.5483) to overall tenderness than was WBSF.

The significance of this phase of the study is that it validates the use of biomechanical strain measurements to effectively predict overall sensory tenderness of cooked steaks from raw steaks, and which compression temperatures were optimal. Based on this evidence, the null hypothesis was accepted. Biomechanical platen values accounted for or were related to biological components of meat that impact cooked meat tenderness and sensory attributes. This study is of significance to the beef industry since the results show the potential of raw compressive measurements to predict cooked sensory tenderness. It also validates that biomechanical values obtained at any temperature between 0 and 6°C are better predictors of sensory traits than at 8 or 10°C, with 2°C producing the best prediction equation. Since processing facilities maintain an environment temperature of 0 to 6°C, this compressive technique allows for online tenderness assessment without temperature adjustment. Identifying which fiber orientation produced the highest R-square value will alleviate multiple cubed sample excision. Based on these results, one 2.54 cm^3 cube of raw *Longissimus dorsi* sample needs to be removed for compression in the perpendicular fiber orientation to obtain the best prediction equation. Results showed that compressing parallel to the fiber orientation at 0 to 4°C yielded overall tenderness prediction equations with R-square

values ranging from 0.65 to 0.74 (Table 6). Compression in the perpendicular fiber orientation at 2 to 4°C yielded overall tenderness prediction equations with R-square values ranging from 0.70 to 0.77 (Table 6), with data collected at 2°C PP producing the best prediction equation for overall tenderness (Table 8).

Because excision of a small amount of loin muscle, orienting the muscle fibers and compressing for 240 sec are not compatible with the speed required for assessment under processing plant conditions. A modification of the biomechanical measuring technique is required if it is suitable for a rapid, non-destructive test that could be adapted to an in-line grading system. Although the compressive tenderness assessment technique developed by Spadaro (1996) was an effective predictor of overall tenderness, it is not sufficiently practical. Thus, this required an additional phase of the study to be performed (Phase 2) in order to reduce compression time and allow testing of an intact loin sample.

Phase 2 - Assessment of Biomechanical Properties of Intact Raw Muscle Sample with a Probe.

Forty fresh loins were collected from a slaughter facility, assigned to one of three compression temperatures (-6.6°C, n = 14; 4.4°C, n = 13; 10ºC, n = 13) and distributed, based on USDA quality grade, somewhat equally among each temperature treatment. Only the data collected from compression testing were subjected to the temperature treatments and compared to other analyses from the same loins. No other physical,

chemical or sensory analyses were performed under the three temperature treatments. Other analyses could not have temperature restraints applied due to the nature of the data collection technique. Most, but not all, loin samples were treated to every temperature treatment during compression due to insufficient sample numbers. This range of temperatures was selected so that compressive measurements could be performed over the range of temperatures anticipated in a meat packing plant environment (4.4 and 10°C), and the water in the sample was in a fluid state. The 4.4 and 10°C measurements could then be compared to muscle with water in a relatively solid state (-6.6°C). Since the solid form of water has infinite viscoelasticity, data from samples compressed at –6.6°C would serve as a control for biomechanical measurements against samples with intracellular fluid in the liquid state (4.4 and 10°C). Although forty loins were available, the entire loin was not at my disposal. There was sufficient loin for platen and probe compression samples as well as physical, chemical and sensory analyses. Sufficient numbers of samples were available for statistical validation.

The objective of Phase 2 was to test three null hypotheses: 1) probe compression values are predictive of platen compression values, 2) probe compression values are as predictive of sensory tenderness as platen compression values, and 3) removing replicate probe compression values that are greater than 45% of the mean improved the ability to predict sensory tenderness using biomechanical values from the probe compression.

For probe compression data (ISTFPR, FSTFPR and EDPR presented at the bottom of Table 9), four surface measurements were taken at random locations in the center portion of the muscle (Figure 7). A formula to determine the percent difference

between the samples (% difference = (maximum value – minimum value)/maximum value x 100) and the sample mean was constructed and acceptable prove values set at a tolerance of $\leq$ 45%. It was determined that this was a generous percent difference since other physical and chemical analysis data allow only a 5-10% difference in data values, and this was a new technique with limited data to establish an appropriate range of acceptable values. For some samples, one of the four probe compression measurements was an outlier when compared to the other three values. This could have been caused by indigenous grizzle (connective tissue) within the muscle and would be an obvious anomaly. Therefore, if the percent difference between an actual probe compression value and the probe compression mean for that particular sample was greater than 45%, the single outlying datum was removed. A maximum of only one data value per set of four was removed. For further clarification of the probe compression data, the initial four probe values are termed "Raw Data" and the data set with the calculated outlying value removed is termed "Adjusted Data". Raw and Adjusted Data only apply to probe compression values.

Mean values for physical, chemical, sensory and biomechanical analyses across temperature treatments are shown in Table 9. Samples from loins subjected to physical, chemical and sensory evaluation were assigned to different temperatures, but not physically held at those temperatures. Rather, their presence in a treatment column was done for statistical assignment. Only the compression testing samples underwent temperature treatment. The data for each loin were allotted to one of the three temperature treatments depending upon assignment of a loin to a compression

temperature. The only analysis that showed significant differences between the temperature treatments was color space lightness (L*) values. Those loin samples that were assigned to 4.4°C were darker ($P<0.05$) than those samples held at -6.6° or 10°C. Otherwise, no significant differences were observed between temperature groups for all other physical, chemical, sensory or biomechanical analyses. Although a storage temperature effect was not expected in this study for physical and chemical values, storage temperature can affect some physical, chemical and sensory analyses. Meat is aged at refrigerated temperatures, which allows for the muscle tissue to begin degradation. Aging weakens muscle fibers, produces small changes in connective tissue and Warner-Bratzler shear force values decrease with refrigerated aging (Bouton and others 1975). Proteolysis of myofibrillar proteins by calcium-dependent proteases and lysosomal enzymes is the major contributor to meat tenderization during postmortem storage (Koohmaraie and others 1988). Thus, less tissue degradation results in tissue structure that remains firm, which can result in lower sensory tenderness scores and higher WBSF values.

Data from both cubed specimens compressed with a platen and probe compression of intact muscle were analyzed to determine if sample temperature during compression had an effect on biomechanical properties. No significant differences between temperature treatments were observed (Table 9). Regardless of lack of temperature effect, the data were separated and analyzed by temperature treatment to determine if one temperature was more advantageous than another (Table 9). Since not

all loins were treated to every compression temperature, data were not pooled and analyzed.

Pairwise correlation coefficients were computed for all variables (Tables 10, 11, 12, 13, and 14) in an effort to identify the degree of their mathematical relationship to become predictors of overall sensory tenderness regardless of sample temperature. Tables 10, 11, 12, and 13 show correlations between all variables based on "Raw Data" from probe compressions. Table 14 illustrates correlations between all variables based on "Adjusted Data" from probe compressions. Variables of primary interest were those associated with overall sensory tenderness, especially Warner-Bratzler shear force (WBSF) and Texture Analyzer (TA) values for platen specimens and probe compression.

USDA quality grade (QG) was highly correlated with marbling (MARB) ($p<0.001$) and both QG and MARB were negatively correlated with percent moisture (MOIST) ($P<0.001$) and positively correlated with percent fat (FAT) ($P<0.001$). Thus, as QG and MARB increased, so did FAT, but MOIST decreased. However, only MARB had a significant relationship with protein (PROT) ($P<0.05$), in which as MARB increased, PROT amount decreased. This is supported the bulk density theory of marbling, which is a marbling increases, it displaces protein. Yield grade (YG) did not correlate as strongly with MOIST ($P<0.05$) and FAT ($P<0.05$) as did QG and MARB (Table 10). QG and MARB are directly related since MARB is one of the two components (maturity is the second, and maturity did not vary within this population) of QG. As intramuscular fat or marbling is deposited throughout the loin muscle, QG increases. In addition, a higher MARB score would result in a greater FAT content of

the muscle, and as FAT amount increases, a dilution effect is imposed on MOIST and PROT content.

Although significant correlations were observed between color space values for lightness (L*) and redness (a*) values ($P<0.01$), the correlation coefficient was not strong (Table 10). Redness (a*) and yellowness (b*) values had a much stronger relationship ($P<0.001$) and were both negatively related to MOIST ($P<0.01$). Yellowness (b*) values had a slightly larger relationship with FAT ($P<0.001$) than did a* values ($P<0.01$). However, only a* values had a significant relationship with PROT. Redness (a*) and yellowness (b*) values exhibited a positive relationship with sensory evaluation scores for CTAMT ($P<0.01$), MFTEND ($P<0.01$) and OVERALL ($P<0.01$). Redness (a*) and yellowness (b*) values were both negatively related to WBSF values ($P<0.05$). The only relationship observed between color space values and biomechanical testing was between b* and ISTFPLC ($P<0.05$). This relationship appears coincidental since no other correlation was observed between biomechanical measurements and color space values.

Some chemical traits were also correlated with physical, sensory and biomechanical attributes (Table 11). pH values were negatively related ($P < 0.05$) to EDPR, but positively related to FSTFPR ($P<0.05$). As expected, percent moisture was negatively related to FAT ($P < 0.001$), but positively correlated with PROT ($P<0.001$). A significant relationship was also observed between FAT and PROT ($P<0.001$). Sensory variables were not significantly correlated with MOIST or FAT, but were correlated with PROT. Percent protein was negatively correlated with CTAMT

(P<0.01), MFTEND (P<0.01) and OVERALL (P<0.001) indicating that as percent PROT decreased, these sensory values increased. This could be attributed to the relationship between fat and protein. Intramuscular fat has an influential role in beef palatability and an increase in fat could result in an increase in sensory tenderness scores. However, PROT accounted for $\leq$ 25% of the variation that might be attributed to predicting sensory values. As observed between PROT and WBSF, the higher the level of PROT, the higher the WBSF value (P<0.01), but with the same degree of predictive effectiveness as with the sensory traits. A greater amount of protein content results in a greater amount of protein coagulation during heating. Coagulated protein requires a greater degree of force to shear through the sample than does a sample with a higher fat and less protein content. The only significant correlation between proximate analysis variables and TA probe compression was between PROT and EDPR (P<0.05). Percent total and soluble collagen were positively correlated (P<0.001), indicating that a higher percent value of one would result in a higher percentage of the other but the predictive relationship was not high.

Correlations of sensory and biomechanical measures are shown in Tables 12 and 13. Juiciness was positively associated with CTAMT (P<0.05), MFTEND (P<0.001) and OVERALL (P<0.001). Connective tissue amount scores were positively related (P<0.001) to MFTEND and OVERALL as well as EDPPC (P<0.01). However, CTAMT was inversely related (P<0.01) to ISTFPPC and FSTFPPC. A significant relationship (P<0.001) was observed between MFTEND and OVERALL, indicating that the more tender the muscle fiber, the more tender the overall tenderness value. Muscle fiber

tenderness and OVERALL were positively correlated to EDPPC ($P<0.001$) and EDPR ($P<0.05$), but negatively correlated to ISTFPPC ($P<0.01$), FSTFPPC ($P<0.01$) and FSTFPR ($P<0.05$). Stiffness values had an inverse relationship with their respective energy dissipated values. The results indicate that this relationship extends to other data variables as well. If a variable has an inverse relationship with initial and final stiffness, then it has a positive correlation with energy dissipated.

Correlation coefficients for biomechanical traits are outlined in Table 13. Warner-Bratzler shear force values were inversely and highly related ($P<0.001$) to all sensory attributes. Warner-Bratzler shear force measurements were not correlated with TA measurements. Platen compression values for samples compressed with fibers orientated perpendicularly were highly correlated with other biomechanical measurements for perpendicular fiber orientation. However, those values for parallel fiber orientation did not all correlate significantly with other parallel fiber orientation measurements. EDPPC was inversely related ($P<0.001$) to ISTFPPC and FSTFPPC meaning that the more stiff the sample, the less energy dissipated during compression. The same trend was observed in Spadaro (1996), Marburger (1999) and Spadaro and others (2002). Stiffness values (ISTF, FSTF) for fibers in the perpendicular orientation were positively correlated ($P<0.001$), but stiffness values for parallel orientation did not exhibit a significant relationship. However, for the parallel fiber orientated compression, only FSTFPLC and EDPLC were negatively ($P<0.001$) related.

Probe compression values were highly correlated ($P<0.001$) with one another. ISTFPR and FSTFPR were positively correlated while each were negatively correlated to

EDPR. These results support the findings of Spadaro (1996), Marburger (1999) and Spadaro and others (2002), in which the stiffer the sample, the less energy dissipated during compression or the more stiff a sample, the less energy that can be absorbed into the material. The only platen compression value that was correlated with probe compression was between ISTFPPC and FSTFPR ($P<0.05$). This correlation appears purely coincidental since no other correlations were observed between platen and probe compression values. This correlation could possibly be attributed to the fact that the relationship is between stiffness values, such as comparing 'like' measurements to each other.

Table 14 shows the correlations between all variables and the adjusted probe compression values (ISTFPR, FSTFPR and EDPR). All other correlation relationships between physical, chemical, sensory and biomechanical traits remained the same. With the outlying probe compression values removed, changes in correlation coefficients and relationships with other variables were observed. ISTFPR and FSTFPR were positively related ($P<0.05$) to pH and negatively correlated ($P<0.05$) to OVERALL. Prior to the data adjustment, no correlation was observed between ISTFPR and pH or OVERALL (tenderness). Slight changes in the correlations between probe compression and other variables did occur after adjusting for the percent difference between sample values. FSTFPR continued to have a negative correlation with MFTEND ($P<0.05$) and EDPR remained negatively correlated with pH ($P<0.05$). ISTFPR and FSTFPR remained highly correlated ($P<0.001$) to each other as well as to EDPR ($P<0.001$). Based on the lack of significant correlations between platen and probe compression values (Tables 13

and 14), there does not appear to be sufficient evidence to support the hypothesis that platen compression values can be predicted from probe compression values. Although platen compression provided effective prediction equations, the process of excising a cubed sample and orientating muscle fibers in a uniform orientation is not practical to the goal of Phase 2. Platen compression also is unnecessary in developing prediction equations using probe compression. Therefore, there is no advantage to predicting platen values from probe compression except to show that there is a relationship between platen and probe compression.

Although statistical analysis showed that temperature had no significant effect on compression values, data were separated based on sample temperature during TA compression testing to determine if one temperature produced more optimal correlation coefficients than other temperatures. Data were then separated based on sample temperature during compression and pairwise correlation coefficients were computed for all variables (Tables 15, 16, 17, 18, 19 and 20). Since sample temperature was only treated to TA measurements, Tables 15 through 20 depict correlation coefficients between all variables and biomechanical measurements for each compression temperature. WBSF did not undergo temperature treatment due to the nature of the protocol for WBSF assessment, but is still included in the biomechanical category. TA compressive values are correlated to WBSF, but other physical, chemical and sensory variable correlations to WBSF remained the same as outlined in Tables 13 and 14. Tables 15, 16, and 17 show correlations between all variables based on “Raw Data” from

probe compressions and Tables 18, 19, and 20 are the correlations between all variables based on "Adjusted Data" from probe compressions.

Platen compression of samples tempered to -6.6°C (Table 15) resulted in ISTFPLC and FSTFPLC being highly correlated to EDPLC ($P<0.001$). Stiffness values (ISTF and FSTF) for perpendicular fiber orientation were positively correlated to each other ($P<0.001$), but both negatively correlated to EDPPC. As observed previously, the more stiff the sample, the less energy dissipated. At -6.6°C, only platen compression values for perpendicular fiber orientation exhibited significant correlations with sensory attributes. Both ISTFPPC and FSTFPPC had negative relationships with CTAMT ($P<0.05$), MFTEND ($P<0.01$) and OVERALL ($P<0.01$) whereas EDPPC was directly correlated to CTAMT ($P<0.01$), MFTEND ($P<0.01$) and OVERALL ($P<0.01$).

Biomechanical property values for probe compression of samples tempered to -6.6°C (Table 15) correlated highly to each other, but were not as highly related to sensory properties. Only EDPR was correlated to MFTEND and OVERALL ($P<0.05$), and EDPR was the only probe compression variable correlated to QG ($P<0.01$) and MARB ($P<0.05$) at this compression temperature of -6.6°C. It was also observed that platen compression values for stiffness (ISTF, FSTF) in the perpendicular fiber orientation correlated highly ($P<0.001$) with ISTFPR and FSTPR. EDPPC also exhibited correlations with ISTFPR ($P<0.01$), FSTFPR ($P<0.001$) and EDPR ($P<0.01$). Apparently, at –6.6°C, there exists the potential to predict platen compression values from probe compression values. During cubed sample compression, the platen covers

the entire sample surface, whereas with probe compression, the probe only covers 2 mm of the surface. At –6.6°C, the intracellular fluid is in a near-solid state, and it is possible that viscoelasticity of the solid state is being assessed to the same degree for both the platen and probe. When the intracellular fluid is in a liquid state, there is allowance for more deformation by the probe than the platen, resulting in differences in data values and perhaps lack of correlation between the compression techniques.

A high correlation between stiffness values and energy dissipated values, regardless of platen or probe compression, was expected. As noted in Table 15, platen compression in the perpendicular fiber orientation had a stronger relationship with sensory MFTEND and OVERALL than parallel compressive measurements. Platen compression values also had a strong relationship with all probe compression values. Based on these observations, the biomechanical properties of the perpendicular fiber orientation may be similar to those of the intact muscle undergoing probe compression.

Samples tempered to 4.4°C and treated to the TA platen compression technique (Table 16) showed that compression values for the same fiber orientation were not always related. The only significant correlation observed for parallel fiber orientation values was between FSTFPLC and EDPLC ($P<0.001$). Also at this temperature, it appeared that only FSTFPLC and EDPLC had an effect on or were related to sensory attributes. FSTFPLC was positively correlated ($P<0.05$) to CTAMT, MFTEND and OVERALL, and negatively correlated to MOIST ($P<0.05$). As EDPLC increased in value, so did MOIST ($P<0.05$) and YG ($P<0.05$), but sensory values for JUICY ($P<0.05$), CTAMT ($P<0.05$), MFTEND ($P<0.05$), OVERALL ($P<0.05$) decreased. The

only significant effect ISTFPLC had was on yellowness (b*). Color space values did not show a correlation to platen or probe compression values under other correlations, and this observed relationship may be due to the small sample size. ISTFPPC and FSTFPPC were positively correlated to QG and MARB ($P<0.01$) whereas EDPPC was negatively correlated to QG and MARB ($P<0.05$).

Probe measurements of the same samples tempered to 4.4°C (Table 16) were highly correlated ($P<0.001$) to one other, with an inverse relationship between stiffness values (ISTFPR, FSTFPR) and energy dissipated (EDPR) values. A similar trend was found in Tables 13, 14 and 15 and by Spadaro (1996), Marburger (1999), and Spadaro and others (2002). No other correlations between these measurements and physical, chemical, sensory or other biomechanical traits were noted. Based on the lack of significant correlation between platen and probe compression values, there is not enough evidence to support the hypothesis that platen compression values can be predicted from probe compression values at 4.4°C. Although platen compression provided effective prediction equations, the process of excising a cubed sample and orientating muscle fibers in a uniform orientation is not practical to the goal of Phase 2. Therefore, there is no advantage to predicting platen values from probe compression except to show that there was a relationship between platen and probe compression.

Platen compressed samples at 10°C (Table 17) resulted in both ISTFPLC and FSTFPLC being correlated to FSTFPR ($P<0.05$), but only ISTFPLC correlated to ISTFPR ($P<0.05$). As for energy dissipated value correlations, EDPLC was the only

biomechanical trait to have a correlation to MOIST ($P<0.05$) and EDPPC the only biomechanical trait to be correlated ($P<0.05$) with CTAMT, MFTEND and OVERALL. Based on the lack of significant correlation between platen and probe compression values, there is not enough evidence to support the hypothesis that platen compression values can be predicted from probe compression values at 10°C. Platen compression is not a variable in developing prediction equations using probe compression, thus there is no advantage to predicting platen values from probe compression except to show that there was a relationship between platen and probe compression.

Tables 18, 19 and 20 list the correlation coefficients for "Adjusted Data" for biomechanical values at each compression temperature. Only probe compression biomechanical measurements underwent the removal of outlying data to be termed "Adjusted Data". Platen compression values and the physical, chemical and sensory data were not adjusted, as discussed above. Table 18 outlines those coefficients for TA values at -6.6°C. As seen under other conditions, probe compression values correlated highly with each other, with stiffness (ISTF, FSTF) values being correlated ($P<0.001$) and having a negatively correlation to EDPR.

It was observed that ISTFPR had a positive correlation to ISTFPPC ($P<0.05$) which may be due to both measurements accounting for the same parameter of initial stiffness. ISTFPR was also inversely related to EDPPC ($P<0.05$). Correlation coefficients indicated that as FSTPR increased, so did ISTFPPC ($P<0.01$) and FSTFPPC ($P<0.01$), but EDPPC values declined ($P<0.01$). Energy dissipated values for probe compression showed a negative relationship ($P<0.05$) between QG and MARB but a

directly correlation (P<0.05) to EDPPC. It appears that at -6.6°C, all probe compression values correlated to EDPPC to some degree. Stronger significance levels for this same observation were observed for the raw data (Table 18).

There was the same relationship between probe samples compressed at 4.4°C (Table 19) as under -6.6°C conditions. No other significant relationships existed between probe compression values and other physical, chemical, sensory or biomechanical traits. Based on the lack of significant correlation between platen and probe compression values for samples analyzed at 4.4°C, there is not enough evidence to support the hypothesis that platen compression values can be predicted from probe compression values. The only advantage to predicting platen values from probe compression was to determine if there was a relationship between platen and probe compression.

Table 20 lists correlations between variables for "Adjusted Data" obtained at 10°C compression treatment. A significant correlation was observed between pH and probe values (Table 20). It was observed that as stiffness values increased and energy dissipated values decreased, pH values increased (P<0.05). Based on the lack of significant correlation between platen and probe compression values for data analyzed at 10°C, there is not enough evidence to support the hypothesis that platen compression values can be predicted from probe compression values. Although platen compression provided effective prediction equations, the process destroys the sample, making it impractical to the goal of Phase 2. Therefore, there is no advantage to predicting platen

values from probe compression except to show that there was a relationship between platen and probe compression.

In summary, Tables 13 through 20 exhibit consistent relationship trends across all temperatures for both platen and probe compression values. Stiffness values, regardless of fiber orientation, or platen or probe compression, were positively related to each other to varying degrees of significance, and stiffness values were consistently negatively related to energy dissipated values, regardless of fiber orientation, or platen or probe compression.

No significant differences between temperature treatments were found, but regression equations were derived based on compression values for all temperatures and regression equations at each individual compression temperature tested (Tables 21 through 24). The purpose of developing regression equations is to determine if there is a predictive relationship between biomechanical measurements and sensory attributes, with overall tenderness being the most important sensory variable. Strong prediction equations will help to alleviate the restraints of predicting beef tenderness using a trained sensory panel, which includes being time consuming, costly, not rapid and destroying the sample. Developing prediction equations with high predictability for overall tenderness would be an asset to industry and researchers alike by providing a rapid, non-destructive method of assessing tenderness. The STEPWISE option of SAS for deriving regression equations selects those variables that meet a significance level of $P< 0.1500$ in order to enter the model and chooses the minimum number of variables that meet these criteria. This significance level was selected by the SAS program. When evaluating those

formulas that take into account all testing temperatures (Table 21), a prediction equation for overall tenderness (OVERALL) using biomechanical values for initial stiffness parallel to fibers of the platen sample (ISTFPLC), initial stiffness perpendicular to fibers of the platen sample (ISTFPPC), energy dissipated perpendicular to fibers of the platen sample (EDPPC) and energy dissipated of probe compression (EDPR) of the "Raw Data" had the greatest prediction potential for overall sensory tenderness ($R^2 = 0.47$). When evaluating the "Adjusted Data", the final stiffness of probe compression (FSTFPR) and EDPPC had the greatest prediction potential for overall sensory tenderness ($R^2 = 0.40$). For muscle fiber tenderness (MFTEND), EDPPC and FSTFPR produced an equation with the greatest predictability ($R^2 = 0.39$) for "Adjusted Data" whereas EDPPC and EDPR were incorporated into the equation for "Raw Data" ($R^2 = 0.38$). Predictive equations for juiciness (JUICY) and connective tissue amount (CTAMT) for both "Raw" and "Adjusted Data" yielded the same prediction equation with the level of predictability ($R^2 = 0.07$, JUICY; $R^2 = 0.22$, CTAMT). Platen and probe compression measurements were combined within the predictive equations to demonstrate the effectiveness of biomechanical measurements to predict sensory traits. However, collecting platen and probe compressive values is impractical in regards to sample preparation and destruction of the sample. Utilizing probe compression values only would salvage the sample and save time. Evaluation of effectiveness of probe compression to predict sensory traits is discussed later in the paper.

Although compression temperature did not have a significant effect on biomechanical values, data were separated based on compression testing temperature and

predictive equations constructed to evaluate if one testing temperature might prove to be more optimal than others. This range of temperatures (-6.6 to 10°C) was selected so that compressive measurements could be performed on carcasses exposed to various temperatures that might occur in a packing plant environment. The range of 4.4 to 10°C is more typical and accounts for water in the sample being in a fluid state. These measurements could then be compared to muscle with water in a being in near-solid state (-6.6°C). Since the solid form of water has infinite viscoelasticity, data from samples compressed at –6.6°C would serve as a "control" for biomechanical measurements against samples with intracellular fluid in the liquid state (4.4 and 10°C).

Table 22 lists prediction equations for "Raw" and "Adjusted Data" of samples compressed at -6.6°C. For OVERALL, the equation with the greatest predictability included final stiffness perpendicular to fibers for platen compression (FSTFPPC) (R^2 = 0.48). The juiciness prediction included final stiffness parallel to fibers for platen compression (FSTFPLC) (R^2 = 0.26) and CTAMT included energy dissipated perpendicular to fibers for platen compression (EDPPC) (R^2 = 0.42). Muscle fiber tenderness did differ between the "Raw" and "Adjusted Data". "Raw Data" for MFTEND yielded a prediction equation with an R-square value of 0.77 and included both platen compression and probe compression variables (FSTFPPC, EDPLC and FSTFPR). The equation utilizing "Adjusted Data" only incorporated FSTFPPC and did not have as high a predictability (R^2 = 0.48).

Predictions using “Raw” and “Adjusted Data” for samples compressed at 4.4°C did not give advantage of one data set over another (Table 23). With the exception of MFTEND of “Raw Data” for samples at -6.6°C, samples compressed at 4.4°C had higher R-square values than those for the colder temperature. Predication equations for OVERALL ($R^2 = 0.54$) and MFTEND ($R^2 = 0.54$) both incorporated platen compression energy dissipated values for both fiber orientations (EDPLC and EDPPC). The platen compression method still lacks the ability to accurately predict CTAMT ($R^2 = 0.39$) and predict JUICY ($R^2 = 0.50$).

Of all the test temperatures, samples compressed at 10°C (Table 24) were the most effective predictors of sensory traits, with the exception of JUICY. No combination of variables met the $P< 0.15$ significance level and were not entered into the model. Neither the “Raw Data” nor “Adjusted Data” sets proved to be better. The equation with the greatest prediction potential for OVERALL ($R^2 = 0.71$), MFTEND ($R^2 = 0.73$) and CTAMT ($R^2 = 0.55$) utilized FSTFPLC and EDPPC.

Even though compression temperature did not have a significant effect on biomechanical values, equations constructed from data separated based on compression testing temperature were more effective predictors of cooked sensory tenderness (Tables 22, 23, and 24) than if the data, regardless of temperature, were pooled (Table 21). By separating the data based on compression temperature, it was observed that the greatest predictability of sensory tenderness was from 10ºC ($R^2 = 0.71$), followed by 4.4°C ($R^2 =$

0.54) and -6.6°C (R^2 = 0.48), all of which had higher R-square values than the pooled data (R^2 = 0.40).

Regression models are useful approximations for determining if an independent variable has a predictive effect on the dependent variable. It is the easiest method of interpreting if an equation is a good predictor. Choosing a model based solely on R-square values may not be practical. The variables that are included in the model may not be easily obtained or measured, therefore requiring that more than just the R-square value needs to be taken into consideration in regards to an equations prediction potential. Whether an R-square value is considered large or small can depend up on the context of the study. It is best to consider the root means squared error (RMSE) and Mallow's Cp for the equation in conjunction with the R–square value. RMSE is the statistic whose value is minimized during the parameter estimation process, and determines the width of the confidence intervals for predictions. It is measured in the same units as the data, rather than squared units, and is representative of the size of a typical error. It is important to remember that the width of the confidence intervals is proportional to the RMSE and how much of a relative decrease in the width of the confidence intervals would be noticeable on a plot. RMSE is a measure of the lack of fit while Mallow's Cp is the total square errors. There is no set criteria for an acceptable RMSE or Cp value. Thus, the higher the R-square is, the better the model is. The lower the RMSE and Cp are, the better the model is.

It is also necessary to consider the degree of increase in predictability by adding additional variables to the equation. For example, is a 3% increase in prediction worth

adding another independent variable to a regression model to decrease the RMSE and Cp? By adding additional data to collect, you open the possibility of the collector not doing a proper job of measuring and obtaining solid data.

R-square, RMSE and Cp are taken into account in Tables 21 through 24. In Tables 21 through 24, equations for JUICY and CTAMT yield the same R-square and RMSE for both "Raw Data" and "Adjusted Data". Review of the equation's Cp shows that there are advantages to using one data set over another. For all temperatures (Table 21), there is no advantage to eliminating outlying data in order to strengthen the prediction potential of an equation for JUICY. However, for CTAMT, it was observed that the prediction equation using "Adjusted Data" was a better predictor. There is little difference in predictability for MFTEND between "Raw Data" and "Adjusted Data" when evaluating the R-square value and RMSE ($R^2 = 0.38$ vs. $R^2 = 0.39$, respectively; RMSE = 0.787 vs. RMSE = 0.784, respectively). However, evaluation of the Cp shows that eliminating outlying data points does yield the better prediction equation.

Prediction equations for OVERALL showed that there was little difference in prediction potential between "Raw Data" and "Adjusted Data" (Table 21). Evaluation of the RMSE and Cp show little difference, but the R-square for "Raw Data" is greater than that for "Adjusted Data" ($R^2 = 0.47$ vs. $R^2 = 0.40$, respectively). However, one must consider the equation itself prior to determining if is good or unacceptable. For "Raw Data", the equation incorporates four variables, whereas "Adjusted Data" only utilizes two variables. From these results, there is no reason to remove replicate probe

compression values that are greater than 45% of the mean in order to improve the ability to predict sensory tenderness using biomechanical values from the probe compression.

However, when data was segregated by compression temperature, significant improvement in predictability of JUICY, CTAMT and OVERALL was obtained at -6.6°C by using "Adjusted Data" over "Raw Data" (Table 22). Although R-square values and RMSE are identical between the two data sets, the Cp shows the better prediction equation. The opposite was observed for MFTEND obtained at -6.6°C, in which there was an advantage to using "Raw Data" (Table 22), with a 28.3% increase in MFTEND prediction. Although R-square, RMSE and Cp need to be considered, "Raw Data" equations yielded higher R-square values and lower RMSEs. However, one must consider the equation itself prior to determining if is good or unacceptable. Before accepting or rejecting the null hypothesis that removing replicate probe compression values in order to improve the ability to predict sensory tenderness using biomechanical values from the probe compression, the number of variables utilized in the equation need to be considered when evaluating these two data sets. Is it worth adding two additional variables to improve predictability? For "Raw Data", the equation incorporates three variables, whereas "Adjusted Data" only utilizes one variable. Based on these results, there is no reason to remove replicate probe compression values that are greater than 45% of the mean in order to improve the ability to predict sensory tenderness using biomechanical values from the probe compression.

At 4.4°C (Table 23), R-square and RMSE are the same for all sensory traits between "Raw Data" and "Adjusted Data". Therefore, one must look to Cp in order to identify the better prediction equation. For JUICY and CTAMT, the lower Cp values for "Adjusted Data" indicate that removing eliminating outlying data values does improve prediction potential. For MFTEND and OVERALL, "Raw Data" yields lower Cp values, indicating that better prediction of these sensory traits can be obtained by no removing outlying data. At this temperature, the intracellular fluid in the sample is in a liquid state versus a solid state at -6.6°C. This may the cause of the variation in predictability between temperatures and between data sets. It is also noteworthy that muscle tissue in practice will not be tested at -6.6°C, but would be tested at approximately 4.4°C. Based on the statistical parameters in Table 23, one could not state that removing outlying data values would yield better prediction equations for all sensory traits.

At 10°C (Table 24), R-square and RMSE are the same for all sensory traits between "Raw Data" and "Adjusted Data". Therefore, one must look to Cp in order to identify the better prediction equation. For CTAMT, the lower Cp value for "Adjusted Data" indicated that removing eliminating outlying data values does improve prediction potential. However, for MFTEND and OVERALL, "Raw Data" yields lower Cp values, indicating that a better prediction of these sensory traits can be obtained by not removing outlying data. At this temperature, the intracellular fluid in the sample is in a liquid state versus a solid state at -6.6°C. This may be the cause of the variation in predictability

between temperatures and between data sets. Unlike 4.4°C, carcasses will not be held at 10°C due to spoilage and safety concerns. Based on this information, regardless of the improvement in predictability of 10°C over 4.4°C, utilizing prediction equations for MFTEND and OVERALL at 10°C are not feasible.

Predicting overall sensory tenderness from biomechanical measurements of raw *Longissimus dorsi* muscle was the critical variable that was trying to be predicted was the primary objective of this study. When data were segregated by compression temperature, there was significant improvement in OVERALL (tenderness) prediction as sample temperature increased (Tables 22, 23 and 24). As compression temperature decreased from 10°C to 4.4° to –6.6°C, so did predictability for overall tenderness (R^2 = 0.71, R^2 = 0.54 and R^2 = 0.48, respectively). There was only a 5.9% increase in predictability with 4.4°C over -6.6°C, but a 27.1% increase with 10°C over 4.4°C.

The differences in prediction potential may be due to the influence of water and the "fluidity" of the muscle tissue on biomechanical properties. At -6.6°C, the water in the sample is beginning to crystallize and transition from a liquid to a solid whereas at 4.4 and 10°C, the intracellular fluid in the sample is in a liquid state and the associated muscle tissues are softer. The energy dissipated represents the amount of energy that is exerted against the compression plate or probe by the sample under constant compression (strain). Fluids dissipate 100% energy, therefore at refrigerated temperatures above the freezing point of water, energy dissipated would be incorporated into the prediction equation. It is also noteworthy that in practice, muscle tissue in the

carcass would not be tested at -6.6°C nor 10°C, but would be tested at approximately 4.4°C. Based on this information, regardless of the improvement in predictability of OVERALL, using 10°C or –6.6°C over 4.4°C is not feasible.

Tables 21 through 24 indicate that there is no advantage to using "Raw Data" over "Adjusted Data" to predict OVERALL. With all temperatures pooled, there is little difference in predictability for OVERALL. However, at –6.6 and 10°C, there is stronger prediction equations derived using "Adjusted Data". At 4.4°C, better prediction is found with "Raw Data". Thus, one would reject the hypothesis that removing outlying probe compression values will produce better prediction potential and it could be concluded that use of "Raw Data" at 4.4°C was a better predictor of tenderness.

One of the objectives of this study was to further evaluate other compressive methods as a potential tenderness assessment tool that can accurately, rapidly and non-destructively predict the tenderness of a beef sample. To achieve this, multiple measurements with a 2 mm diameter probe compression technique was used to predict sensory tenderness. Tables 25 through 28 give various sensory trait prediction equations using only probe compression values. The STEPWISE option of SAS was not utilized to develop these equations, but rather the equations were forced and developed using all three variables derived from four 0.25 s probe compressions (ISTFPR, FSTFPR, EDPR) per loin.

Prediction equations for sensory traits utilizing TA probe compression values for all data over all compression temperatures are outlined in Table 25. As expected, the

highest R-square values for each sensory trait were observed in those equations that incorporated all three probe measurements. However, for the "Adjusted Data" set, there were alternate equations, not listed in the table, which only utilized two variables but had a high R-square value. Although the R-square values was high, the RMSE and Cp values were not lower than the equation that utilized three variables. Equations using ISTFPR and FSTPR for MFTEND, OVERALL and CTAMT yielded R-square values of 0.13, 0.14, and 0.08, respectively, as compared to the three variable equations (R^2 = 0.13, 0.14, and 0.09, respectively). RMSE and Cp values did not differ much, if at all, between the two data sets. Thus, it could be concluded that eliminating outlying data does not produce better prediction equations based on R-square, RSME and Cp values.

To better evaluate the effect of temperature, the data were segregated based on compression temperature and the regression equations developed. Table 26 outlines those prediction equations for samples compressed at –6.6°C. By separating data based on temperature treatment, R-square values were improved over pooled temperatures (Table 25). The highest R-square values were derived from equations using ISTFPR, FSTFPR and EDPR. Greater prediction potential was observed for sensory traits using "Raw Data" at this temperature, with a slightly higher predictability of OVERALL for "Raw Data" (R^2 = 0.33) versus "Adjusted Data" (R^2 = 0.29). Although not listed in the table, within the "Adjusted Data" set, a simpler equation for JUICY was possible, using only ISTFPR and EDPR and yields the same R-square value (R^2 = 0.12) as the three variable equation. RMSE and Cp values did not differ much between the two data sets, however, higher R-square values and lower RMSE and Cp values were obtained using

"Raw Data". Therefore, it can be concluded that eliminating outlying data does not produce better prediction equations.

A tremendous improvement in predictability of sensory traits can be observed in Table 27 for those samples compressed at 4.4°C, particularly with the "Adjusted Data" vs. the "Raw Data". Equations using "Adjusted Data" had higher R-square values and lower RMSE and Cp values for all sensory traits. For MFTEND prediction, the "Adjusted Data" accounted for 21% more of the variation ($R^2 = 0.73$) in the samples than did the "Raw Data" ($R^2 = 0.51$). Also, within the "Adjusted Data" set, probe compression values could accurately predict OVERALL (tenderness) 70.73% of the time whereas the "Raw Data" set prediction was only 52.28% of the time. Better predictability was also observed with "Adjusted Data" for JUICY ($R^2 = 0.30$) and CTAMT ($R^2 = 0.55$). Thus, at 4.4°C, eliminating outlying data produced more accurate prediction equations and this sample temperature was more conducive to predictability.

Improved predictability at 10°C with "Adjusted Data" over the "Raw Data" was observed in Table 28, but the advantage of one over the other is slight. At 10°C, improvements in R-square value of the "Adjusted Data" over the "Raw Data" were not as large as they were with the 4.4°C "Adjusted Data". R-square values of "Adjusted Data" for MFTEND ($R^2 = 0.67$) and OVERALL ($R^2 = 0.70$) at 10°C were slightly lower than the "Adjusted Data" for the same variables ($R^2 = 0.73$ and 0.71, respectively) at 4.4°C. However, for "Raw Data", MFTEND ($R^2 = 0.67$) and OVERALL ($R^2 = 0.70$) at 10°C had higher predictability than the same variables at 4.4 °C ($R^2 = 0.51$ and 0.53,

respectively). It can be concluded that from Tables 26 through 28, that there is an advantage to eliminating outlying data and compressing at refrigerated temperatures, particularly 4.4°C, which produced equations with the greatest predictability for sensory tenderness.

The differences in prediction potential may be due to the influence of water on biomechanical properties as well as fluidity of intramuscular fat. At -6.6°C, the water in the sample is beginning to crystallize and transition from a liquid to a solid whereas at 4.4 and 10°C, the intracellular fluid in the sample is in a liquid state. Also, at 4.4 and 10°C, muscle tissue and intramuscular fat becomes warm and softens, where as at -6.6°C, fat is in a firm, solid state. Intramuscular fat that is more fluid, or less viscous, would have an impact on compressive measurements. Industry regulations do not allow muscle tissue to reach 10°C prior to or during fabrication, which is at the processing step where this objective measurement could be implemented. The higher R-square value, lower RMSE, lower Cp and temperature of "Adjusted Data" for 4.4°C samples (Table 27) yielded the best prediction equation for OVERALL in an on-line process (OVERALL = 15.60995 + 0.14377 ISTFPR + -0.20226 FSTFPR + -427.06157 EDPR). Based on this conclusion, one would accept the hypothesis that removing outlying probe compression values produce better prediction equations for OVERALL sensory tenderness,

Although probe compression temperature did not have a significant effect on biomechanical values, equations constructed from probe data separated based on sample

temperature were more effective predictors of cooked sensory tenderness (Tables 26, 27 and 28). By separating the data based on compression temperature, predictability for sensory tenderness was greatest at 4.4ºC (R^2 = 0.71), followed by 10°C (R^2 = 0.70) and -6.6°C (R^2 = 0.29), all of which had higher R-square values than the pooled temperature prediction for tenderness (R^2 = 0.14).

Comparison of probe compression prediction equations (Tables 25 through 28) to equations incorporating platen and probe compression equations (Tables 21 through 24) for OVERALL tenderness showed that better predictability was derived from platen compression or combined platen and probe compression values for "Raw Data" for data obtained at all temperatures, -6.6 and 4.4°C (Tables 21 through 24) than for "Raw Data" obtained from probe compression values for all temperatures, -6.6 and 4.4°C (Tables 25 through 28). However, "Raw Data" from probe compression values produced higher predictability for OVERALL at 10°C (Table 28) than "Raw Data" using platen compression values (Table 24). For "Adjusted Data", better predictability was observed using platen or combined platen and probe compression for all temperatures and –6.6°C (Tables 21 and 22) when compared to "Adjusted Data" using probe compression at all temperatures and -6.6°C (Tables 25 and 26). As temperature increased to 4.4 and 10°C, probe compression values were better predictors of OVERALL (Tables 27 and 28) than platen compression (Tables 23 and 24). The greatest prediction equation for OVERALL tenderness was derived using only probe compression values from "Adjusted Data" at 4.4°C (R^2 = 0.71, RMSE = 0.47, Cp = 4.0). Therefore, it cannot be concluded that probe

compression values are better predictors of sensory tenderness than platen compression regardless of sample temperatures, but probe compression values are better predictors of tenderness at 4.4 and 10°C than at -6.6°C when compared to platen compression.

To better evaluate the advantage of the probe compression, it should be compared to current tenderness assessment techniques. Warner –Bratzler shear force values were obtained using the standard WBSF protocol and regressed against sensory evaluation traits and R-square values were derived (Table 29). WBSF values were not obtained on samples treated to tempered to one of three temperature treatments (-6.6, 4.4 or 10°C). Therefore, equations derived for OVERALL tenderness using probe compression values should be compared to prediction equations using WBSF for data obtained at all temperatures rather than samples segregated by temperature treatment. WBSF for those loins assigned to a specific temperature were used to generate WBSF R-square values for comparison to those same loins whose temperature was adjusted to -6.6, 4.4 or 10°C and measured by probe compression. However, since the temperature adjusted loins were "treated" differently for the probe measurements but not for the WBSF, the R-square value only applies to that subset of loins (Table 29). Overall, the greatest prediction equations for OVERALL came from probe compression "Adjusted Data" at 4.4° and 10°C (R^2 = 0.71 and 0.70, respectively), accounting for more of the variation in the sample than did WBSF (R^2 = 0.55) at all temperatures or the subset of loins for 4.4°C (R^2 = 0.45) or 10°C (R^2 = 0.65). All probe compression data at 4.4° and 10°C (both raw and adjusted) were better predictors of sensory traits than was WBSF, with the exception

of CTAMT using “Raw Data”. However, when samples were not segregated by compression temperature treatment, WBSF was a better predictor of sensory traits, except for JUICY, than TA probe compression values (Table 29).

Spadaro (1996) and Spadaro and others (2002) compressed cubed beef loin samples and found that the biomechanical parameters of stiffness and total energy dissipated in the parallel and perpendicular fiber orientations could be used to effectively predict overall sensory tenderness better than WBSF. In their studies, overall sensory tenderness was highly correlated to final stiffness and energy dissipated in the parallel fiber orientation ($r = 0.86$ and $r = -0.91$). This compressive model of using energy dissipated in the parallel fiber orientation exceeded the WBSF correlation to overall sensory tenderness by 53%. Spadaro and others (2002) constructed a model that would predict overall tenderness of beef loin steaks using energy dissipated in a parallel fiber orientation or final stiffness in a parallel fiber orientation. Both correlated highly to overall sensory tenderness ($r = -0.95$ and $r = 0.95$, respectively). Warner-Bratzler shear force values on the same set of samples were correlated to overall sensory panel tenderness, but yielded a much lower correlation ($r = 0.55$) value. The obvious advantage to this compressive technique was that overall tenderness could be predicted on raw samples, thus eliminating the need for cooking, and subsequent sensory panel testing.

Marburger (1999) tested the compressive technique and mathematical models developed by Spadaro and others (2002) to predict muscle tenderness of raw *Longissimus dorsi* samples that varied in tenderness and degree of aging. The energy

dissipated-parallel (EDPL) and initial stiffness-perpendicular (ISTFPP) to the muscle fibers (r = -0.86 and r = 0.85, respectively) were effective predictors of sensory tenderness in raw samples, whereas the Warner-Bratzler shear force (WBSF) of cooked samples was less effective (than biomechanical parameters) for predicting tenderness (r = -0.79). Less energy was dissipated on steaks that had a high overall tenderness scores and parallel fiber orientation readings correlated higher (r =-0.86) with overall sensory tenderness scores than did the perpendicular fiber orientation (r = -0.80). Energy dissipated from samples (2.54 cm^3) with the strain applied parallel to the fiber orientation accounted for 73.3% of the variation in tenderness and was a more accurate assessment of tenderness than WBSF (61.9%). Regardless of degree of aging, each biomechanical property measurement accounted for more variation in the sample than did WBSF, and did so more effectively. Marburger (1996) confirmed that the application of an objective, biomechanical strain to raw muscle specimens could effectively predict overall sensory tenderness of cooked steaks more effectively than WBSF.

In this study, the compressive platen technique was compared to a new non-destructive probe compression technique. Higher predictions for overall sensory tenderness (R^2 = 0.71 for 4.4°C and R^2 = 0.70 for 10°C) were achieved using a probe compression method than the traditional WBSF (R^2 = 0.55 for all temperatures, R^2 = 0.45 for 4.4°C subset and R^2 = 0.65 for 10°C subset).

The greatest prediction potential for overall sensory tenderness (R^2 = 0.71) was observed using the probe compression technique at 4.4°C (OVERALL = 15.60995 +

0.14377 ISTFPR + -0.20226 FSTFPR + -427.06157 EDPR). This exceeded the predictability of WBSF (R^2 = 0.55 for all temperatures) for the same sample set by 15%. R-square values (Tables 27, 28) for equations using ISTFPR, FSTFPR and EDPR were higher for samples compressed at 4.4° and 10°C (R^2 = 0.71 and R^2 = 0.70, respectively) than equations using the same TA variables and compressing at -6.6ºC (R^2 = 0.29). These results indicate that compression at refrigerated temperatures (4.4º and 10ºC) were necessary to effect better predictability of overall tenderness than at freezing temperatures (-6.6ºC).

Due to the small number of loin samples available to perform this study, a validation study of the results is not feasible. Ideally, a validation study would include two-thirds of the data undergoing regression analysis. The remaining one-third of the samples will be used to test the regression analysis. In this study, the most samples available for a two-thirds regression analysis was 27. These numbers were insufficient to perform the validation study. It is suggested that a larger study be performed in the future with ample number of samples to validate the prediction equations.

In summary, based on the lack of significant correlations between platen and probe compression values, one would reject the null hypothesis that platen compression values can be predicted from probe compression values. In addition, it cannot be concluded that probe compression values are consistently better predictors of sensory tenderness than platen compression regardless of sample temperatures, but probe compression values are better predictors of tenderness at 4.4 and 10°C than at -6.6°C when compared to platen compression. Therefore, one would accept the null hypothesis

that probe compression values are as predictive of sensory tenderness as platen compression values. This is due to high R-square values, low RMSE and Cp values, non-destructive nature of the technique, and the muscle temperature that produced the greatest predictability with probe compression is consistent with carcass temperature in industry. Finally, evidence showed that there is no consistent improvement in predictability with removal of replicate probe compression values that are greater than 45% of the mean in order to improve the ability to predict sensory tenderness using biomechanical values from the probe compression regardless of sample temperature. However, removing replicate probe compression values that are greater than 45% of the mean for samples compressed at 4.4 and 10°C produced greater prediction equations for tenderness. Again, these temperatures are more consistent with carcass temperature in industry. Therefore, one would accept the null hypothesis that removing replicate probe compression values that are greater than 45% of the mean does improve the ability to predict sensory tenderness using biomechanical values from the probe compression.

Based on observations in this study, a non-destructive TA compression of raw beef loin steaks using a 2 mm diameter probe (0.635 cm) at refrigerated temperatures (4.4º or 10ºC) was a better predictor of overall sensory tenderness than WBSF, with fifteen percent more of the variation in tenderness was explained than with WBSF values. Probe compression values were better predictors of OVERALL tenderness than equations using TA platen compressions performed at 4.4°C and 10°C. This study confirmed observations of Spadaro (1996) and Marburger (1999) that compressive measurements were more effective predictors of cooked sensory tenderness than WBSF

values and those equations of Spadaro (1996) could be adapted to produce a non-destructive objective tenderness assessment tool.

CONCLUSIONS

The overall goal of this study was to develop a more rapid, accurate and non-destructive objective instrumental method for measuring the tenderness of raw beef loins by modifying the compressive technique developed by Spadaro (1996) and Spadaro and others (2002) and to verify this new technique. The study also evaluated the effect of loin temperature and fiber orientation during compression on predictability of overall tenderness.

The objective of Phase 1 in this study was to determine if sample temperature and fiber orientation during compression had an effect on biomechanical compressive measurements and if these biomechanical compressive measurements could potentially predict overall sensory tenderness. This platen compression method was also compared to values derived from the Warner-Bratzler shear device.

The significance of this phase of the study is that it validates the use of biomechanical strain measurements to effectively predict overall sensory tenderness of cooked steaks from raw steaks. This may be of significant importance to the beef industry since the results validate that biomechanical values obtained at any temperature between 0 and 6°C are better predictors of sensory traits than at 8 or 10°C. Since processing facilities maintain an environment temperature of 0 to 6°C, this compressive technique allows for online tenderness assessment without temperature adjustment or special facilities for testing.

Fiber orientation did have a significant effect on biomechanical values. Fibers orientated in a parallel (PL) direction had lower stiffness (ISTF, FSTF) values and greater ED ($P<0.05$) than perpendicular (PP) fiber values. By identifying which fiber orientation produced the highest R-square value alleviates multiple cubed sample excision. Based on these results, one 2.54 cm^3 cube of raw *Longissimus dorsi* sample needs to be removed for compression and either parallel or perpendicular fiber orientation compression is satisfactory. Results showed that compressing parallel to the fiber orientation at 0 to 4°C yielded overall tenderness prediction equations with R-square values ranging from 0.65 to 0.74. Compression in the perpendicular fiber orientation at 2 to 4°C yielded overall tenderness prediction equations with R-square values ranging from 0.70 to 0.77.

Prediction equations derived from regression analysis were computed for all compression variables and regression formulas. It was concluded that the most effective predictor of overall cooked beef tenderness derived from a raw sample using a platen to compress excised cubed samples comes from perpendicularly oriented fibers at 2°C (R^2 = 0.77, RMSE = 0.44) using a platen, followed by PL samples at 0°C (R^2 = 0.74, RMSE = 0.46).

All compression values, especially 2ºC PP (R^2 = 0.77), had higher predictability of overall sensory tenderness than did WBSF (R^2 = 0.11), indicating the predictive effectiveness of these values over that of WBSF. This indicates that the TA generated biomechanical values could alleviate researchers of utilizing the time consuming technique of WBSF and provide for better overall sensory tenderness prediction. It also

validates use of sample temperatures less than 6°C, which can be beneficial to the meat industry. Because excision of a small amount of loin muscle, orienting the muscle fibers and compressing for 240 sec are not compatible with the speed required for assessment under processing plant conditions, a modification of the biomechanical measuring technique is required if it is suitable for a rapid, non-destructive test that could be adapted to an in-line grading system.

The objective of Phase 2 in this study was to determine if the biomechanical measuring technique developed by Spadaro (1996) could be modified and if this modified technique could effectively predict overall sensory tenderness of cooked steaks by assessing biomechanical values by probe compression of raw, intact steaks at different refrigerated sample temperatures.

Raw beef loin steaks (2.54 cm thick) were compressed 0.635 cm using a 2 mm diameter probe at –6.6°C, 4.4°C and 10°C. Although probe compression temperature did not have a significant effect on biomechanical values, equations constructed from probe data separated based on sample temperature were more effective predictors of cooked sensory than data from all temperatures pooled. By separating these data based on compression temperature, predictability for sensory tenderness was greatest at 4.4ºC (R^2 = 0.71), followed by 10°C (R^2 = 0.70) and -6.6°C (R^2 = 0.29), all of which had higher R-square values than the pooled temperature prediction for tenderness (R^2 = 0.14). It is also noteworthy that in practice, muscle tissue in the carcass would not be tested at -6.6°C nor 10°C, but would be tested at approximately 4.4°C. Based on this

information, regardless of the improvement in predictability of OVERALL, using 10°C or –6.6°C over 4.4°C is not practical.

This study also addressed if removing outlying probe compression values that are greater than 45% of the mean improved the predictability of overall sensory tenderness using probe compression values. Prediction equations utilizing TA probe compression values for all data at all compression temperatures showed that eliminating outlying data does not produce better prediction equations. When data were separated based on temperature at compression, at –6.6°C, eliminating outlying data does not produce better prediction equations, but at 4.4 and 10°C, there is an advantage to eliminating outlying data, particularly 4.4°C , which produced equations with the greatest predictability (R^2 = 0.71, RMSE = 0.47, Cp = 4.0). Based on this, one would accept that removing outlying probe compression values would produce better prediction equations for overall sensory tenderness at approximately 4.4°C.

To better evaluate the advantage of the probe compression, it was compared to Warner –Bratzler shear force. The greatest prediction equations for overall sensory tenderness came from probe compression values, with outlying data values removed, at 4.4° and 10°C (R^2 = 0.71 and 0.70, respectively), accounting for more of the variation in the sample than did WBSF (R^2 = 0.55) at all temperatures or the subset of loins for 4.4°C (R^2 = 0.45) or 10°C (R^2 = 0.65). However, when samples were not segregated by compression temperature treatment, WBSF was a better predictor of sensory traits, except for juiciness, than TA probe compression values.

The significance of this study was that it validated the use of biomechanical probe measurements to more rapidly and effectively predict overall sensory tenderness of raw steaks without sample destruction. Based on observations in this study, a non-destructive TA probe compression of raw beef loin steaks using a 2 mm diameter probe compressed 0.635 cm at refrigerated temperatures (4.4º or 10ºC) was a better predictor of overall sensory tenderness than WBSF. Fifteen percent more of the variation in tenderness was explained than with WBSF values. This innovative technique could guarantee tenderness to consumers, be integrated into on-line grading systems and be utilized as a powerful research tool.

REFERENCES

AMSA. 1995. Research Guidelines for Cookery, Sensory Evaluation and Instrumental Tenderness Measurements of Fresh Meat. American Meat Science Association, National Live Stock and Meat Board, Chicago, IL.

AOAC. 1995. Official Methods of Analysis. 16th edition. AOAC International, Arlington, VA.

Basset O, Buquet B, Abouelkaram S, Delachartre P, Culioli J. 2000. Application of texture image analysis for the classification of bovine meat. Food Chem. 69(4):437-445.

Batcher OM, Dawson EH, Gilpin GL, Eisen JN. 1962. Quality and physical composition of various cuts of raw and cooked pork. Food Tech. 16(4):104-109.

Beattie RJ, Bell SF, Farmer LJ, Moss BW, Patterson D. 2004. Preliminary investigation of the application of Raman spectroscopy to the prediction of the sensory quality of beef silverside. Meat Sci. 66(4):903-913.

Beilken SL, Eadie LM, Griffiths I, Jones PN, Harris PV. 1991. Assessment of the textural quality of meat patties: correlation of instrumental and sensory attributes. J. Food Sci. 56(6):1465-1469, 1475.

Berry BW. 1983. Measurement of meat texture. American Meat Science Association. Reciprocal Meat Conference Proceedings. 36:103-107.

Bett KL. 1993. Measuring sensory properties of meat in the laboratory. Food Tech. 47(11):121-126, 134.

Bouton PE, Harris PV, Shorthose WR. 1971. Effect of ultimate pH upon the water-holding capacity and tenderness of mutton. J. Food Sci. 36(3):435-441.

Bouton PE, Harris PV. 1972a. A comparison of some objective methods used to assess meat tenderness. J. Food Sci. 37(2):218-222.

Bouton PE, Harris PV. 1972b. The effects of some post-slaughter treatments on mechanical properties of bovine and ovine muscle. J. Food Sci. 37(4):539-543.

Bouton PE, Harris PV. 1972c. The effects of cooking temperature and time on some mechanical properties of meat. J. Food Sci. 37(1):140-144.

Bouton PE, Harris PV, Shorthose WR. 1975. Changes in shear parameters of meat associated with structural changes produced by aging, cooking and myofibrilar contraction. J. Food Sci. 40(6):1122-1126.

Brandt MA, Skinner EZ, Coleman JA. 1963. Texture profile method. J. Food Sci. 28(4):404-409.

Bratzler LJ. 1932. Measuring the tenderness of meat by means of a mechanical shear. [M.S. thesis], Kansas State College, Manhattan, KS.

Byrne CE, Downey G, Troy DJ, Buckley DJ. 1998. non-destructive prediction of selected quality attributes of beef by near-infrared reflectance spectroscopy between 750 and 1098 nm. Meat Sci. 49(4):399-409.

Caine WR, Aalhus JL, Best DR, Dugan MER, Jeremiah LE. 2003. Relationship of texture profile analysis and Warner-Bratzler shear force with sensory characteristics of beef rib steaks. Meat Sci. 64(4):333-339.

Campion DR, Crouse JD, Dikeman ME. 1975. Predictive value of USDA quality grade factors for cooked meat palatability. J. Food Sci. 40(6):1225-1228.

Cardello AV, Segars RA. 1989. Effects of sample size and prior mastication on texture judgments. J. Sensory Stud. 4(1):1-18.

Carpenter ZL. 1974. Beef quality grade standards-need for modifications? American Meat Science Association. Reciprocal Meat Conference Proceedings. 27:122-142.

Carpenter ZL, Smith GC, Butler OD. 1972. Assessment of beef tenderness with the Armour Tenderometer. J. Food Sci. 37(1):126-129.

Cover S, Ritchey SJ, Hostetler RL. 1962. Tenderness of beef. I. The connective tissue component of tenderness. J. Food Sci. 27(5):469-473.

Cross HR, Carpenter ZL, Smith GC. 1973. Effects of intramuscular collagen and elastin on bovine muscle tenderness. J. Food Sci. 38(6):998-1003.

Cross HR, Belk KE. 1994. Objective measurements of carcass and meat quality. Meat Sci. 36(1, 2):191-202.

Culler RD, Parrish FC Jr., Smith GC, Cross HR. 1978. Relationship of myofibril fragmentation index to certain chemical, physical and sensory characteristics of bovine longissimus muscle. J. Food Sci. 43(4):1177-1180.

Davey CL, Gilbert KV. 1969. Studies in meat tenderness. 7. Changes in the fine structure of meat during aging. J. Food Sci. 34(1):69-74.

Davis GW, Smith GC, Carpenter ZL, Dutson TR, Cross HR. 1979. Tenderness variations among beef steaks from carcasses of the same USDA quality grade. J. Anim. Sci. 49(1):103-114.

Deatherage FE, Gernatz G. 1952. A comparative study of tenderness determination by sensory panel and by shear strength measurements. Food Tech. 6 (7):260-265.

Dikeman ME. 1996. The relationship of animal leanness to meat tenderness. American Meat Science Association. Reciprocal Meat Conference Proceedings. 49:87-101.

Dikeman ME, Tuma HJ, Glimp HA, Gregory KE, Allen DM. 1972. Evaluation of the tenderometer for predicting bovine muscle tenderness. J. Anim Sci. 34(6):960-962.

Dikeman ME, Crouse JD. 1975. Chemical composition of carcasses from Hereford, Limousin and Simmental crossbred cattle as related to growth and meat palatability. J. Anim. Sci. 40(3):463-467.

Dolezal HG, Smith GC, Savell JW, Carpenter ZL. 1982. Comparison of subcutaneous fat thickness, marbling and quality grade for predicting palatability of beef. J. Food Sci. 47(2):397-401.

Field RA, Pearson AM, Schweigert BS. 1970. Labile collagen from epimysial and intramuscular connective tissue as related to Warner-Bratzler shear values. Agric. Food Chem. 18(2):280-283.

Fielder MM, Mullins AM, Skellenger MM, Whitehead R, Moschette DS. 1963. Subjective and objective evaluations of fabricated cuts of beef. Food Tech. 17(4):95-100.

George MH, Tatum JD, Dolezal HG, Morgan JB, Wise JW, Calkins CR, Gordon T, Reagan JO, Smith GC. 1997. Comparison of USDA quality grade with Tendertec for the assessment of beef palatability. J. Anim. Sci. 75(6):1538-1546.

Harris JJ, Miller RK, Savell JW, Cross HR, Ringer LJ. 1992. Evaluation of the tenderness of beef top sirloin steaks. J. Food Sci. 57(1):6-9, 15.

Harris PV, Shorthose WR. 1988. Meat texture. In Developments in Meat Science, R.A. Lawrie (Ed.), p 245-296. Elsevier Applied Science Publishers, New York, NY.

Herring HK, Cassens RG, Briskey EJ. 1965. Further studies on bovine muscle tenderness as influenced by carcass position sarcomere length, and fiber diameter. J. Food Sci. 30(6):1049-1054.

Hill F. 1966. The solubility of intramuscular collagen in meat animals of various ages. J. Food Sci. 31(2):161-166.

Hinnergardt LC, Tuomy JM. 1970. A penetrometer test to measure meat tenderness. J. Food Sci. 35(3):312-315.

Huang Y, Lacey RE, Moore LL, Miller RK, Whittaker AD, Ophir J. 1997. Wavelet textural features from ultrasonic elastograms for meat quality prediction. Transactions of the ASAE. 40(6):1741-1748.

Huffman DL. 1974. An evaluation of the tenderometer for measuring beef tenderness. J. Anim. Sci. 38(2):287-294

Jack FR, Paterson A, Piggott JR. 1995. Perceived texture: direct and indirect methods for use in product development. Int. J. Food Sci. Tech. 30(1):1-12.

Jennings TB, Berry BW, Joseph AL. 1978. Influence of fat thickness, marbling and length of aging on beef palatability and shelf-life characteristics. J. Anim. Sci. 46(3):658-665.

Jeremiah LE, Phillips DM. 2000. Evaluation of a probe for predicting beef tenderness. Meat Sci. 55(4):493-502.

Kapsalis JG, Moskowitz HR. 1977. The psychophysics and physics of food texture. Food Tech. 31(4):91-99.

Kingston OL. 1989. Consumer preferences for loin and topside steaks from beef carcasses of different classification criteria. Rev Mark Agric Econ. 57(1/3):118-128.

Kolar K. 1990. Colorimetric determination of hydroxyproline as a measure of collagen content in meat products. NMKL collaborative study. Assoc. Off. Anal. Chem. 73(1):54-57.

Koohmaraie M, Seideman SC, Schollmeyer JE, Dutson TR, Babiker AS. 1988. Factors associated with the tenderness of three bovine muscles. J. Food Sci. 53(2):407-410.

Koohmaraie M, Wheeler TL, Shackelford SD. 1995. Beef tenderness: regulation and prediction. CSIRO Meat Industry Research Conference. 4A:1-25.

Lepetit J, Culioli J. 1992. Mechanical properties of meat. Proceedings of International Congress of Meat Science and Technology, Clermont, France. 38:135-151.

Lewis GJ, Purslow PP. 1990. Connective tissue differences in the strength of cooked meat across the muscle fiber direction due to test specimen size. Meat Sci. 28(3):183-194.

Li J, Tan J, Martz FA, Heymann H. 1999. Image texture features as indicators of beef tenderness. Meat Sci. 53(1):17-22.

Li J, Tan J, Shatadal P. 2001. Classification of tough and tender beef by image texture analysis. Meat Sci. 57(4):341-346.

Liu Y, Lyon BG, Windham WR, Realini CA, Pringle TDD, Duckett S. 2003. Prediction of color, texture and sensory characteristics of beef steaks by visible and near infrared reflectance spectroscopy. A feasibility study. Meat Sci. 65(3):1107-1115.

Locker RH, Hagyard CJ. 1963. A cold shortening effect in beef muscles. J. Food Agric. 14(11):787-781.

Lozano MSR. 1995. Ultrasonic elastography to evaluate beef and pork quality. [Ph.D. dissertation], Texas A&M University, College Station.

Luchak GL, Miller RK, Belk KE, Hale DS, Michaelsen SA, Johnson DD, West RL, Leak RW, Cross HR, Savell JW. 1998. Determination of sensory, chemical and cooking characteristics of retail beef cuts differing in intramuscular and external fat. Meat Sci. 50(1):55-72.

Marburger RM. 1999. Biomechanical characterization of meat tenderness. [M.S. thesis], Texas A&M University, College Station.

Marsh BB, Leet NG. 1966. Studies in meat tenderness. 3. The effects of cold shortening on tenderness. J. Food Sci. 31(3):450-454.

McBee JL Jr., Wiles JA. 1967. Influence of marbling and carcass grade on the physical and chemical characteristics of beef. J. Anim. Sci. 26(4):701-704.

Meilgaard M, Ceville GV, Carr BT. 1991. Sensory Evaluation Techniques. CRC Press, Inc., Boca Raton, FL.

Miller JA, Topel DG, Rust RE. 1976. USDA beef grading: a failure in consumer information? J. of Marketing. 40(1):25-31.

Moller AJ. 1981. Analysis of Warner-Bratzler shear pattern with regard to myofibrillar and connective tissue components of tenderness. Meat Sci. 5(4):247-260.

Morgan JB, Savell JW, Hale DS, Miller RK, Griffin DB, Cross HR, Shackelford SD. 1991. National beef tenderness survey. J. Anim. Sci. 69(8):3274-3283.

Murray AC, Jeremiah LE, Martin AH. 1983. Muscle fiber orientation and its effect on measurements of tenderness of bovine longissimus dorsi muscle. Food Tech. 18(5):607-617.

Olson DG, Parrish FC Jr., Stromer MH. 1976. Myofibril fragmentation and shear resistance of three bovine muscles during postmortem storage. J. Food Sci. 41(5):1036-1041.

Palmer AZ, Carpenter JW, Alsmeyer RL, Chapman HL, Kirk WG. 1958. Simple correlations between carcass grade, marbling, ether extract of loin eye and beef tenderness. J. Anim. Sci. 17(4):1153.

Park B, Whittaker AD, Miller RK, Hale DS. 1994. Ultrasonic spectral analysis for beef attributes. J. Food Sci. 59(4):697-701, 724.

Park B, Chen YR, Hruschka WR, Shackelford SD, Koohmaraie M. 1998. Near-infrared reflectance analysis for predicting beef longissimus tenderness. J. Anim. Sci. 76(8):2115-2120.

Parrish FC Jr. 1974. Relationship of marbling to meat tenderness. Proc. Meat Ind. Res. Conf. Am. Meat Inst., Arlington, VA. P 117-131.

Parrish FC Jr., Olson DG, Miner BE, Rust RE. 1973. Effect of degree of marbling and internal temperature of doneness on beef rib steaks. J. Anim. Sci. 37(2):430-434.

Parrish FC Jr., Vandell CJ, Culler RD. 1973. Effect of maturity and marbling on the myofibril fragmentation index of bovine longissimus muscle. J. Food Sci. 44(6):1668-1971.

Pearson AM. 1963. Objective and subjective measurements for meat tenderness. Proceedings Meat Tenderness Symposium. Campbell's Soup Co., Camden, NJ. 1:135-158.

Perry D, Thompson JM, Hwang IH, Butchers A, Egan AF. 2001. Relationship between objective measurements and taste panel assessment of beef quality. Australian J. of Experimental Agriculture. 41(7):981-989.

Pool MF, Klose AA. 1969. The relation of force to sample dimensions in objective measurement of tenderness of poultry meat. J. Food Sci. 34(6):524-527.

Purchas RW. 1973. Some aspects of raw meat tenderness. J. Food Sci. 38(4):556-559.

Reagan JO, Buyck MJ. 1995. Beef customer satisfaction. The National Livestock and Meat Board with Texas A&M University, Colorado State University and Yankelovich Partners, Inc. pp:2-21.

Rhodes DN, Jones RCD, Chrystall BB, Harries JM. 1972. Meat texture. J. Texture Stud. 3(3):298-309.

Rodbotten R, Nilsen BN, Hildrum KI. 2000. Prediction of beef quality attributes from early post-mortem near infrared reflectance spectra. Food Chemistry. 69(4):427-436.

SAS (Statistical Analysis System). 1985. v8.1. SAS Institute, Cary, NC.

Savell JW, Cross HR. 1988. The role of fat in the palatability of beef, pork, and lamb . In: Designing Foods; Animal Product Options in the Market Place. Washington, D.C.: National Academy Press. p 345-355.

Savell JW, Cross HR, Francis JJ, Wise JW, Hale DS, Wilkes DL, Smith GC. 1989. National consumer retail beef study: Interaction of trim level price ad grade on consumer acceptance of beef steaks and roasts. J. Food Quality. 12(4):251-274.

Segars RA, Nordstrom HA, Kapsalis JG. 1974. Textural characteristics of beef muscles. J. Texture Stud. 5(3):283-297.

Shackelford SD, Morgan JB, Cross HR, Savell JW. 1991a. Identification of threshold levels for Warner-Bratzler shear force in beef top loin steaks. J. Muscle Foods. 2(4):289-296.

Shackelford SD, Koohmaraie M, Whipple G, Wheeler TL, Miller MF, Crouse JD, Reagan JO. 1991b. Predictors of beef tenderness: development and verification. J. Food Sci. 56(5):1130-1135, 1140.

Shackelford SD, Koohmaraie M, Wheeler TL. 1994. The efficacy of adding a minimum adjusted fat thickness requirement to the USDA beef quality grading standards for select grade beef. J. Anim. Sci. 72(6):1502-1507.

Shackelford SD, Wheeler TL, Koohmaraie M. 1995. Relationship between shear force and trained sensory panel tenderness ratings of 10 major muscles from *Bos indicus* and *Bos taurus* cattle. J. Anim. Sci. 73(10):3333-3340.

Shackelford SD, Wheeler TL, Koohmaraie M. 1998. Coupling of image analysis and tenderness classification to simultaneously evaluate carcass cutability, longissimus area, subprimal cut weights and tenderness of beef. J. Anim. Sci. 76(10):2631-2640.

Shama F, Sherman P. 1973. Evaluation of some textural properties of foods with the Instron Universal Testing Machine. J. Texture Stud. 4(3):344-352.

Smith GC, Carpenter ZL, Cross HR, Murphey CE, Abraham HC, Savell, JW, Davis GW, Berry BW, Parrish FC Jr. 1984. Relationship of USDA marbling groups to palatability of cooked beef. J. Food Qual. 7(4):289-308.

Smith GC, Savell JW, Cross HR, Carpenter ZL, Murphey CE, Davis GW, Abraham HC, Parrish FC Jr, Berry BW. 1987. Relationship of USDA quality grades to palatability of cooked beef. J. Food Qual. 10(4):269-286.

Smith GC, Dolezal HG, Savell JW. 1995. The Final Report of the National Beef Quality Audit. Colorado State University, Fort Collins, Oklahoma State University, Stillwater, and Texas A&M University, College Station.

Spadaro MV. 1996. Biomechanical characterization of meat texture. [Ph.D. dissertation], Texas A&M University, College Station.

Spadaro MV, Allen DH, Keeton JT, Moreira RG, Boleman RM. 2002. Biomechanical characterization of meat texture. J. Texture Stud. 33(1):59-87.

Stanley DW, Pearson GP, Coxworth VE. 1971. Evaluation of certain physical properties of meat using a Universal Testing machine. J. Food Sci. 36(2):256-260.

Swatland HJ, Findlay CJ. 1997. On-line probe prediction of beef toughness, correlating sensory evaluation with fluorescence detection of connective tissue and dynamic analysis of overall toughness. Food Qual, Preference. 8(3):233-239.

Szczesniak AS. 1963. Objective measurements of food texture. J. Food Sci. 28(4):410-420.

Szczesniak AS. 1966. Texture measurements. Food Tech. 20(10):1292-1298.

Szczesniak AS. 1968. Correlations between objective and sensory texture measurements. Food Tech. 22(8):49-54.

Szczesniak AS. 1969. The whys and whats of objective texture measurements. Can. Inst. Food Tech. 2(4):150-156.

Szczesniak AS. 1972. Instrumental methods of texture measurement. Food Tech. 26(1):50-56, 63.

Szczesniak AS. 1977. An overview of recent advances in food texture research. Food Tech. 31(4):71-75, 90.

Szczesniak AS, Brandt MA, Friedman H. 1963. Development of standard rating scales for mechanical parameters of texture and correlation between the objective and the sensory methods of texture evaluation. J. Food. Sci. 28(4):397-403.

Szczesniak AS, Torgeson KW. 1965. Methods of meat texture measurement viewed from the background of factors affecting tenderness. Adv. Food Res. 14:33-165.

Tatum JD, Smith GC, Berry BW, Murphey CE, Williams FL, Carpenter ZL. 1980. Carcass characteristics, time on feed and cooked beef palatability attributes. J. Anim. Sci. 50(5):833-840.

Tornberg E, Fjelkner-Modig S, Ruderus H, Glantz RO, Randow K, Stafford D. 1985. Clinically recorded masticatory patterns as related to the sensory evaluation of meat and meat products. J. Food Sci. 50(4):1059-1066.

Voisey PW. 1976. Engineering assessment and critique of instruments used for meat tenderness evaluation. J. Texture Stud. 7(1):11-48.

Voisey PW, Larmond E. 1974. Examination of factors affecting performance of the Warner-Bratzler meat shear test. J. Inst. Can. Sci. Tech. Aliment. 7(4):243-249.

Walter MJ, Goll DE, Anderson LP, Kline EA. 1963. Effect of marbling and maturity on beef tenderness. J. Anim. Sci., Midwestern Section Abstracts. 22:1115.

Webb NB, Rao NM, Ceville GV, Hamann DD. 1975. Texture evaluation of frankfurters by dynamic testing. J. Texture Stud. 6(3):329-342.

Wheeler TL, Koohmaraie M. 1991. A modified procedure for simultaneous extraction and subsequent assay of calcium-dependent and lysosomal protease systems from a skeletal biopsy. J. Animal Sci. 69(4):1559-1565.

Wheeler TL, Cundiff LV, Koch RM. 1994. Effect of marbling degree on beef palatability in *Bos taurus* and *Bos indicus* cattle. J. Anim. Sci. 72(12):3145-3151.

Whipple G, Koohmaraie M, Dikeman ME, Crouse JD. 1990. Predicting beef longissimus tenderness from various biochemical and histological muscle traits. J. Anim. Sci. 68(12):4193-4199.

Wulf DM, O'Connor SF, Tatum JD, Smith GC. 1997. Using objective measures of muscle color to predict beef longissimus tenderness. J. Anim. Sci. 75(3):684-692.

Wyle AM, Vote DJ, Roeber DL, Cannell RC, Belk KE, Scanga JA, Goldberg M, Tatum JD, Smith GC. 2003. Effectiveness of the SmartMV prototype BeefCam System to sort beef carcasses into expected palatability groups. J. Anim. Sci. 81(2):441-448.

APPENDIX A

Experimental Techniques of Spadaro (1996)

Characterization of the Linear Viscoelastic Range and Relaxation Time

These experiments were aimed at characterizing boundaries of the deformation range, within which behavior and the relaxation time for *Longissimus dorsi* muscle could be specified as linear viscoelastic (see Biomechanics of Meat Tissues).

Sample Preparation

Five bovine *Longissimus dorsi* muscles of undetermined USDA quality grade were obtained from local retail stores (Randalls, Inc. and Kroger, Inc.). Samples were vacuum packaged and stored at -40°C until analyzed.

Muscles were tempered to 5°C four days prior to the day of analysis. When the temperature was homogeneous throughout the muscles, samples were cut parallel and perpendicular to the myofiber direction into cubes of 30 mm side length. Temperature of the cubes was allowed to equilibrate to room temperature (21$\pm$ 2°C).

Characterization of the Linear Viscoelastic Range

From each of three randomly selected muscles, eight cubic specimens were obtained as described above and randomly assigned to one of two treatments: parallel and perpendicular to the myofiber directions.

Self-adhesive medium grain sand paper (3M, Inc., St. Paul, MN) was fixed with cyanoacrylate (superglue) on two parallel faces of teach individual cube, and the set was

placed onto the platform of a TA.XT2 Texture Analyzer (Texture Technologies Corp., Scarsdale, NY/Stable Micro Systems, Godalming, Surrey, UK) with its crosshead in contact with the upper face. Application of a compressive constant strain was applied for 4 minutes, after which the compression was stopped, and tension was immediately applied at same strain level and time interval. These experiments were conducted at strain levels of 1%, 2%, 3%, 4% and 5%. Stress decay vs. time was recorded for each muscle section in the experiment at a speed of 50 points/sec and data were saved in ASCII file format for further analysis. Tests were triggered at a contact force of 0.015 N.

Characterization of Stress Relaxation Time

The two remaining muscles were used to determine relation times under linear conditions as described in the previous paragraph. Again, eight cubic samples from each muscle were randomly assigned to one of two treatments: parallel and perpendicular to the myofiber direction.

Each specimen was placed onto the platform of a TA.XT2 Texture Analyzer (Texture Technologies Corp., Scarsdale, NY/Stable Micro Systems, Godalming, Surrey, UK) and compressed for 2, 3, 4, 5, and 6 minutes at a constant 3% strain level. Stress decay vs. time was recorded at a speed of 50 points /sec and data were saved in ASCII file format for further analysis. Tests were triggered at a contact force of 0.015N.

Data Analysis

Experimental data were non-linearly curve fitted over equation (14) with three exponential terms plus an infinite equilibrium term (see Biomechanics of Meat Tissues). The software package used was Matlab v4.2c.1 (The MathWorks, Inc., Natick, MA). (Copies of codes used, mainprog.m and opfun.m, can be found in Appendix C of Spadaro (1996)).

Sensitivity of the Technique

After characterization of the linear viscoelastic range and stress relation time, it was necessary to determine whether mechanical characterization of muscle tissues was sensitive enough to discriminate levels of tenderness as judged by a trained sensory panel, as well as Warner-Bratzler shear force measurements. *Longissimus dorsi* muscles from animals representing extremes in tenderness were selected: old cows or bulls (around 4 years of age), and young USDA Choice steers (approximately 18 months old).

Sample Preparation

Eight *Longissimus dorsi* muscles from Anus steers (approximately 18 months old) graded USDA Choice were obtained from Rosenthal Meat Science Center at Texas A&M University, after being aged for 20 days at 5°C. Eight *Longissimus dorsi* muscles from cows and bulls (approximately 48 months old) graded USDA Utility were obtained 24 h postmortem from a commercial slaughter house (L&H, San Antonio, TX).

Four steaks, 25 mm thick, were removed from each muscle, individually vacuum packaged, and stored at -40°C for subsequent trained sensory and Warner-Bratzler shear force analyses. The remaining portion of the muscles were vacuum packaged and stored at -40°C until analyzed.

Muscles were tempered to 5°C four days prior to the day of stress relation analysis. When the temperature was homogeneous throughout the muscles, samples were cut parallel and perpendicular to the myofiber direction into cubes of 30 mm side length. Temperature of the cubes was allowed to equilibrate to room temperature (21$\pm$2°C).

Steaks for sensory and Warner-Bratzler shear force analyses were tempered at 2°C for 24 h prior to cooking.

Stress-Relaxation Analysis

Eight cubic samples were obtained from each muscle as described above and randomly assigned to one of two treatments: parallel and perpendicular to the myofiber direction.

Each specimen was placed on the platform of a TA.XT2 Texture Analyzer and compressed for 4 minutes at a 3% strain level. Stress decay vs. time was recorded at a speed of 50 points/sec and data were saved in ASCII file format for further analysis. Tests were triggered at a contact force of 0.015N.

Sensory Analysis

From each *Longissimus dorsi* muscle, two steaks were broiled to an internal temperature of 40°C, turned, and broiling continued to an internal endpoint temperature of 70°C on Farberware electric broilers (Farberware, Bronx, NY). The internal temperature was monitoring using a copper constantan thermocouple probe attached to a Honeywell recording thermometer (Honeywell, Scarborough, ON, Canada).

Warm, 13 mm side length cubic samples were served in duplicate to a six-member sensory panel trained according to methods described by Cross et al. (1978) and Meilgaard et al. (1991). The descriptive attribute panel evaluated each sample for juiciness (8=extremely juicy, 1 = extremely dry); fiber tenderness (8=extremely tender, 1=extremely tough); overall tenderness (8-extremely tender, 1 =extremely tough) and connective tissue amount (8=none, 1=abundant) using an eight-point structured scale.

Warner-Bratzler Shear Force Analysis

One steak was cooked using the same procedure described for Sensory Analysis, and was allowed to cool for 2 hr at 23$\pm$1°C. Ten 13 mm cores were removed from each steak parallel to the myofiber direction. Each core was sheared competently through once with a Warner-Bratzler shear machine. Force for each cut was recorded in pounds as the mean of 10 cores.

Data Analysis

Stress relation data were processed in the same manner as it was explained for the previous subsection (see Characterization of the Linear Viscoelastic Range and Relation Time).

Sensory and shear force data were analyzed using a blocked one way analysis of variance. Tukey's test was used to discriminate differences between treatments. The software package used for statistical analysis was SAS v6.08 (SAS Institute, Cary, NC).

Characterization of the Mechanical Properties of Angleton Cattle

Having characterized the linear viscoelastic range of the meat material, its general relaxation time, and the ability of mechanical properties to discriminate textural attributes, the next objective was to generate the data necessary to evaluate the performance of stiffness and energy values obtained during the initial masticatory process (see Biomechanics of Meat Tissues), and compare those values to the subjective sensory and objective Warner-Bratzler tools used to judge meat texture.

Sample Preparation

Longissimus dorsi muscle samples located at the 7^{th} and 8^{th} rib juncture were taken from 50 carcasses assigned to the Angleton genetic control beef carcass program (see Introduction) were collected. All samples were vacuum packaged and aged at 5°C for 10 days.

From each *Longissimus dorsi* muscle, 25 mm thick steaks were removed and utilized by different scientists within the Animal science Department at Texas A&M University: steaks 1 and 3 were for sensory analysis, steak 2 for Warner-Bratzler shear force analysis, steak 4 was assigned as a backup for sensory or shear force analysis, and steaks 5 and 6 for calpain/calpastatin enzyme analysis. Steaks 7 and 8 were left uncut and were collected by the author for material and mechanical characterization. Samples were kept frozen at -40°C until analyzed.

Muscles were tempered to 5°C four days prior to the day of stress relaxation analysis. When the temperature was homogeneous throughout the muscles, samples were cut parallel and perpendicular to the myofiber direction into cubes of 30 mm side length. Temperature of the cubes was allowed to equilibrate to room temperature (21 ± 2°C) immediately prior to testing.

Stress-Relaxation Analysis

Eight cubic samples obtained from each muscle as described above were randomly assigned to one of two treatments: parallel and perpendicular to the myofiber direction.

Each specimen was placed on the platform of a TA.XT2 Texture Analyzer and compressed for 4 minutes at a 3% strain level. Stress decay vs. time was recorded at a speed of 50 points/sec and data were saved in ASCII file format for further analysis. Tests were triggered at a contact force of 0.015N.

Data Analysis

Stress relation data were processed in the same manner as it was explained for the previous subsection (see Characterization of the Linear Viscoelastic Range and Relation Time). Equation (18) was applied to obtain creep compliance functions, and the analytical solutions were obtained using Matlab v4.2c.1 (The MathWorks, Inc., Natick, MA). Appendix C (of Spadaro (1996)) contains copies of codes used: creep.m and final.m.

Sensory and shear force results previously obtained for these cattle were furnished by Davis and Taylor (1995). These data were correlated to predict tenderness values obtained using stiffness and energy dissipated models. The software package used for statistical analysis was SAS v6.08 (SAS Institute, Cary, NC).

APPENDIX B

NAME: _____ **DATE:** _____ **STUDY: Boleman Tenderness**

Sample	Juiciness	Muscle Fiber Tenderness	Connective Tissue Amount	Overall Tenderness
Warm Up				

JUICINESS

8 Extremely Juicy
7 Very Juicy
6 Moderately Juicy
5 Slightly Juicy
4 Slightly Dry
3 Moderately Dry
2 Very Dry
1 Extremely Dry

MUSCLE FIBER/OVERALL TENDERNESS

8 Extremely Tender
7 Very Tender
6 Moderately Tender
5 Slightly Tender
4 Slightly Tough
3 Moderately Tough
2 Very Tough
1 Extremely Tough

CONNECTIVE TISSUE AMOUNT

8 None
7 Practically None
6 Traces
5 Slight
4 Moderate
3 Slightly Abundant
2 Moderately Abundant
1 Abundant

APPENDIX C

TABLE 1. Least square means of platen Texture Analyzer compression values as affected by fiber orientation.

Compression Variable	Muscle Fiber Orientation				
	PL[1]	(SEM) [1]	PP[1]	(SEM) [1]	P value
ISTF (Pa)[1]	22413 [a]	1505.49	34955 [b]	1556.82	<0.0001
FSTF (Pa)[1]	17663 [a]	1189.41	27471 [b]	1230.18	<0.0001
ED (J/m^3)[1]	2.491 [a]	0.094	1.804 [b]	0.097	<0.0001

[ab] Mean values with like superscripts across a row are not significantly different (P>0.05).
[1] Variable abbreviation explanation: PL = Parallel fiber orientation; PP = Perpendicular fiber orientation; SE = Standard Error; ISTF = Initial Stiffness; FSTF = Final Stiffness; ED = Energy Dissipated.

TABLE 2. Least square means of platen Texture Analyzer compression values as affected by temperature (ºC) during compression.

Compression Variable	Temperature (ºC)						
	0	2	4	6	8	10	P Value
ISTF (Pa)[1]	31962 [a]	33648 [a]	28375 [ab]	31597 [a]	23959 [b]	22564 [b]	0.0030
FSTF (Pa)[1]	25043 [a]	26479 [a]	22295 [ab]	24888 [a]	18863 [b]	17834 [b]	0.0038
ED (J/m^3)[1]	2.151 [ab]	1.776 [b]	2.198 [ab]	1.856 [b]	2.572 [a]	2.332 [a]	0.0010

[ab] Mean values with like superscripts across a row are not significantly different (P>0.05).

[1] Variable abbreviation explanation: ISTF = Initial Stiffness; FSTF = Final Stiffness; ED = Energy Dissipated.

* Standard Error: ISTF 0°C = 2458.47; ISTF 2°C = 2425.94; ISTF 4°C = 2558.79; ISTF 6°C = 2426.04; ISTF 8°C = 2586.9; ISTF 10°C = 2392.77; FSTF 0°C = 1946.1; FSTF 2°C = 1920.27; FSTF 4°C = 2025.67; FSTF 6°C = 1920.35; FSTF 8°C = 2047.95; FSTF 10°C = 1894.0; ED 0°C, ED 6°C = 0.1475; ED 2°C = 0.1475; ED 4°C = 0.1552; ED 8°C = 0.1569; ED 10°C = 0.1455.

TABLE 3. R-square values for prediction equations for juiciness based on fiber orientation and temperature (ºC).

Fiber Orientation[1]	Temperature (ºC)	Equation variables [1]	R^2
PL	0	ISTF ISTF2 ISTF3 FSTF FSTF2 FSTF3 ED ED2 ED3	0.5556
PL	0	ISTF ISTF2 ISTF3 FSTF FSTF2 FSTF3 ED ED3	0.5556
PL	0	ISTF ISTF2 ISTF3 FSTF FSTF2 FSTF3 ED2 ED3	0.5556
PL	2	ISTF ISTF2 ISTF3 FSTF FSTF2 FSTF3 ED ED2 ED3	0.5615
PL	4	ISTF ISTF2 ISTF3 FSTF FSTF2 FSTF3 ED ED2 ED3	0.6473
PL	4	ISTF ISTF2 ISTF3 FSTF2 FSTF3 ED ED2 ED3	0.6458
PL	6	ISTF ISTF2 ISTF3 FSTF FSTF2 FSTF3 ED ED2 ED3	0.6782
PL	8	ISTF ISTF2 ISTF3 FSTF FSTF2 FSTF3 ED ED2 ED3	0.2180
PL	8	ISTF ISTF2 ISTF3 FSTF FSTF2 FSTF3 ED ED3	0.2180
PL	10	ISTF ISTF2 ISTF3 FSTF FSTF2 FSTF3 ED ED3	0.4579
PL	10	ISTF ISTF3 FSTF FSTF2 FSTF3 ED ED2 ED3	0.4579
PL	10	ISTF ISTF3 FSTF FSTF2 FSTF3 ED ED3	0.4579
PP	0	ISTF ISTF2 ISTF3 FSTF FSTF2 FSTF3 ED ED2 ED3	0.7175
PP	0	ISTF ISTF2 ISTF3 FSTF FSTF2 FSTF3 ED2 ED3	0.7110
PP	2	ISTF ISTF2 ISTF3 FSTF FSTF2 FSTF3 ED ED2 ED3	0.7570
PP	2	ISTF ISTF2 ISTF3 FSTF FSTF2 ED ED2 ED3	0.7532
PP	4	ISTF ISTF2 ISTF3 FSTF FSTF2 FSTF3 ED ED2 ED3	0.3275
PP	4	ISTF ISTF2 ISTF3 FSTF FSTF2 ED ED2 ED3	0.3275
PP	4	ISTF ISTF2 FSTF FSTF2 FSTF3 ED ED2 ED3	0.3275
PP	6	ISTF ISTF2 ISTF3 FSTF FSTF2 FSTF3 ED ED2 ED3	0.6778
PP	6	ISTF ISTF2 ISTF3 FSTF FSTF2 FSTF3 ED ED3	0.6735
PP	6	ISTF ISTF2 ISTF3 FSTF FSTF2 FSTF3 ED3	0.6728
PP	8	ISTF ISTF3 FSTF FSTF2 FSTF3 ED ED2 ED3	0.7276
PP	8	ISTF ISTF2 ISTF3 FSTF FSTF3 ED ED2 ED3	0.7275
PP	8	ISTF ISTF3 FSTF FSTF3 ED ED2 ED3	0.7271
PP	10	ISTF ISTF2 ISTF3 FSTF FSTF2 FSTF3 ED ED2 ED3	0.5472

[1] Variable abbreviation explanation: PL = Parallel fiber orientation; PP = Perpendicular fiber orientation; SE = Standard Error; ISTF = Initial Stiffness; FSTF = Final Stiffness; ED = Energy Dissipated; ISTF2 = ISTF x ISTF; ISTF3 = ISTF2 x ISTF; FSTF2 = FSTF x FSTF; FSTF3 = FSTF2 x FSTF; ED2 = ED x ED; ED3 = ED2 x ED.

TABLE 4. R-square values for prediction equations for connective tissue based on fiber orientation and temperature (°C).

Fiber Orientation[1]	Temperature (°C)	Equation variables [1]	R^2
PL	0	ISTF ISTF2 ISTF3 FSTF FSTF2 FSTF3 ED ED2 ED3	0.5409
PL	0	ISTF ISTF2 ISTF3 FSTF FSTF2 FSTF3 ED2 ED3	0.5409
PL	2	ISTF ISTF2 ISTF3 FSTF FSTF2 FSTF3 ED ED2 ED3	0.6491
PL	4	ISTF ISTF2 ISTF3 FSTF FSTF2 FSTF3 ED ED2 ED3	0.3840
PL	4	ISTF ISTF2 ISTF3 FSTF FSTF2 FSTF3 ED2 ED3	0.3840
PL	6	ISTF ISTF2 ISTF3 FSTF FSTF2 FSTF3 ED ED2 ED3	0.5232
PL	6	ISTF ISTF2 ISTF3 FSTF FSTF2 ED ED2 ED3	0.5229
PL	8	ISTF ISTF2 ISTF3 FSTF FSTF2 FSTF3 ED ED2 ED3	0.3249
PL	8	ISTF ISTF2 ISTF3 FSTF2 FSTF3 ED ED2 ED3	0.3248
PL	8	ISTF ISTF3 FSTF FSTF2 ED ED2 ED3	0.3238
PL	8	ISTF FSTF FSTF2 ED ED2 ED3	0.3235
PL	10	ISTF ISTF2 ISTF3 FSTF FSTF2 FSTF3 ED ED2 ED3	0.5347
PP	0	ISTF ISTF2 ISTF3 FSTF FSTF2 FSTF3 ED ED2 ED3	0.5359
PP	2	ISTF ISTF2 ISTF3 FSTF FSTF2 FSTF3 ED ED2 ED3	0.7867
PP	4	ISTF ISTF2 ISTF3 FSTF FSTF2 FSTF3 ED ED2 ED3	0.7181
PP	4	ISTF2 ISTF3 FSTF FSTF2 FSTF3 ED ED2 ED3	0.7181
PP	6	ISTF ISTF2 ISTF3 FSTF FSTF2 FSTF3 ED ED2 ED3	0.3956
PP	8	ISTF ISTF2 FSTF FSTF2 FSTF3 ED ED2 ED3	0.3990
PP	10	ISTF ISTF2 ISTF3 FSTF FSTF2 FSTF3 ED ED2 ED3	0.2056

[1] Variable abbreviation explanation: PL = Parallel fiber orientation; PP = Perpendicular fiber orientation; SE = Standard Error; ISTF = Initial Stiffness; FSTF = Final Stiffness; ED = Energy Dissipated; ISTF2 = ISTF x ISTF; ISTF3 = ISTF2 x ISTF; FSTF2 = FSTF x FSTF; FSTF3 = FSTF2 x FSTF; ED2 = ED x ED; ED3 = ED2 x ED.

TABLE 5. R-square values for prediction equations for muscle fiber tenderness based on fiber orientation and temperature (ºC).

Fiber Orientation[1]	Temperature (ºC)	Equation variables [1]	R^2
PL	0	ISTF ISTF2 ISTF3 FSTF FSTF2 FSTF3 ED ED2 ED3	0.6835
PL	2	ISTF ISTF2 ISTF3 FSTF FSTF2 FSTF3 ED ED2 ED3	0.6457
PL	2	ISTF ISTF2 ISTF3 FSTF FSTF2 FSTF3 ED ED3	0.6456
PL	2	ISTF ISTF2 ISTF3 FSTF FSTF2 FSTF3 ED ED2	0.6456
PL	2	ISTF ISTF2 ISTF3 FSTF2 FSTF3 ED2 ED3	0.6432
PL	4	ISTF ISTF2 ISTF3 FSTF FSTF2 FSTF3 ED ED2 ED3	0.6518
PL	4	ISTF ISTF2 ISTF3 FSTF FSTF2 FSTF3 ED2 ED3	0.6499
PL	6	ISTF ISTF2 ISTF3 FSTF FSTF2 FSTF3 ED ED2 ED3	0.5784
PL	8	ISTF ISTF2 ISTF3 FSTF FSTF2 FSTF3 ED ED2 ED3	0.6120
PL	10	ISTF ISTF2 ISTF3 FSTF FSTF2 FSTF3 ED ED2 ED3	0.5551
PP	0	ISTF ISTF2 ISTF3 FSTF FSTF2 FSTF3 ED ED2 ED3	0.5106
PP	2	ISTF ISTF2 ISTF3 FSTF FSTF2 FSTF3 ED ED2 ED3	0.7290
PP	4	ISTF ISTF2 ISTF3 FSTF FSTF2 FSTF3 ED ED2 ED3	0.7315
PP	4	ISTF ISTF2 ISTF3 FSTF FSTF2 FSTF3 ED2 ED3	0.7309
PP	4	ISTF2 ISTF3 FSTF2 FSTF3 ED ED2 ED3	0.7308
PP	4	ISTF2 ISTF3 FSTF2 FSTF3 ED2 ED3	0.7301
PP	6	ISTF ISTF2 ISTF3 FSTF FSTF2 FSTF3 ED ED2 ED3	0.5827
PP	8	ISTF ISTF3 FSTF FSTF2 FSTF3 ED ED2 ED3	0.6496
PP	10	ISTF ISTF2 ISTF3 FSTF FSTF2 FSTF3 ED ED2 ED3	0.5171
PP	10	ISTF ISTF2 ISTF3 FSTF FSTF2 FSTF3 ED2 ED3	0.5132

[1] Variable abbreviation explanation: PL = Parallel fiber orientation; PP = Perpendicular fiber orientation; SE = Standard Error; ISTF = Initial Stiffness; FSTF = Final Stiffness; ED = Energy Dissipated; ISTF2 = ISTF x ISTF; ISTF3 = ISTF2 x ISTF; FSTF2 = FSTF x FSTF; FSTF3 = FSTF2 x FSTF; ED2 = ED x ED; ED3 = ED2 x ED.

TABLE 6. R-square values for prediction equations for overall sensory tenderness based on fiber orientation and temperature (ºC).

Fiber Orientation[1]	Temperature (ºC)	Equation variables [1]	R^2
PL	0	ISTF ISTF2 ISTF3 FSTF FSTF2 FSTF3 ED ED2 ED3	0.7370
PL	0	ISTF ISTF2 ISTF3 FSTF FSTF2 FSTF3 ED ED2	0.7183
PL	0	ISTF ISTF2 ISTF3 FSTF FSTF2 FSTF3 ED ED3	0.7149
PL	2	ISTF ISTF2 ISTF3 FSTF FSTF2 FSTF3 ED ED2 ED3	0.6592
PL	2	ISTF ISTF2 ISTF3 FSTF2 FSTF3 ED ED2 ED3	0.6591
PL	4	ISTF ISTF2 ISTF3 FSTF FSTF2 FSTF3 ED ED2 ED3	0.6512
PL	4	ISTF ISTF2 ISTF3 FSTF FSTF2 FSTF3 ED2 ED3	0.6508
PL	6	ISTF ISTF2 ISTF3 FSTF FSTF2 FSTF3 ED ED2 ED3	0.5146
PL	6	ISTF2 ISTF3 FSTF FSTF2 FSTF3 ED ED2 ED3	0.5146
PL	8	ISTF ISTF2 ISTF3 FSTF FSTF2 FSTF3 ED ED2 ED3	0.5295
PL	8	ISTF ISTF2 ISTF3 FSTF2 FSTF3 ED ED2 ED3	0.5295
PL	10	ISTF ISTF2 ISTF3 FSTF FSTF2 FSTF3 ED ED2 ED3	0.5208
PP	0	ISTF ISTF2 ISTF3 FSTF FSTF2 FSTF3 ED ED2 ED3	0.4946
PP	2	ISTF ISTF2 ISTF3 FSTF FSTF2 FSTF3 ED ED2 ED3	0.7746
PP	4	ISTF ISTF2 ISTF3 FSTF FSTF2 FSTF3 ED ED2 ED3	0.6984
PP	4	ISTF2 ISTF3 FSTF FSTF2 FSTF3 ED ED2 ED3	0.6982
PP	4	ISTF ISTF3 FSTF FSTF3 ED ED2 ED3	0.6976
PP	6	ISTF ISTF2 ISTF3 FSTF FSTF2 FSTF3 ED ED2 ED3	0.4827
PP	6	ISTF ISTF2 ISTF3 FSTF FSTF2 FSTF3 ED ED3	0.4827
PP	8	ISTF ISTF3 FSTF FSTF2 FSTF3 ED ED2 ED3	0.5118
PP	10	ISTF ISTF2 ISTF3 FSTF FSTF2 FSTF3 ED ED2 ED3	0.4170
PP	10	ISTF ISTF2 ISTF3 FSTF FSTF2 FSTF3 ED2 ED3	0.4150

[1] Variable abbreviation explanation: PL = Parallel fiber orientation; PP = Perpendicular fiber orientation; SE = Standard Error; ISTF = Initial Stiffness; FSTF = Final Stiffness; ED = Energy Dissipated; ISTF2 = ISTF x ISTF; ISTF3 = ISTF2 x ISTF; FSTF2 = FSTF x FSTF; FSTF3 = FSTF2 x FSTF; ED2 = ED x ED; ED3 = ED2 x ED.

TABLE 7. R-square values for prediction equations for Warner-Bratzler Shear based on fiber orientation and temperature (ºC).

Fiber Orientation[1]	Temperature (ºC)	Equation variables [1]	R^2
PL	0	ISTF ISTF2 ISTF3 FSTF FSTF2 FSTF3 ED ED2 ED3	0.5124
PL	0	ISTF ISTF2 ISTF3 FSTF FSTF2 FSTF3 ED ED2	0.5112
PL	2	ISTF ISTF2 ISTF3 FSTF FSTF2 FSTF3 ED ED2 ED3	0.6344
PL	2	ISTF ISTF2 ISTF3 FSTF2 FSTF3 ED ED2 ED3	0.6344
PL	2	ISTF ISTF2 ISTF3 FSTF FSTF3 ED ED2 ED3	0.6316
PL	4	ISTF ISTF2 ISTF3 FSTF FSTF2 FSTF3 ED ED2 ED3	0.2605
PL	4	ISTF ISTF2 FSTF FSTF2 FSTF3 ED ED2 ED3	0.2605
PL	4	ISTF ISTF3 FSTF FSTF2 ED ED2 ED3	0.2603
PL	6	ISTF ISTF2 ISTF3 FSTF FSTF2 FSTF3 ED ED2 ED3	0.1894
PL	6	ISTF2 ISTF3 FSTF FSTF2 FSTF3 ED ED2 ED3	0.1881
PL	8	ISTF ISTF2 ISTF3 FSTF FSTF2 FSTF3 ED ED2 ED3	0.5702
PL	10	ISTF ISTF2 ISTF3 FSTF FSTF2 FSTF3 ED ED2 ED3	0.4553
PL	10	ISTF ISTF2 ISTF3 FSTF FSTF2 ED ED2 ED3	0.4550
PL	10	ISTF ISTF3 FSTF FSTF2 ED ED2 ED3	0.4527
PP	0	ISTF ISTF2 ISTF3 FSTF FSTF2 FSTF3 ED ED2 ED3	0.3445
PP	2	ISTF ISTF2 ISTF3 FSTF FSTF2 FSTF3 ED ED2 ED3	0.8035
PP	4	ISTF ISTF2 ISTF3 FSTF FSTF2 FSTF3 ED ED2 ED3	0.7138
PP	6	ISTF ISTF2 ISTF3 FSTF FSTF2 FSTF3 ED ED2 ED3	0.1846
PP	6	ISTF ISTF2 ISTF3 FSTF FSTF2 FSTF3 ED ED2	0.1814
PP	8	ISTF ISTF2 ISTF3 FSTF FSTF2 FSTF3 ED ED2 ED3	0.8792
PP	10	ISTF ISTF2 ISTF3 FSTF FSTF2 FSTF3 ED ED2 ED3	0.7304

[1] Variable abbreviation explanation: PL = Parallel fiber orientation; PP = Perpendicular fiber orientation; SE = Standard Error; ISTF = Initial Stiffness; FSTF = Final Stiffness; ED = Energy Dissipated; ISTF2 = ISTF x ISTF; ISTF3 = ISTF2 x ISTF; FSTF2 = FSTF x FSTF; FSTF3 = FSTF2 x FSTF; ED2 = ED x ED; ED3 = ED2 x ED.

TABLE 8. Prediction equations incorporating fiber orientation and temperature (ºC) during platen compression with the highest R^2 values for sensory attributes using Warner-Bratzler shear values and TA compressions values.[1]

Equation	β value	R^2	RMSE
JUICINESS			
PP 2ºC			
Intercept	29.84017	0.7532	0.420
ISTF (Pa)	-0.00133		
ISTF2 (Pa)	1.850409 E-8		
ISTF3 (Pa)	-2.9212 E--14		
FSTF (Pa)	0.00112		
FSTF2 (Pa)	-2.05868 E-8		
ED (J/m^3)	-20.32239		
ED2 (J/m^3)	9.19959		
ED3 (J/m^3)	-1.55331		
Warner-Bratzler			
Intercept	4.99732	0.0323	0.575
WBSF (kg)	0.11582		
CONNECTIVE TISSUE			
PP 2ºC			
Intercept	8.85820	0.7867	0.332
ISTF (Pa)	-0.00469		
ISTF2 (Pa)	9.412472 E-8		
ISTF3 (Pa)	-5.1583 E-13		
FSTF (Pa)	0.00637		
FSTF2 (Pa)	-1.6304 E-7		
FSTF3 (Pa)	1.14638 E-12		
ED (J/m^3)	-13.13299		
ED2 (J/m^3)	8.06773		
ED3 (J/m^3)	-1.52544		
Warner-Bratzler			
Intercept	6.89034	0.0343	0.468
WBSF (kg)	-0.09716		

Equation	β value	R^2	RMSE
MUSCLE FIBER TENDERNESS			
PP 4ºC			
Intercept	2.82723	0.7301	0.453
ISTF2 (Pa)	-1.13275 E-8		
ISTF3 (Pa)	1.70355 E-13		
FSTF2 (Pa)	1.965086 E-8		
FSTF3 (Pa)	-3.5767 E-13		
ED2 (J/m^3)	1.47635		
ED3 (J/m^3)	-0.36618		
Warner-Bratzler			
Intercept	7.04387	0.1024	0.597
WBSF (kg)	-0.2218		
OVERALL TENDERNESS			
PP 2ºC			
Intercept	5.56159	0.7746	0.441
ISTF (Pa)	-0.00943		
ISTF2 (Pa)	1.774793 E-7		
ISTF3 (Pa)	-1.0302 E-12		
FSTF (Pa)	0.01354		
FSTF2 (Pa)	-3.2039 E-7		
FSTF3 (Pa)	2.33633 E-12		
ED (J/m^3)	-47.57349		
ED2 (J/m^3)	31.57059		
ED3 (J/m^3)	-6.02842		
Warner-Bratzler			
Intercept	7.00546	0.1103	0.581
WBSF (kg)	-0.22552		

[1] Variable abbreviation explanation: PL = Parallel fiber orientation; PP = Perpendicular fiber orientation; ISTF = Initial Stiffness; FSTF = Final Stiffness; ED = Energy Dissipated; ISTF2 = ISTF x ISTF; ISTF3 = ISTF2 x ISTF; FSTF2 = FSTF x FSTF; FSTF3 = FSTF2 x FSTF; ED2 = ED x ED; ED3 = ED2 x ED; WBSF = Warner Bratzler Shear Force value; R^2 = R-square; RMSE = Root Mean Squared Error.

TABLE 9. Mean values of physical, chemical, sensory and biomechanical traits of *Longissimus dorsi* samples evaluated at three holding temperatures (Phase 2).

Variable[1]	-6.6ºC	(S.E.M.)	4.4ºC	(S.E.M.)	10ºC	(S.E.M.)	Range of Values	P Value
	n=14		n=13		n=13			
Physical Data								
QG	423.570	(±8.79)	433.310	(±9.12)	443.460	(±9.12)	295 – 483	0.3032
MARB	485.360	(±21.57)	500.000	(±22.39)	530.380	(±22.39)	290 – 650	0.3494
YG	2.971	(±0.18)	2.914	(±0.18)	2.947	(±0.18)	1.93 – 4.58	0.9747
L*	46.419[a]	(±0.63)	43.940[b]	(±0.66)	46.136[a]	(±0.66)	40.36 – 50.42	0.0205
a*	15.813	(±0.60)	16.160	(±0.62)	16.255	(±0.62)	11.39 – 20.24	0.8645
b*	6.425	(±0.44)	6.007	(±0.46)	6.8573	(±0.46)	3.40 – 9.76	0.4349
WBSF (kg)	2.528	(±0.12)	2.339	(±0.13)	2.481	(±0.13)	1.4037 – 3.5276	0.5515
Chemical Data								
pH	5.364	(±0.04)	5.301	(±0.04)	5.255	(±0.04)	5.05 – 5.66	0.1619
MOIST (%)	71.846	(±0.36)	71.9131	(±0.38)	72.1196	(±0.38)	68.35 – 74.14	0.8638
FAT (%)	5.018	(±0.42)	4.729	(±0.44)	4.732	(±0.44)	2.31 – 8.96	0.8607
PROT (%)	25.0372	(±0.25)	25.255	(±0.26)	25.522	(±0.26)	23.66 – 28.44	0.4133
TOTCOL (mg/g)	3.483	(±0.18)	3.6511	(±0.19)	3.596	(±0.19)	2.42 – 4.83	0.8041
SOLCOL (%)	8.934	(±0.57)	8.755	(±0.59)	8.368	(±0.59)	4.61 – 13.19	0.7844
CALPST (act/g)	2.400	(±0.09)	2.513	(±0.09)	2.614	(±0.09)	2.05 – 3.32	0.2384
Sensory Data								
CKYLD (%)	84.364	(±0.73)	83.095	(±0.76)	82.724	(±0.76)	77.2 – 87.44	0.2749
JUICY	6.061	(±0.16)	5.615	(±0.17)	5.769	(±0.17)	4.2 – 7.4	0.1691
CTAMT	7.304	(±0.18)	7.319	(±0.19)	6.969	(±0.19)	5.6 – 8	0.3312
MFTEND	6.479	(±0.26)	6.396	(±0.27)	6.162	(±0.27)	3.6 – 7.75	0.6932
OVERALL	6.493	(±0.27)	6.450	(±0.28)	6.212	(±0.28)	3.6 – 8	0.7378
Platen Compression Data								
ISTFPLC (Pa)	12319	(±6538.43)	25371	(±7062.31)	12156	(±7062.31)	6414.10 – 162541.5	0.3186
FSTFPLC (Pa)	10063	(±764.05)	10771	(±825.27)	9884.7	(±825.27)	5238.17 – 16340.51	0.7239
ISTFPPC (Pa)	12116	(±892.25)	11478	(±963.74)	11960	(±963.74)	8020.48 – 21741.12	0.8831
FSTFPPC (Pa)	9537.2	(±714.75)	9212.8	(±772.02)	9534.2	(±772.02)	6287.38 – 17609.65	0.9420
EDPLC (J/m^3)	3.8659	(±0.25)	3.5546	(±0.27)	3.8251	(±0.27)	2.0819 – 61711	0.6695
EDPPC (J/m^3)	3.7483	(±0.28)	3.6971	(±0.22)	3.6384	(±0.22)	1.9449 – 5.1662	0.9377

TABLE 9. Continued.

Variable[1]	-6.6ºC	(S.E.M.)	4.4ºC	(S.E.M.)	10ºC	(S.E.M.)	Range of Values	P Value
Raw Data for Probe Compression								
ISTFPR (Pa)	218.57	(±14.94)	218.42	(±15.50)	201.16	(±15.50)	94.389 – 333.542	0.6587
FSTFPR (Pa)	182.28	(±12.63)	185.77	(±13.11)	171.15	(±13.11)	81.232 – 284.871	0.7135
EDPR (kJ/m^3)	8.15	(±0.49)	8.45	(±0.50)	8.40	(±0.50)	5.57 – 13.596	0.8949
Adjusted Data for Probe Compression								
ISTFPR (Pa)	199.73	(±14.72)	182.58	(±15.27)	197.31	(±15.27)	92.148 – 347.107	0.6890
FSTFPR (Pa)	165.65	(±12.38)	155.73	(±12.85)	167.87	(±12.85)	77.763 – 298.843	0.7767
EDPR (kJ/m^3)	8.48	(±0.61)	9.16	(±0.63)	8.60	(±0.63)	4.645 – 15.596	0.7173

[a] Mean values with like superscripts across a row are not significantly different (P>0.05).

[1] Variable abbreviations: QG=Quality Grade; MARB=Marbling; YG=Yield Grade; MOIST=Moisture; PROT=Protein; SOLCOL=Soluble Collagen; TOTCOL=Total Collagen; CALPST =Calpastatin; CKYLD= Cook Yield; CTAMT=Connective Tissue Amount; MFTEND=Muscle Fiber Tenderness; OVERALL= Overall Tenderness; WBSF=Warner-Bratzler Shear Force; ISTFPLC=Initial Stiffness of Parallel Fibers-Platen Compression; FSTFPLC=Final Stiffness of Parallel Fibers-Platen Compression; EDPLC=Energy Dissipated in Parallel Fibers-Platen Compression; ISTFPPC=Initial Stiffness of Perpendicular Fibers-Platen Compression; FSTFPPC=Final Stiffness of Perpendicular Fibers-Platen Compression; EDPPC= Energy Dissipated in Perpendicular Fibers-Platen Compression; ISTFPR=Initial Stiffness-Probe Compression; FSTFPR=Final Stiffness-Probe Compression; EDPR=Energy Dissipated-Probe Compression.

TABLE 10. Pairwise correlation coefficients of "Raw Data" pooled over compression temperatures for physical traits of *Longissimus dorsi* samples (Phase 2).

Variable[1]	QG	MARB	YG	L*	a*	b*
Physical Data						
QG	--------	0.956***	0.200	-0.026	0.427**	0.396*
MARB	0.956***	---------	0.282	0.031	0.442**	0.449**
YG	0.200	0.282	---------	0.013	0.290	0.276
L*	-0.026	0.031	0.013	---------	-0.404**	-0.071
a*	0.427**	0.442**	0.290	-0.404**	---------	0.876***
b*	0.396**	0.449**	0.276	-0.071	0.876***	---------
CKYLD (%)	0.041	0.071	0.097	0.169	0.198	0.278
WBSF (kg)	-0.012	-0.074	-0.252	0.063	-0.361*	-0.331*
Chemical Data						
pH	0.018	-0.043	0.020	0.119	-0.113	-0.149
MOIST (%)	-0.507***	-0.598***	-0.313*	0.136	-0.415**	-0.431**
FAT (%)	0.620***	0.729***	0.313*	0.004	0.474**	0.519***
PROT (%)	-0.216	-0.349*	-0.101	0.018	-0.350*	-0.303
SOLCOL (%)	-0.254	-0.263	-0.264	0.024	-0.161	-0.264
TOTCOL (%)	0.048	0.085	-0.289	-0.031	-0.125	-0.190
CALPST(act/g)	-0.127	-0.090	-0.049	-0.017	-0.096	-0.073
Sensory Data						
JUICY	-0.112	-0.099	0.078	0.144	0.083	0.197
CTAMT	-0.058	0.007	0.144	-0.092	0.469**	0.449**
MFTEND	-0.030	0.021	0.129	-0.013	0.453**	0.448**
OVERALL	-0.035	0.025	0.142	-0.012	0.441**	0.446**
Platen Compression Data						
ISTFPLC (Pa)	0.121	0.133	0.113	0.023	0.216	0.329*
FSTFPLC (Pa)	-0.121	-0.171	-0.078	-0.255	0.000	-0.056
ISTFPPC (Pa)	0.275	0.301	0.170	0.126	-0.010	0.066
FSTFPPC (Pa)	0.285	0.310	0.182	0.117	-0.022	0.049
EDPLC (J/m^3)	0.101	0.146	0.031	0.215	0.078	0.111
EDPPC (J/m^3)	-0.296	-0.305	-0.107	-0.148	0.154	0.097
Raw Data for Probe Compression						
ISTFPR (Pa)	0.089	0.016	-0.155	0.079	0.091	0.147
FSTFPR (Pa)	0.016	-0.052	-0.178	0.112	0.031	0.084
EDPR (J/m^3)	-0.140	-0.035	0.118	-0.061	0.051	0.020

*P<0.05 Significant
**P<0.01 Highly Significant
***P<0.001 Very Highly Significant

[1] Variable abbreviations: QG=Quality Grade; MARB=Marbling; YG=Yield Grade; MOIST=Moisture; PROT=Protein; SOLCOL=Soluble Collagen; TOTCOL=Total Collagen; CALPST =Calpastatin; CKYLD= Cook Yield; CTAMT=Connective Tissue Amount; MFTEND=Muscle Fiber Tenderness; OVERALL= Overall Tenderness; WBSF=Warner-Bratzler Shear Force; ISTFPLC=Initial Stiffness of Parallel Fibers-Platen Compression; FSTFPLC=Final Stiffness of Parallel Fibers-Platen Compression; EDPLC=Energy Dissipated in Parallel Fibers-Platen Compression; ISTFPPC=Initial Stiffness of Perpendicular Fibers-Platen Compression; FSTFPPC=Final Stiffness of Perpendicular Fibers-Platen Compression; EDPPC= Energy Dissipated in Perpendicular Fibers-Platen Compression; ISTFPR=Initial Stiffness-Probe Compression; FSTFPR=Final Stiffness-Probe Compression; EDPR=Energy Dissipated-Probe Compression.

TABLE 11. Pairwise correlation coefficients of "Raw Data" pooled over compression temperatures for chemical traits of *Longissimus dorsi* samples (Phase 2).

Variable[1]	pH	%MOIST	%FAT	%PROT	SOLCOL	TOTCOL	CALPST
Physical Data							
QG	0.018	-0.507***	0.620***	-0.216	-0.254	0.048	-0.127
MARB	-0.043	-0.598***	0.729***	-0.349*	-0.263	0.085	-0.090
YG	0.020	-0.313*	0.313*	-0.101	-0.264	-0.289	-0.049
L*	0.120	0.136	0.004	0.018	0.024	-0.031	-0.017
a*	-0.113	-0.415**	0.474**	-0.350*	-0.161	-0.125	-0.096
b*	-0.149	-0.431**	0.519***	-0.303	-0.264	-0.190	-0.073
CKYLD (%)	0.069	-0.270	0.299	-0.178	0.159	-0.0171	-0.278
WBSF (kg)	-0.030	0.234	-0.230	0.479**	0.152	0.0817	0.052
Chemical Data							
pH	--------	0.093	-0.029	0.077	0.154	0.093	0.115
MOIST (%)	0.093	--------	-0.914***	0.493***	0.064	-0.182	0.244
FAT (%)	-0.029	-0.914***	--------	-0.614***	-0.133	0.224	-0.192
PROT (%)	0.077	0.493***	-0.614***	--------	0.205	-0.214	0.088
SOLCOL (%)	0.154	0.064	-0.133	0.205	--------	0.552***	-0.099
TOTCOL (%)	0.093	-0.182	0.224	-0.214	0.552***	--------	0.110
CALPST (act/g)	0.115	0.244	-0.192	0.088	-0.099	0.110	-------
Sensory Data							
JUICY	0.029	0.119	-0.013	-0.229	-0.143	-0.2651	-0.033
CTAMT	-0.093	-0.283	0.289	-0.437**	-0.026	-0.0767	-0.206
MFTEND	-0.051	-0.155	0.237	-0.484**	-0.078	-0.0932	-0.147
OVERALL	-0.079	-0.159	0.238	-0.487***	-0.087	-0.0891	-0.120
Platen Compression Data							
ISTFPLC (Pa)	0.106	-0.286	0.217	-0.044	0.157	0.2310	-0.038
FSTFPLC (Pa)	0.063	-0.096	-0.046	0.128	0.132	0.0181	0.241
ISTFPPC (Pa)	0.076	-0.063	0.061	0.103	-0.084	-0.2315	0.042
FSTFPPC (Pa)	0.067	-0.068	0.056	0.120	-0.087	-0.2257	0.059
EDPLC (J/m^3)	0.033	-0.008	0.113	-0.078	-0.037	0.0703	-0.229
EDPPC (J/m^3)	-0.029	0.122	-0.047	-0.168	-0.073	0.1071	-0.059
Raw Data for Probe Compression							
ISTFPR (Pa)	0.277	0.097	-0.092	0.238	-0.101	-0.2676	-0.011
FSTFPR (Pa)	0.307*	0.178	-0.176	0.265	-0.057	-0.2476	0.021
EDPR (J/m^3)	-0.347*	-0.052	0.099	-0.314*	0.112	0.2168	0.111

*P<0.05 Significant
**P<0.01 Highly Significant
***P<0.001 Very Highly Significant

[1] Variable abbreviations: QG=Quality Grade; MARB=Marbling; YG=Yield Grade; MOIST=Moisture; PROT=Protein; SOLCOL=Soluble Collagen; TOTCOL=Total Collagen; CALPST =Calpastatin; CKYLD= Cook Yield; CTAMT=Connective Tissue Amount; MFTEND=Muscle Fiber Tenderness; OVERALL= Overall Tenderness; WBSF=Warner-Bratzler Shear Force; ISTFPLC=Initial Stiffness of Parallel Fibers-Platen Compression; FSTFPLC=Final Stiffness of Parallel Fibers-Platen Compression; EDPLC=Energy Dissipated in Parallel Fibers-Platen Compression; ISTFPPC=Initial Stiffness of Perpendicular Fibers-Platen Compression; FSTFPPC=Final Stiffness of Perpendicular Fibers-Platen Compression; EDPPC= Energy Dissipated in Perpendicular Fibers-Platen Compression; ISTFPR=Initial Stiffness-Probe Compression; FSTFPR=Final Stiffness-Probe Compression; EDPR=Energy Dissipated-Probe Compression.

TABLE 12. Pairwise correlation coefficients of "Raw Data" pooled over compression temperatures for sensory traits of *Longissimus dorsi* samples (Phase 2).

Variable[1]	CKYLD	JUICY	CTAMT	MFTEND	OVERALL
Physical Data					
QG	0.041	-0.112	-0.058	-0.030	-0.035
MARB	0.071	-0.099	0.007	0.021	0.025
YG	0.097	0.078	0.144	0.129	0.142
L*	0.169	0.144	-0.092	-0.013	-0.012
a*	0.198	0.083	0.469**	0.453**	0.441**
b*	0.278	0.197	0.449**	0.448**	0.446**
CKYLD (%)	--------	-0.218	0.200	0.142	0.141
WBSF (kg)	-0.141	-0.225	-0.755***	-0.736***	-0.740***
Chemical Data					
pH	0.069	0.029	-0.093	-0.051	-0.079
MOIST (%)	-0.270	0.119	-0.283	-0.155	-0.159
FAT (%)	0.299	-0.013	0.289	0.237	0.238
PROT (%)	-0.178	-0.229	-0.437**	-0.484**	-0.487***
SOLCOL (%)	0.159	-0.143	-0.026	-0.078	-0.087
TOTCOL (%)	-0.017	-0.265	-0.077	-0.093	-0.089
CALPST (act/g)	-0.278	-0.033	-0.206	-0.147	-0.120
Sensory Data					
JUICY	-0.218	--------	0.379*	0.495***	0.492***
CTAMT	0.200	0.379*	--------	0.928***	0.922***
MFTEND	0.142	0.495***	0.928***	--------	0.996***
OVERALL	0.141	0.492***	0.922***	0.996***	--------
Platen Compression Data					
ISTFPLC (Pa)	0.211	-0.001	0.202	0.115	0.149
FSTFPLC (Pa)	0.084	0.143	0.073	0.018	0.028
ISTFPPC (Pa)	-0.177	-0.045	-0.398**	-0.422**	-0.416**
FSTFPPC (Pa)	-0.204	-0.064	-0.411**	-0.441**	-0.434**
EDPLC (J/m^3)	0.048	-0.272	0.034	0.031	0.019
EDPPC (J/m^3)	0.078	0.212	0.471**	0.541***	0.534***
Raw Data for Probe Compression					
ISTFPR (Pa)	0.032	-0.078	-0.187	-0.281	-0.305
FSTFPR (Pa)	0.014	-0.110	-0.236	-0.325*	-0.347*
EDPR (J/m^3)	0.004	0.194	0.223	0.357*	0.376*

*P<0.05 Significant
**P<0.01 Highly Significant
***P<0.001 Very Highly Significant

[1] Variable abbreviations: QG=Quality Grade; MARB=Marbling; YG=Yield Grade; MOIST=Moisture; PROT=Protein; SOLCOL=Soluble Collagen; TOTCOL=Total Collagen; CALPST =Calpastatin; CKYLD= Cook Yield; CTAMT=Connective Tissue Amount; MFTEND=Muscle Fiber Tenderness; OVERALL= Overall Tenderness; WBSF=Warner-Bratzler Shear Force; ISTFPLC=Initial Stiffness of Parallel Fibers-Platen Compression; FSTFPLC=Final Stiffness of Parallel Fibers-Platen Compression; EDPLC=Energy Dissipated in Parallel Fibers-Platen Compression; ISTFPPC=Initial Stiffness of Perpendicular Fibers-Platen Compression; FSTFPPC=Final Stiffness of Perpendicular Fibers-Platen Compression; EDPPC= Energy Dissipated in Perpendicular Fibers-Platen Compression; ISTFPR=Initial Stiffness-Probe Compression; FSTFPR=Final Stiffness-Probe Compression; EDPR=Energy Dissipated-Probe Compression.

TABLE 13. Pairwise correlation coefficients of "Raw Data" pooled over compression temperatures for biomechanical traits of *Longissimus dorsi* samples (Phase 2).

Variable[1]	WBSF	ISTFPLC	FSTFPLC	ISTFPPC	FSTFPPC	EDPLC	EDPPC	ISTFPR	FSTFPR	EDPR
Physical Data										
QG	-0.012	0.121	-0.121	0.275	0.285	0.101	-0.296	0.089	0.016	-0.140
MARB	-0.074	0.133	-0.171	0.301	0.301	0.146	-0.305	0.016	-0.052	-0.035
YG	-0.252	0.113	-0.078	0.167	0.182	0.031	-0.107	-0.155	-0.178	0.118
L*	0.063	0.023	-0.255	0.126	0.117	0.215	-0.148	0.079	0.112	-0.061
a*	-0.361*	0.216	0.000	-0.010	-0.022	0.078	0.154	0.091	0.031	0.051
b*	-0.331*	0.329*	-0.056	0.066	0.049	0.111	0.097	0.147	0.084	0.020
CKYLD (%)	-0.141	0.211	0.084	-0.177	-0.204	0.048	0.078	0.032	0.014	0.004
WBSF(kg)	--------	-0.233	-0.067	0.268	0.279	-0.005	-0.290	0.251	0.239	-0.156
Chemical Data										
pH	-0.030	0.106	0.063	0.076	0.067	0.033	-0.029	0.277	0.307*	-0.347*
MOIST(%)	0.234	-0.286	-0.096	-0.063	-0.068	-0.008	0.122	0.097	0.177	-0.052
FAT(%)	-0.230	0.217	-0.046	0.061	0.056	0.113	-0.047	-0.092	-0.176	0.099
PROT(%)	0.479**	-0.044	0.128	0.103	0.120	-0.078	-0.168	0.238	0.265	-0.314*
SOLCOL(%)	0.152	0.157	0.132	-0.084	-0.087	-0.037	-0.073	-0.101	-0.057	0.112
TOTCOL(%)	0.082	0.231	0.018	-0.232	-0.226	0.070	0.107	-0.268	-0.248	0.217
CALPST(act/g)	0.052	-0.038	0.241	0.042	0.059	-0.229	-0.059	-0.011	0.021	0.111
Sensory Data										
JUICY	-0.225	-0.001	0.143	-0.045	-0.064	-0.272	0.212	-0.078	-0.110	0.194
CTAMT	-0.755***	0.202	0.073	-0.398**	-0.411**	0.034	0.471**	-0.187	-0.236	0.223
MFTEND	-0.736***	0.115	0.018	-0.422**	-0.441**	0.031	0.541***	-0.281	-0.325*	0.357*
OVERALL	-0.740***	0.149	0.028	-0.416**	-0.434**	0.019	0.534***	-0.305	-0.347*	0.376*
Platen Compression Data										
ISTFPLC(Pa)	-0.233	--------	0.300	-0.069	-0.073	-0.243	0.008	0.163	0.147	-0.157
FSTFPLC(Pa)	-0.067	0.300	--------	-0.279	-0.298	-0.885***	0.112	0.061	0.056	-0.037
ISTFPPC (Pa)	0.268	-0.069	-0.279	--------	0.997***	0.152	-0.892***	0.299	0.325*	-0.164
FSTFPPC (Pa)	0.279	-0.073	-0.289	0.997***	--------	0.153	-0.904***	0.274	0.300	-0.151
EDPLC (J/m^3)	-0.005	-0.243	-0.885***	0.152	0.153	---------	0.018	0.045	0.049	-0.155
EDPPC (J/m^3)	-0.290	0.008	0.112	-0.892***	-0.904***	0.018	--------	-0.194	-0.235	0.139

TABLE 13 Continued.

Variable[1]	WBSF	ISTFPLC	FSTFPLC	ISTFPPC	FSTFPPC	EDPLC	EDPPC	ISTFPR	FSTFPR	EDPR
Raw Data for Probe Compression										
ISTFPR (Pa)	0.251	0.163	0.061	0.299	0.274	0.045	-0.194	--------	0.977***	-0.787***
FSTFPR (Pa)	0.239	0.147	0.056	0.325*	0.300	0.049	-0.235	0.977***	--------	-0.785***
EDPR (J/m^3)	-0.156	-0.157	-0.037	-0.164	-0.151	-0.155	0.014	-0.787***	-0.785***	-------

*P<0.05 Significant
**P<0.01 Highly Significant
***P<0.001 Very Highly Significant
[1] Variable abbreviations: QG=Quality Grade; MARB=Marbling; YG=Yield Grade; MOIST=Moisture; PROT=Protein; SOLCOL=Soluble Collagen; TOTCOL=Total Collagen; CALPST =Calpastatin; CKYLD= Cook Yield; CTAMT=Connective Tissue Amount; MFTEND=Muscle Fiber Tenderness; OVERALL= Overall Tenderness; WBSF=Warner-Bratzler Shear Force; ISTFPLC=Initial Stiffness of Parallel Fibers-Platen Compression; FSTFPLC=Final Stiffness of Parallel Fibers-Platen Compression; EDPLC=Energy Dissipated in Parallel Fibers-Platen Compression; ISTFPPC=Initial Stiffness of Perpendicular Fibers-Platen Compression; FSTFPPC=Final Stiffness of Perpendicular Fibers-Platen Compression; EDPPC= Energy Dissipated in Perpendicular Fibers-Platen Compression; ISTFPR=Initial Stiffness-Probe Compression; FSTFPR=Final Stiffness-Probe Compression; EDPR=Energy Dissipated-Probe Compression.

TABLE 14. Pairwise correlation coefficients of "Adjusted Data" pooled over compression temperatures for biomechanical traits of *Longissimus dorsi* samples (Phase 2).

Variable[1]	WBSF	ISTFPLC	FSTFPLC	ISTFPPC	FSTFPPC	EDPLC	EDPPC	ISTFPR	FSTFPR	EDPR
Physical Data										
QG	-0.012	0.121	-0.121	0.275	0.285	0.101	-0.296	0.107	0.025	-0.106
MARB	-0.074	0.133	-0.171	0.301	0.301	0.146	-0.305	0.060	-0.019	-0.035
YG	-0.252	0.113	-0.078	0.167	0.182	0.031	-0.107	-0.220	-0.256	0.093
L*	0.063	0.023	-0.255	0.126	0.117	0.215	-0.148	0.071	0.124	-0.060
a*	-0.361*	0.216	0.000	-0.010	-0.022	0.078	0.154	-0.054	-0.119	0.111
b*	-0.331*	0.329*	-0.056	0.066	0.049	0.111	0.097	-0.027	-0.092	0.084
CKYLD (%)	-0.141	0.211	0.084	-0.177	-0.204	0.048	0.078	-0.026	-0.048	0.029
WBSF(kg)	--------	-0.233	-0.067	0.268	0.279	-0.005	-0.290	0.161	0.139	-0.062
Chemical Data										
pH	-0.030	0.106	0.063	0.076	0.067	0.033	-0.029	0.328*	0.370*	-0.317*
MOIST(%)	0.234	-0.286	-0.096	-0.063	-0.068	-0.008	0.122	-0.036	0.065	-0.045
FAT(%)	-0.230	0.217	-0.046	0.061	0.056	0.113	-0.047	0.001	-0.103	0.036
PROT(%)	0.479**	-0.044	0.128	0.103	0.120	-0.078	-0.168	0.131	0.158	-0.216
SOLCOL(%)	0.152	0.157	0.132	-0.084	-0.087	-0.037	-0.073	-0.018	0.038	0.120
TOTCOL(%)	0.082	0.231	0.018	-0.232	-0.226	0.070	0.107	-0.061	-0.040	0.174
CALPST(act/g)	0.052	-0.038	0.241	0.042	0.059	-0.229	-0.059	-0.083	-0.042	0.161
Sensory Data										
JUICY	-0.225	-0.001	0.143	-0.045	-0.064	-0.272	0.212	-0.163	-0.199	0.185
CTAMT	-0.755***	0.202	0.073	-0.398**	-0.411**	0.034	0.471**	-0.183	-0.238	0.137
MFTEND	-0.736***	0.115	0.018	-0.422**	-0.441**	0.031	0.541***	-0.298	-0.343*	0.272
OVERALL	-0.740***	0.149	0.028	-0.416**	-0.434**	0.019	0.534***	-0.321*	-0.363*	0.288
Platen Compression Data										
ISTFPLC(Pa)	-0.233	--------	0.300	-0.069	-0.073	-0.243	0.008	0.128	0.113	-0.118
FSTFPLC(Pa)	-0.067	0.300	--------	-0.279	-0.298	-0.885***	0.112	0.115	0.107	-0.039
ISTFPPC (Pa)	0.268	-0.069	-0.279	--------	0.997***	0.152	-0.892***	0.127	0.172	-0.063
FSTFPPC (Pa)	0.279	-0.073	-0.289	0.997***	--------	0.153	-0.904***	0.106	0.149	-0.052
EDPLC (J/m^3)	-0.005	-0.243	-0.885***	0.152	0.153	--------	0.018	0.048	0.056	-0.169
EDPPC (J/m^3)	-0.290	0.008	0.112	-0.892***	-0.904***	0.018	--------	-0.127	-0.185	0.064

TABLE 14 Continued.

Variable[1]	WBSF	ISTFPLC	FSTFPLC	ISTFPPC	FSTFPPC	EDPLC	EDPPC	ISTFPR	FSTFPR	EDPR
Adjusted Data for Probe Compression										
ISTFPR (Pa)	0.161	0.128	0.155	0.127	0.106	0.048	-0.127	--------	0.960***	-0.898***
FSTFPR (Pa)	0.139	0.113	0.107	0.172	0.149	0.056	-0.185	0.960***	-------	-0.862***
EDPR (J/m^3)	-0.062	-0.118	-0.039	-0.063	-0.052	-0.169	0.064	-0.898***	-0.862***	-------

*P<0.05 Significant
**P<0.01 Highly Significant
***P<0.001 Very Highly Significant
[1] Variable abbreviations: QG=Quality Grade; MARB=Marbling; YG=Yield Grade; MOIST=Moisture; PROT=Protein; SOLCOL=Soluble Collagen; TOTCOL=Total Collagen; CALPST =Calpastatin; CKYLD= Cook Yield; CTAMT=Connective Tissue Amount; MFTEND=Muscle Fiber Tenderness; OVERALL= Overall Tenderness; WBSF=Warner-Bratzler Shear Force; ISTFPLC=Initial Stiffness of Parallel Fibers-Platen Compression; FSTFPLC=Final Stiffness of Parallel Fibers-Platen Compression; EDPLC=Energy Dissipated in Parallel Fibers-Platen Compression; ISTFPPC=Initial Stiffness of Perpendicular Fibers-Platen Compression; FSTFPPC=Final Stiffness of Perpendicular Fibers-Platen Compression; EDPPC= Energy Dissipated in Perpendicular Fibers-Platen Compression; ISTFPR=Initial Stiffness-Probe Compression; FSTFPR=Final Stiffness-Probe Compression; EDPR=Energy Dissipated-Probe Compression.

TABLE 15. Pairwise correlation coefficients of "Raw Data" biomechanical traits of *Longissimus dorsi* samples (Phase 2) tempered to -6.6ºC prior to compression.

Variable[1]	WBSF	ISTFPLC	FSTFPLC	ISTFPPC	FSTFPPC	EDPLC	EDPPC	ISTFPR	FSTFPR	EDPR
Physical Data										
QG	…	-0.134	-0.143	0.230	0.244	0.239	-0.289	0.368	0.218	-0.674**
MARB	…	-0.227	-0.244	0.230	0.246	0.366	-0.273	0.286	0.135	-0.538*
YG	…	-0.173	-0.180	-0.138	-0.068	0.085	0.140	-0.336	-0.369	0.227
L*	…	-0.450	-0.460	0.067	0.084	0.494	-0.155	-0.037	0.095	0.056
a*	…	0.107	0.093	0.001	-0.009	0.102	0.145	0.233	0.110	-0.170
b*	…	-0.096	-0.177	0.024	0.021	0.320	0.175	0.182	0.084	-0.030
CKYLD (%)	…	0.304	0.282	-0.307	-0.351	-0.081	0.227	-0.127	-0.159	0.045
WBSF(kg)	--------	-0.361	-0.334	0.424	0.466	0.081	-0.427	0.380	0.310	-0.357
Chemical Data										
pH	…	0.305	0.328	0.059	0.056	-0.275	-0.191	-0.064	0.069	-0.384
MOIST(%)	…	0.029	0.064	0.085	0.076	-0.180	-0.111	-0.015	0.173	0.143
FAT(%)	…	-0.133	-0.162	-0.115	-0.108	0.302	0.092	-0.075	-0.242	-0.155
PROT(%)	…	-0.051	-0.037	0.394	0.431	0.010	-0.286	0.428	0.422	-0.411
SOLCOL(%)	…	0.138	0.153	-0.222	-0.264	-0.031	0.137	-0.247	-0.086	0.226
TOTCOL(%)	…	-0.329	-0.327	-0.194	-0.203	0.364	0.121	-0.474	-0.426	0.164
CALPST(act/g)	…	0.250	0.218	-0.328	-0.336	-0.134	0.219	-0.413	-0.313	0.467
Sensory Data										
JUICY	…	0.480	0.505	-0.327	-0.342	-0.494	0.429	-0.084	-0.083	0.286
CTAMT	…	0.103	0.082	-0.593*	-0.616*	0.150	0.650**	-0.392	-0.448	0.497
MFTEND	…	0.177	0.160	-0.663**	-0.689**	0.032	0.686**	-0.400	-0.434	0.531*
OVERALL	…	0.172	0.155	-0.664**	-0.691**	0.337	0.690**	-0.416	-0.444	0.561*
Platen Compression Data										
ISTFPLC(Pa)	-0.361	--------	0.998***	-0.277	-0.333	-0.894***	0.268	0.033	0.005	-0.007
FSTFPLC(Pa)	-0.334	0.998***	--------	-0.263	-0.319	-0.911***	0.251	0.038	0.017	-0.020
ISTFPPC (Pa)	0.424	-0.277	-0.263	--------	0.996***	0.248	-0.941***	0.811***	0.888***	-0.699**
FSTFPPC (Pa)	0.466	-0.333	-0.319	0.996***	--------	0.285	-0.938***	0.787***	0.862***	-0.688**
EDPLC (J/m^3)	0.081	-0.894***	-0.911***	0.248	0.285	--------	-0.187	0.011	0.018	-0.059
EDPPC (J/m^3)	-0.427	0.269	0.251	-0.941***	-0.938***	-0.187	--------	-0.742**	-0.829***	0.737**

TABLE 15 Continued.

Variable[1]	WBSF	ISTFPLC	FSTFPLC	ISTFPPC	FSTFPPC	EDPLC	EDPPC	ISTFPR	FSTFPR	EDPR
Raw Data for Probe Compression										
ISTFPR (Pa)	0.380	0.033	0.038	0.811***	0.787***	0.011	-0.742**	--------	0.947***	-0.743**
FSTFPR (Pa)	0.310	0.005	0.017	0.888***	0.862***	0.018	-0.829***	0.947***	-------	-0.713**
EDPR (J/m^3)	-0.357	-0.007	-0.020	-0.699**	-0.688**	-0.059	0.737**	-0.743**	-0.713**	-------

*P<0.05 Significant
**P<0.01 Highly Significant
***P<0.001 Very Highly Significant
[1] Variable abbreviations: QG=Quality Grade; MARB=Marbling; YG=Yield Grade; MOIST=Moisture; PROT=Protein; SOLCOL=Soluble Collagen; TOTCOL=Total Collagen; CALPST =Calpastatin; CKYLD= Cook Yield; CTAMT=Connective Tissue Amount; MFTEND=Muscle Fiber Tenderness; OVERALL= Overall Tenderness; WBSF=Warner-Bratzler Shear Force; ISTFPLC=Initial Stiffness of Parallel Fibers-Platen Compression; FSTFPLC=Final Stiffness of Parallel Fibers-Platen Compression; EDPLC=Energy Dissipated in Parallel Fibers-Platen Compression; ISTFPPC=Initial Stiffness of Perpendicular Fibers-Platen Compression; FSTFPPC=Final Stiffness of Perpendicular Fibers-Platen Compression; EDPPC= Energy Dissipated in Perpendicular Fibers-Platen Compression; ISTFPR=Initial Stiffness-Probe Compression; FSTFPR=Final Stiffness-Probe Compression; EDPR=Energy Dissipated-Probe Compression.

TABLE 16. Pairwise correlation coefficients of "Raw Data" biomechanical traits of *Longissimus dorsi* samples (Phase 2) tempered to 4.4ºC prior to compression.

Variable[1]	WBSF	ISTFPLC	FSTFPLC	ISTFPPC	FSTFPPC	EDPLC	EDPPC	ISTFPR	FSTFPR	EDPR
Physical Data										
QG	…	0.388	0.173	0.735**	0.729**	-0.533	-0.648*	-0.061	-0.108	0.301
MARB	…	0.385	0.173	0.736**	0.730**	-0.533	-0.651*	-0.063	-0.110	0.302
YG	…	0.289	0.638*	0.276	0.266	-0.563	-0.283	0.177	0.151	-0.092
L*	…	0.347	-0.177	0.158	0.130	0.111	0.038	0.431	0.416	-0.156
a*	…	0.492	0.262	0.244	0.238	-0.217	-0.307	0.251	0.229	-0.214
b*	…	0.724**	0.304	0.210	0.191	-0.322	-0.198	0.442	0.409	-0.309
CKYLD (%)	…	0.340	0.110	-0.262	-0.267	0.172	0.039	0.210	0.224	-0.210
WBSF(kg)	--------	-0.498	-0.305	0.067	0.047	0.246	0.048	0.367	0.392	-0.136
Chemical Data										
pH	…	0.182	-0.392	0.171	0.159	0.266	-0.029	0.464	0.436	-0.099
MOIST(%)	…	-0.438	-0.566*	-0.218	-0.221	0.566*	0.432	0.312	0.341	-0.357
FAT(%)	…	0.430	0.462	0.328	0.316	-0.553	-0.386	-0.122	-0.158	0.320
PROT(%)	…	-0.114	-0.072	-0.359	-0.361	0.271	0.240	0.422	0.462	-0.520
SOLCOL(%)	…	0.208	0.057	0.168	0.174	0.077	-0.484	-0.092	-0.085	0.044
TOTCOL(%)	…	0.419	0.253	-0.056	-0.058	-0.109	-0.106	-0.275	-0.295	0.365
CALPST(act/g)	…	-0.155	-0.068	0.070	0.057	0.002	0.253	0.268	0.246	0.026
Sensory Data										
JUICY	…	0.090	0.290	0.229	0.211	-0.571*	-0.017	-0.037	-0.068	0.232
CTAMT	…	0.432	0.625*	-0.165	-0.158	-0.582*	0.079	-0.261	-0.289	0.198
MFTEND	…	0.299	0.579*	-0.202	-0.198	-0.636*	0.224	-0.340	-0.378	0.381
OVERALL	…	0.348	0.578*	-0.230	-0.227	-0.616*	0.256	-0.345	-0.383	0.358
Platen Compression Data										
ISTFPLC(Pa)	-0.498	--------	0.334	-0.036	-0.049	-0.252	-0.010	0.203	0.176	-0.257
FSTFPLC(Pa)	-0.305	0.334	--------	-0.224	-0.227	-0.871***	0.038	-0.294	-0.312	0.291
ISTFPPC (Pa)	0.067	-0.036	-0.224	--------	0.999***	-0.106	-0.873***	0.125	0.104	0.094
FSTFPPC (Pa)	0.047	-0.049	-0.227	0.999***	--------	-0.103	-0.885***	0.095	0.074	0.114
EDPLC (J/m^3)	0.246	-0.252	-0.871***	-0.106	-0.103	--------	0.212	0.316	0.349	-0.443
EDPPC (J/m^3)	0.048	-0.010	0.038	-0.872**	-0.885***	0.212	--------	0.127	0.138	-0.252

TABLE 16 Continued.

Variable[1]	WBSF	ISTFPLC	FSTFPLC	ISTFPPC	FSTFPPC	EDPLC	EDPPC	ISTFPR	FSTFPR	EDPR
Raw Data for Probe Compression										
ISTFPR (Pa)	0.367	0.203	-0.294	0.125	0.095	0.316	0.127	--------	0.998***	-0.847***
FSTFPR (Pa)	0.392	0.176	-0.312	0.104	0.074	0.349	0.138	0.998***	-------	-0.863***
EDPR (J/m^3)	-0.136	-0.257	0.291	0.094	0.114	-0.443	-0.252	-0.841***	-0.863***	-------

*P<0.05 Significant
**P<0.01 Highly Significant
***P<0.001 Very Highly Significant
[1] Variable abbreviations: QG=Quality Grade; MARB=Marbling; YG=Yield Grade; MOIST=Moisture; PROT=Protein; SOLCOL=Soluble Collagen; TOTCOL=Total Collagen; CALPST =Calpastatin; CKYLD= Cook Yield; CTAMT=Connective Tissue Amount; MFTEND=Muscle Fiber Tenderness; OVERALL= Overall Tenderness; WBSF=Warner-Bratzler Shear Force; ISTFPLC=Initial Stiffness of Parallel Fibers-Platen Compression; FSTFPLC=Final Stiffness of Parallel Fibers-Platen Compression; EDPLC=Energy Dissipated in Parallel Fibers-Platen Compression; ISTFPPC=Initial Stiffness of Perpendicular Fibers-Platen Compression; FSTFPPC=Final Stiffness of Perpendicular Fibers-Platen Compression; EDPPC= Energy Dissipated in Perpendicular Fibers-Platen Compression; ISTFPR=Initial Stiffness-Probe Compression; FSTFPR=Final Stiffness-Probe Compression; EDPR=Energy Dissipated-Probe Compression.

TABLE 17. Pairwise correlation coefficients of "Raw Data" biomechanical traits of *Longissimus dorsi* samples (Phase 2) tempered to 10°C prior to compression.

Variable[1]	WBSF	ISTFPLC	FSTFPLC	ISTFPPC	FSTFPPC	EDPLC	EDPPC	ISTFPR	FSTFPR	EDPR
Physical Data										
QG	…	-0.329	-0.333	0.049	0.040	0.336	-0.017	-0.240	-0.230	0.181
MARB	…	-0.329	-0.333	0.046	0.037	0.335	-0.015	-0.237	-0.227	0.178
YG	…	-0.547	-0.553	0.341	0.316	0.458	-0.127	-0.414	-0.406	0.234
L*	…	-0.022	0.013	0.083	0.100	-0.253	-0.405	-0.046	-0.028	-0.027
a*	…	-0.232	-0.253	-0.186	-0.217	0.277	0.518	-0.164	-0.209	0.341
b*	…	-0.233	-0.248	-0.068	-0.097	0.168	0.346	-0.139	-0.191	0.339
CKYLD (%)	…	-0.132	-0.114	0.004	-0.019	0.019	-0.048	-0.205	-0.212	0.280
WBSF(kg)	--------	0.355	0.363	0.246	0.271	-0.326	-0.438	0.105	0.139	-0.023
Chemical Data										
pH	…	0.188	0.164	-0.026	-0.019	0.220	0.085	0.441	0.458	-0.539
MOIST(%)	…	0.340	0.368	-0.070	-0.059	-0.575*	-0.028	-0.117	-0.112	0.188
FAT(%)	…	-0.418	-0.435	-0.030	-0.052	0.534	0.181	-0.109	-0.123	0.120
PROT(%)	…	0.423	0.434	0.235	0.254	-0.412	-0.374	0.062	0.095	-0.190
SOLCOL(%)	…	0.160	0.179	-0.281	-0.270	-0.141	0.241	-0.077	-0.053	0.148
TOTCOL(%)	…	0.163	0.177	-0.455	-0.434	-0.118	0.345	0.011	0.035	0.113
CALPST(act/g)	…	0.544	0.532	0.339	0.375	-0.533	-0.456	0.182	0.194	-0.043
Sensory Data										
JUICY	…	-0.412	-0.417	-0.075	-0.087	0.233	0.205	-0.204	-0.250	0.176
CTAMT	…	-0.351	-0.365	-0.407	-0.435	0.358	0.638*	-0.026	-0.080	0.073
MFTEND	…	-0.528	-0.535	-0.329	-0.368	0.480	0.657*	-0.208	-0.262	0.257
OVERALL	…	-0.554	-0.562	-0.275	-0.315	0.492	0.616*	-0.237	-0.292	0.279
Platen Compression Data										
ISTFPLC(Pa)	0.355	--------	0.998***	-0.336	-0.299	-0.845***	0.018	0.591*	0.601*	-0.408
FSTFPLC(Pa)	0.363	0.998***	--------	-0.346	-0.308	-0.868***	0.018	0.563	0.574*	-0.375
ISTFPPC (Pa)	0.246	-0.336	-0.346	--------	0.999***	0.247	-0.877***	-0.305	-0.298	0.100
FSTFPPC (Pa)	0.271	-0.299	-0.308	0.999***	--------	0.210	-0.897***	-0.279	-0.271	0.078
EDPLC (J/m^3)	-0.326	-0.845***	-0.868***	0.247	0.211	--------	0.114	-0.249	-0.259	0.016
EDPPC (J/m^3)	-0.438	0.018	0.018	-0.877***	-0.897***	0.114	--------	0.092	0.072	0.051

TABLE 17 Continued.

Variable[1]	WBSF	ISTFPLC	FSTFPLC	ISTFPPC	FSTFPPC	EDPLC	EDPPC	ISTFPR	FSTFPR	EDPR
Raw Data for Probe Compression										
ISTFPR (Pa)	0.105	0.591*	0.563	-0.305	-0.279	-0.249	0.092	--------	0.998***	-0.847***
FSTFPR (Pa)	0.139	0.601*	0.574*	-0.298	-0.271	-0.259	0.072	0.998***	-------	-0.859***
EDPR (J/m^3)	-0.023	-0.408	-0.375	0.100	0.078	0.016	0.051	-0.847***	-0.859***	-------

*P<0.05 Significant
**P<0.01 Highly Significant
***P<0.001 Very Highly Significant
[1] Variable abbreviations: QG=Quality Grade; MARB=Marbling; YG=Yield Grade; MOIST=Moisture; PROT=Protein; SOLCOL=Soluble Collagen; TOTCOL=Total Collagen; CALPST =Calpastatin; CKYLD= Cook Yield; CTAMT=Connective Tissue Amount; MFTEND=Muscle Fiber Tenderness; OVERALL= Overall Tenderness; WBSF=Warner-Bratzler Shear Force; ISTFPLC=Initial Stiffness of Parallel Fibers-Platen Compression; FSTFPLC=Final Stiffness of Parallel Fibers-Platen Compression; EDPLC=Energy Dissipated in Parallel Fibers-Platen Compression; ISTFPPC=Initial Stiffness of Perpendicular Fibers-Platen Compression; FSTFPPC=Final Stiffness of Perpendicular Fibers-Platen Compression; EDPPC= Energy Dissipated in Perpendicular Fibers-Platen Compression; ISTFPR=Initial Stiffness-Probe Compression; FSTFPR=Final Stiffness-Probe Compression; EDPR=Energy Dissipated-Probe Compression.

TABLE 18. Pairwise correlation coefficients of "Adjusted Data" biomechanical traits of *Longissimus dorsi* samples (Phase 2) tempered to -6.6°C prior to compression.

Variable[1]	WBSF	ISTFPLC	FSTFPLC	ISTFPPC	FSTFPPC	EDPLC	EDPPC	ISTFPR	FSTFPR	EDPR
Physical Data										
QG	…	-0.134	-0.143	0.230	0.244	0.239	-0.289	0.436	0.263	-0.590*
MARB	…	-0.227	-0.244	0.230	0.246	0.366	-0.273	0.422	0.237	-0.530*
YG	…	-0.173	-0.180	-0.138	-0.068	0.085	0.140	-0.213	-0.317	0.080
L*	…	-0.450	-0.460	0.067	0.084	0.494	-0.155	-0.166	0.039	0.150
a*	…	0.107	0.093	0.001	-0.009	0.102	0.145	0.112	-0.031	-0.110
b*	…	-0.096	-0.177	0.024	0.021	0.320	0.175	-0.020	-0.128	0.018
CKYLD (%)	…	0.304	0.282	-0.307	-0.351	-0.081	0.227	0.068	0.031	-0.035
WBSF(kg)	--------	-0.361	-0.334	0.424	0.466	0.081	-0.427	0.192	0.098	-0.271
Chemical Data										
pH	…	0.305	0.328	0.059	0.056	-0.275	-0.191	0.137	0.313	-0.244
MOIST(%)	…	0.029	0.064	0.085	0.076	-0.180	-0.111	-0.266	-0.006	0.356
FAT(%)	…	-0.133	-0.162	-0.115	-0.108	0.302	0.092	0.289	0.056	-0.372
PROT(%)	…	-0.051	-0.037	0.394	0.431	0.010	-0.286	0.082	0.080	-0.198
SOLCOL(%)	…	0.138	0.153	-0.222	-0.264	-0.031	0.137	-0.104	0.121	0.254
TOTCOL(%)	…	0.250	0.218	-0.328	-0.336	-0.134	0.219	-0.342	-0.235	0.426
Sensory Data										
JUICY	…	0.480	0.505	-0.327	-0.342	-0.494	0.429	-0.156	-0.160	0.227
CTAMT	…	0.103	0.082	-0.593*	-0.616*	0.150	0.650*	-0.243	-0.323	0.326
MFTEND	…	0.177	0.160	-0.663**	-0.689**	0.032	0.686**	-0.333	-0.375	0.421
OVERALL	…	0.172	0.155	-0.664**	-0.691**	0.337	0.690**	-0.346	-0.383	0.443
Platen Compression Data										
ISTFPLC(Pa)	-0.361	--------	0.998***	-0.277	-0.333	-0.894***	0.268	0.187	0.147	-0.101
FSTFPLC(Pa)	-0.334	0.998***	--------	-0.263	-0.319	-0.911***	0.251	0.204	0.173	-0.115
ISTFPPC (Pa)	0.424	-0.277	-0.263	--------	0.996***	0.248	-0.941***	0.541*	0.687**	-0.486
FSTFPPC (Pa)	0.466	-0.333	-0.319	0.996***	--------	0.285	-0.938***	0.500	0.639**	-0.466
EDPLC (J/m^3)	0.081	-0.894***	-0.911***	0.248	0.285	--------	-0.187	-0.094	-0.072	0.019
EDPPC (J/m^3)	-0.427	0.269	0.251	-0.941***	-0.938***	-0.187	--------	-0.582*	-0.739**	0.543*

TABLE 18 Continued.

Variable[1]	WBSF	ISTFPLC	FSTFPLC	ISTFPPC	FSTFPPC	EDPLC	EDPPC	ISTFPR	FSTFPR	EDPR
Adjusted Data for Probe Compression										
ISTFPR (Pa)	0.192	0.187	0.204	0.541*	0.500	-0.094	-0.582*	--------	0.895***	-0.936***
FSTFPR (Pa)	0.098	0.147	0.173	0.687**	0.639**	-0.072	-0.739**	0.895***	-------	-0.805***
EDPR (J/m^3)	-0.271	-0.101	-0.115	-0.486	-0.466	0.019	0.543*	-0.936***	-0.805***	-------

*P<0.05 Significant
**P<0.01 Highly Significant
***P<0.001 Very Highly Significant
[1] Variable abbreviations: QG=Quality Grade; MARB=Marbling; YG=Yield Grade; MOIST=Moisture; PROT=Protein; SOLCOL=Soluble Collagen; TOTCOL=Total Collagen; CALPST =Calpastatin; CKYLD= Cook Yield; CTAMT=Connective Tissue Amount; MFTEND=Muscle Fiber Tenderness; OVERALL= Overall Tenderness; WBSF=Warner-Bratzler Shear Force; ISTFPLC=Initial Stiffness of Parallel Fibers-Platen Compression; FSTFPLC=Final Stiffness of Parallel Fibers-Platen Compression; EDPLC=Energy Dissipated in Parallel Fibers-Platen Compression; ISTFPPC=Initial Stiffness of Perpendicular Fibers-Platen Compression; FSTFPPC=Final Stiffness of Perpendicular Fibers-Platen Compression; EDPPC= Energy Dissipated in Perpendicular Fibers-Platen Compression; ISTFPR=Initial Stiffness-Probe Compression; FSTFPR=Final Stiffness-Probe Compression; EDPR=Energy Dissipated-Probe Compression.

TABLE 19. Pairwise correlation coefficients of "Adjusted Data" biomechanical traits of *Longissimus dorsi* samples (Phase 2) tempered to 4.4ºC prior to compression.

Variable[1]	WBSF	ISTFPLC	FSTFPLC	ISTFPPC	FSTFPPC	EDPLC	EDPPC	ISTFPR	FSTFPR	EDPR
Physical Data										
QG	…	0.388	0.173	0.735**	0.729**	-0.533	-0.648*	-0.114	-0.160	0.387
MARB	…	0.385	0.173	0.736**	0.730**	-0.533	-0.651*	-0.116	-0.161	0.389
YG	…	0.289	0.638*	0.276	0.266	-0.563	-0.283	0.032	0.001	-0.045
L*	…	0.347	-0.177	0.158	0.130	0.111	0.038	0.098	0.067	0.020
a*	…	0.492	0.262	0.244	0.238	-0.217	-0.307	0.383	0.357	-0.196
b*	…	0.724**	0.304	0.210	0.191	-0.322	-0.198	0.394	0.349	-0.187
CKYLD (%)	…	0.340	0.110	-0.262	-0.267	0.172	0.039	0.190	0.196	-0.167
WBSF(kg)	--------	-0.498	-0.305	0.067	0.047	0.246	0.048	0.149	0.173	0.072
Chemical Data										
pH	…	0.182	-0.392	0.171	0.159	0.266	-0.029	0.157	0.111	0.050
MOIST(%)	…	-0.438	-0.566	-0.218	-0.221	0.566	0.432	0.275	0.301	-0.369
FAT(%)	…	0.430	0.462	0.328	0.316	-0.553	-0.386	-0.228	-0.265	0.437
PROT(%)	…	-0.114	-0.072	-0.359	-0.361	0.271	0.240	0.192	0.223	-0.439
SOLCOL(%)	…	0.208	0.057	0.168	0.174	0.077	-0.484	-0.097	-0.097	0.052
TOTCOL(%)	…	0.419	0.253	-0.056	-0.058	-0.109	-0.106	-0.339	-0.363	0.391
CALPST(act/g)	…	0.250	0.155	-0.068	0.070	0.002	0.253	-0.097	-0.123	0.152
Sensory Data										
JUICY	…	0.090	0.290	0.229	0.211	-0.571*	-0.017	-0.237	-0.274	0.340
CTAMT	…	0.432	0.625*	-0.165	-0.158	-0.582*	0.079	-0.276	-0.308	0.090
MFTEND	…	0.299	0.579*	-0.202	-0.198	-0.636*	0.224	-0.426	-0.470	0.288
OVERALL	…	0.348	0.578*	-0.230	-0.227	-0.616*	0.256	-0.399	-0.442	0.254
Platen Compression Data										
ISTFPLC(Pa)	-0.498	--------	0.334	-0.036	-0.049	-0.252	-0.010	0.272	0.228	-0.246
FSTFPLC(Pa)	-0.305	0.334	--------	-0.224	-0.227	-0.871***	0.038	-0.457	-0.480	0.314
ISTFPPC (Pa)	0.067	-0.036	-0.224	--------	0.999***	-0.106	-0.873***	-0.013	-0.023	0.222
FSTFPPC (Pa)	0.047	-0.049	-0.227	0.999***	--------	-0.103	-0.885***	-0.031	-0.040	0.233
EDPLC (J/m^3)	0.246	-0.252	-0.871***	-0.106	-0.103	--------	0.212	0.520	0.554	-0.511
EDPPC (J/m^3)	0.048	-0.010	0.038	-0.873***	-0.885***	0.212	--------	0.213	0.213	-0.340

TABLE 19 Continued.

Variable[1]	WBSF	ISTFPLC	FSTFPLC	ISTFPPC	FSTFPPC	EDPLC	EDPPC	ISTFPR	FSTFPR	EDPR
Adjusted Data for Probe Compression										
ISTFPR (Pa)	0.149	0.272	-0.457	0.013	-0.031	0.520	0.213	--------	0.997***	-0.891***
FSTFPR (Pa)	0.173	0.228	-0.480	-0.023	-0.040	0.554	0.213	0.997***	-------	-0.903***
EDPR (J/m^3)	0.072	-0.246	0.320	0.222	0.233	-0.511	-0.340	-0.891***	-0.903***	-------

*P<0.05 Significant
**P<0.01 Highly Significant
***P<0.001 Very Highly Significant
[1] Variable abbreviations: QG=Quality Grade; MARB=Marbling; YG=Yield Grade; MOIST=Moisture; PROT=Protein; SOLCOL=Soluble Collagen; TOTCOL=Total Collagen; CALPST =Calpastatin; CKYLD= Cook Yield; CTAMT=Connective Tissue Amount; MFTEND=Muscle Fiber Tenderness; OVERALL= Overall Tenderness; WBSF=Warner-Bratzler Shear Force; ISTFPLC=Initial Stiffness of Parallel Fibers-Platen Compression; FSTFPLC=Final Stiffness of Parallel Fibers-Platen Compression; EDPLC=Energy Dissipated in Parallel Fibers-Platen Compression; ISTFPPC=Initial Stiffness of Perpendicular Fibers-Platen Compression; FSTFPPC=Final Stiffness of Perpendicular Fibers-Platen Compression; EDPPC= Energy Dissipated in Perpendicular Fibers-Platen Compression; ISTFPR=Initial Stiffness-Probe Compression; FSTFPR=Final Stiffness-Probe Compression; EDPR=Energy Dissipated-Probe Compression.

TABLE 20. Pairwise correlation coefficients of "Adjusted Data" biomechanical traits of *Longissimus dorsi* samples (Phase 2) tempered to 10°C prior to compression.

Variable[1]	WBSF	ISTFPLC	FSTFPLC	ISTFPPC	FSTFPPC	EDPLC	EDPPC	ISTFPR	FSTFPR	EDPR
Physical Data										
QG	…	-0.329	-0.333	0.049	0.040	0.336	-0.017	-0.271	-0.266	0.155
MARB	…	-0.329	-0.333	0.046	0.037	0.335	-0.015	-0.268	-0.263	0.152
YG	…	-0.547	-0.553	0.341	0.316	0.458	-0.127	-0.391	-0.382	0.195
L*	…	-0.022	0.013	0.083	0.100	-0.253	-0.405	0.122	0.134	-0.124
a*	…	-0.232	-0.253	-0.186	-0.217	0.277	0.518	-0.353	-0.384	0.369
b*	…	-0.233	-0.248	-0.068	-0.097	0.168	0.346	-0.345	-0.382	0.357
CKYLD (%)	…	-0.132	-0.114	0.004	-0.019	0.019	-0.048	-0.320	-0.320	0.287
WBSF(kg)	--------	0.355	0.363	0.246	0.271	-0.326	-0.438	0.098	0.123	0.047
Chemical Data										
pH	…	0.188	0.164	-0.026	-0.019	0.220	0.085	0.645*	0.652*	-0.649*
MOIST(%)	…	0.340	0.368	-0.070	-0.059	-0.575*	-0.028	-0.113	-0.105	0.253
FAT(%)	…	-0.418	-0.435	-0.030	-0.052	0.534	0.181	-0.149	-0.161	0.058
PROT(%)	…	0.423	0.434	0.235	0.254	-0.412	-0.374	0.151	0.176	-0.139
SOLCOL(%)	…	0.160	0.179	-0.281	-0.270	-0.141	0.241	0.085	0.102	0.126
TOTCOL(%)	…	0.163	0.177	-0.455	-0.434	-0.118	0.345	0.181	0.194	0.056
CALPST(act/g)	…	0.544	0.532	0.339	0.375	-0.533	-0.456	0.079	0.090	0.046
Sensory Data										
JUICY	…	-0.412	-0.417	-0.075	-0.087	0.233	0.205	-0.269	-0.303	0.164
CTAMT	…	-0.351	-0.365	-0.407	-0.435	0.358	0.638*	-0.071	-0.113	0.021
MFTEND	…	-0.528	-0.535	-0.329	-0.368	0.480	0.657*	-0.222	-0.263	0.179
OVERALL	…	-0.554	-0.562	-0.275	-0.315	0.492	0.616*	-0.264	-0.305	0.206
Platen Compression Data										
ISTFPLC(Pa)	0.355	--------	0.998***	-0.336	-0.299	-0.845***	0.018	0.466	0.474	-0.296
FSTFPLC(Pa)	0.363	0.998***	--------	-0.346	-0.308	-0.868***	0.018	0.446	0.455	-0.266
ISTFPPC (Pa)	0.246	-0.336	-0.346	--------	0.999***	0.247	-0.877***	-0.284	-0.277	0.093
FSTFPPC (Pa)	0.271	-0.299	-0.308	0.999***	--------	0.210	-0.897***	-0.253	-0.246	0.071
EDPLC (J/m^3)	-0.326	-0.845***	-0.868***	0.247	0.211	--------	0.114	-0.136	-0.148	-0.087
EDPPC (J/m^3)	-0.438	0.018	0.018	-0.877***	-0.897***	0.114	--------	0.068	0.052	0.040

TABLE 20 Continued.

Variable[1]	WBSF	ISTFPLC	FSTFPLC	ISTFPPC	FSTFPPC	EDPLC	EDPPC	ISTFPR	FSTFPR	EDPR
Adjusted Data for Probe Compression										
ISTFPR (Pa)	0.098	0.466	0.446	-0.284	-0.253	-0.136	0.068	--------	0.999***	-0.890***
FSTFPR (Pa)	0.123	0.474	0.454	-0.277	-0.246	-0.148	0.052	0.999***	-------	-0.890***
EDPR (J/m^3)	0.047	-0.296	-0.266	0.093	0.071	-0.087	0.040	-0.890***	-0.890***	--------

*P<0.05 Significant
**P<0.01 Highly Significant
***P<0.001 Very Highly Significant
[1] Variable abbreviations: QG=Quality Grade; MARB=Marbling; YG=Yield Grade; MOIST=Moisture; PROT=Protein; SOLCOL=Soluble Collagen; TOTCOL=Total Collagen; CALPST =Calpastatin; CKYLD= Cook Yield; CTAMT=Connective Tissue Amount; MFTEND=Muscle Fiber Tenderness; OVERALL= Overall Tenderness; WBSF=Warner-Bratzler Shear Force; ISTFPLC=Initial Stiffness of Parallel Fibers-Platen Compression; FSTFPLC=Final Stiffness of Parallel Fibers-Platen Compression; EDPLC=Energy Dissipated in Parallel Fibers-Platen Compression; ISTFPPC=Initial Stiffness of Perpendicular Fibers-Platen Compression; FSTFPPC=Final Stiffness of Perpendicular Fibers-Platen Compression; EDPPC= Energy Dissipated in Perpendicular Fibers-Platen Compression; ISTFPR=Initial Stiffness-Probe Compression; FSTFPR=Final Stiffness-Probe Compression; EDPR=Energy Dissipated-Probe Compression.

TABLE 21. Prediction equations for sensory traits utilizing TA platen and probe compression values[1] for pooled data at all compression temperatures (Phase 2).

	Raw data				Adjusted Data				
JUICINESS									
Equation	**β value**	**R^2**	**RMSE**	**Cp**	**Equation**	**β value**	**R^2**	**RMSE**	**Cp**
Intercept	6.52411	0.0737	0.624	9.075	Intercept	6.52411	0.0737	0.624	9.457
EDPLC	-0.18830				EDPLC	-0.18830			
CONNECTIVE TISSUE AMOUNT									
Equation	**β value**	**R^2**	**RMSE**	**Cp**	**Equation**	**β value**	**R^2**	**RMSE**	**Cp**
Intercept	5.62068	0.2214	0.612	1.067	Intercept	5.62068	0.2214	0.612	0.782
EDPPC	0.42429				EDPPC	0.42429			
MUSCLE FIBER TENDERNESS									
Equation	**β value**	**R^2**	**RMSE**	**Cp**	**Equation**	**β value**	**R^2**	**RMSE**	**Cp**
Intercept	2.57073	0.3839	0.787	2.291	Intercept	5.12874	0.3884	0.784	1.721
EDPPC	0.63982				EDPPC	0.61928			
EDPR	165.90497				FSTFPR	-0.00676			
OVERALL TENDERNESS									
Equation	**β value**	**R^2**	**RMSE**	**Cp**	**Equation**	**β value**	**R^2**	**RMSE**	**Cp**
Intercept	-1.29916	0.4678	0.760	2.886	Intercept	5.28221	0.3953	0.787	2.715
ISTFPLC	0.00000930				EDPPC	0.61200			
ISTFPPC	0.00013314				FSTFPR	-0.00729			
EDPPC	1.13170								
EDPR	209.05179								

[1] Variable abbreviation explanation: ISTFPLC=Initial Stiffness of Parallel Fibers-Platen Compression; FSTFPLC=Final Stiffness of Parallel Fibers-Platen Compression; EDPLC=Energy Dissipated in Parallel Fibers-Platen Compression; ISTFPPC=Initial Stiffness of Perpendicular Fibers-Platen Compression; FSTFPPC=Final Stiffness of Perpendicular Fibers-Platen Compression; EDPPC= Energy Dissipated in Perpendicular Fibers-Platen Compression; ISTFPR=Initial Stiffness-Probe Compression; FSTFPR=Final Stiffness-Probe Compression; EDPR=Energy Dissipated-Probe Compression; R^2 = R-square; RMSE = Root Mean Squared Error; Cp = Mallow's Cp.

TABLE 22. Prediction equations for sensory traits utilizing TA platen and probe compression values[1] for pooled data at –6.6ºC (Phase 2).

	Raw data				Adjusted Data				
JUICINESS									
Equation	**β value**	**R^2**	**RMSE**	**Cp**	**Equation**	**β value**	**R^2**	**RMSE**	**Cp**
Intercept	4.93701	0.2554	0.592	20.345	Intercept	4.93701	0.2554	0.592	2.222
FSTFPLC	0.00011166				FSTFPLC	0.00011166			
CONNECTIVE TISSUE AMOUNT									
Equation	**β value**	**R^2**	**RMSE**	**Cp**	**Equation**	**β value**	**R^2**	**RMSE**	**Cp**
Intercept	5.03940	0.4223	0.553	4.496	Intercept	5.03940	0.4223	0.553	2.037
EDPPC	0.60405				EDPPC	0.60405			
MUSCLE FIBER TENDERNESS									
Equation	**β value**	**R^2**	**RMSE**	**Cp**	**Equation**	**β value**	**R^2**	**RMSE**	**Cp**
Intercept	7.09594	0.7660	0.593	3.501	Intercept	9.10983	0.4752	0.810	1.124
FSTFPPC	-0.00070699				FSTFPPC	-0.00027590			
EDPLC	0.51189								
FSTFPR	0.02275								
OVERALL TENDERNESS									
Equation	**β value**	**R^2**	**RMSE**	**Cp**	**Equation**	**β value**	**R^2**	**RMSE**	**Cp**
Intercept	9.15711	0.4769	0.818	12.443	Intercept	9.15711	0.4769	0.818	1.824
FSTFPPC	-0.00027935				FSTFPPC	-0.00027935			

[1] Variable abbreviation explanation: ISTFPLC=Initial Stiffness of Parallel Fibers-Platen Compression; FSTFPLC=Final Stiffness of Parallel Fibers-Platen Compression; EDPLC=Energy Dissipated in Parallel Fibers-Platen Compression; ISTFPPC=Initial Stiffness of Perpendicular Fibers-Platen Compression; FSTFPPC=Final Stiffness of Perpendicular Fibers-Platen Compression; EDPPC= Energy Dissipated in Perpendicular Fibers-Platen Compression; ISTFPR=Initial Stiffness-Probe Compression; FSTFPR=Final Stiffness-Probe Compression; EDPR=Energy Dissipated-Probe Compression; R^2 = R-square; RMSE = Root Mean Squared Error; Cp = Mallow's Cp.

TABLE 23. Prediction equations for sensory traits utilizing TA platen and probe compression values[1] for pooled data at 4.4ºC (Phase 2).

	Raw data				Adjusted Data				
JUICINESS									
Equation	**β value**	**R^2**	**RMSE**	**Cp**	**Equation**	**β value**	**R^2**	**RMSE**	**Cp**
Intercept	11.45486	0.5037	0.504	5.758	Intercept	11.45486	0.5037	0.504	-0.809
FSTFPLC	-0.00020519				FSTFPLC	-0.00020519			
EDPLC	-1.02538				EDPLC	-1.02538			
CONNECTIVE TISSUE AMOUNT									
Equation	**β value**	**R^2**	**RMSE**	**Cp**	**Equation**	**β value**	**R^2**	**RMSE**	**Cp**
Intercept	6.04280	0.3902	0.430	10.033	Intercept	6.04280	0.3902	0.430	-2.772
FSTFPLC	0.00012098				FSTFPLC	0.00012098			
MUSCLE FIBER TENDERNESS									
Equation	**β value**	**R^2**	**RMSE**	**Cp**	**Equation**	**β value**	**R^2**	**RMSE**	**Cp**
Intercept	7.42362	0.5393	0.531	3.859	Intercept	7.42362	0.5393	0.531	9.858
EDPLC	-0.60812				EDPLC	-0.60812			
EDPPC	0.31118				EDPPC	0.31118			
OVERALL TENDERNESS									
Equation	**β value**	**R^2**	**RMSE**	**Cp**	**Equation**	**β value**	**R^2**	**RMSE**	**Cp**
Intercept	7.45088	0.5361	0.593	3.703	Intercept	7.45088	0.5361	0.593	13.032
EDPLC	-0.66424				EDPLC	-0.66424			
EDPPC	0.37355				EDPPC	0.37355			

[1] Variable abbreviation explanation: ISTFPLC=Initial Stiffness of Parallel Fibers-Platen Compression; FSTFPLC=Final Stiffness of Parallel Fibers-Platen Compression; EDPLC=Energy Dissipated in Parallel Fibers-Platen Compression; ISTFPPC=Initial Stiffness of Perpendicular Fibers-Platen Compression; FSTFPPC=Final Stiffness of Perpendicular Fibers-Platen Compression; EDPPC= Energy Dissipated in Perpendicular Fibers-Platen Compression; ISTFPR=Initial Stiffness-Probe Compression; FSTFPR=Final Stiffness-Probe Compression; EDPR=Energy Dissipated-Probe Compression; R^2 = R-square; RMSE = Root Mean Squared Error; Cp = Mallow's Cp.

TABLE 24. Prediction equations for sensory traits utilizing TA platen and probe compression values[1] for pooled data at 10ºC (Phase 2).

	Raw data				Adjusted Data				
JUICINESS									
Equation	**β value**	**R^2**	**RMSE**	**Cp**	**Equation**	**β value**	**R^2**	**RMSE**	**Cp**
No variable met the 0.15 significance level for entry into the model.					No variable met the 0.15 significance level for entry into the model.				
CONNECTIVE TISSUE AMOUNT									
Equation	**β value**	**R^2**	**RMSE**	**Cp**	**Equation**	**β value**	**R^2**	**RMSE**	**Cp**
Intercept	5.43340	0.5481	0.569	6.177	Intercept	5.43340	0.5481	0.569	4.635
FSTFPLC	-0.00010075				FSTFPLC	-0.00010075			
EDPPC	0.67680				EDPPC	0.67680			
MUSCLE FIBER TENDERNESS									
Equation	**β value**	**R^2**	**RMSE**	**Cp**	**Equation**	**β value**	**R^2**	**RMSE**	**Cp**
Intercept	4.47043	0.7307	0.629	8.045	Intercept	4.47043	0.7307	0.629	5.267
FSTFPLC	-0.00021008				FSTFPLC	-0.00021008			
EDPPC	1.00258				EDPPC	1.00258			
OVERALL TENDERNESS									
Equation	**β value**	**R^2**	**RMSE**	**Cp**	**Equation**	**β value**	**R^2**	**RMSE**	**Cp**
Intercept	4.88366	0.7075	0.635	13.211	Intercept	4.88366	0.7075	0.635	9.488
FSTFPLC	-0.00021298				FSTFPLC	-0.00021298			
EDPPC	0.91179				EDPPC	0.91179			

[1] Variable abbreviation explanation: ISTFPLC=Initial Stiffness of Parallel Fibers-Platen Compression; FSTFPLC=Final Stiffness of Parallel Fibers-Platen Compression; EDPLC=Energy Dissipated in Parallel Fibers-Platen Compression; ISTFPPC=Initial Stiffness of Perpendicular Fibers-Platen Compression; FSTFPPC=Final Stiffness of Perpendicular Fibers-Platen Compression; EDPPC= Energy Dissipated in Perpendicular Fibers-Platen Compression; ISTFPR=Initial Stiffness-Probe Compression; FSTFPR=Final Stiffness-Probe Compression; EDPR=Energy Dissipated-Probe Compression; R^2 = R-square; RMSE = Root Mean Squared Error; Cp = Mallow's Cp.

TABLE 25. Prediction equations for sensory traits using TA probe compression values[1] for pooled data at all compression temperatures (Phase 2).

	Raw data					Adjusted Data			
JUICINESS									
Equation	**β value**	**R^2**	**RMSE**	**Cp**	**Equation**	**β value**	**R^2**	**RMSE**	**Cp**
Intercept	4.47474	0.0696	0.626	4.00	Intercept	5.35476	0.0573	0.630	4.00
ISTFPR	0.00879				ISTFPR	0.00622			
FSTFPR	-0.00825				FSTFPR	-0.00750			
EDPR	115.01261				EDPR	55.65510			
CONNECTIVE TISSUE AMOUNT									
Equation	**β value**	**R^2**	**RMSE**	**Cp**	**Equation**	**β value**	**R^2**	**RMSE**	**Cp**
Intercept	6.95781	0.1063	0.663	4.00	Intercept	8.38396	0.0877	0.670	4.00
ISTFPR	0.42429				ISTFPR	0.00585			
FSTFPR	-0.01615				FSTFPR	-0.01198			
EDPR	58.53221				EDPR	-41.28086			
MUSCLE FIBER TENDERNESS									
Equation	**β value**	**R^2**	**RMSE**	**Cp**	**Equation**	**β value**	**R^2**	**RMSE**	**Cp**
Intercept	5.11381	0.1723	0.919	4.00	Intercept	7.31121	0.1304	0.942	4.00
ISTFPR	0.01657				ISTFPR	0.00771			
FSTFPR	-0.02082				FSTFPR	-0.01565			
EDPR	174.25089				EDPR	11.59238			
OVERALL TENDERNESS									
Equation	**β value**	**R^2**	**RMSE**	**Cp**	**Equation**	**β value**	**R^2**	**RMSE**	**Cp**
Intercept	5.20368	0.1827	0.921	4.00	Intercept	7.59887	0.1417	0.944	4.00
ISTFPR	0.01551				ISTFPR	0.00653			
FSTFPR	-0.02000				FSTFPR	-0.01524			
EDPR	177.51707				EDPR	1.32008			

[1] Variable abbreviation explanation: ISTFPR=Initial Stiffness-Probe Compression; FSTFPR=Final Stiffness-Probe Compression; EDPR=Energy Dissipated-Probe Compression; R^2 = R-square; RMSE = Root Mean Squared Error; Cp = Mallock's Cp.

TABLE 26. Prediction equations for sensory traits using TA probe compression values[1] for pooled data at –6.6ºC (Phase 2).

	Raw data				Adjusted Data				
JUICINESS									
Equation	**β value**	**R^2**	**RMSE**	**Cp**	**Equation**	**β value**	**R^2**	**RMSE**	**Cp**
Intercept	3.61799	0.1188	0.706	4.00	Intercept	2.80932	0.0873	0.718	4.00
ISTFPR	0.00302				ISTFPR	0.00843			
FSTFPR	0.00020843				FSTFPR	-0.00321			
EDPR	214.10019				EDPR	247.62804			
CONNECTIVE TISSUE AMOUNT									
Equation	**β value**	**R^2**	**RMSE**	**Cp**	**Equation**	**β value**	**R^2**	**RMSE**	**Cp**
Intercept	5.85788	0.2983	0.668	4.00	Intercept	2.73344	0.2305	0.700	4.00
ISTFPR	0.00703				ISTFPR	0.01628			
FSTFPR	-0.00953				FSTFPR	-0.01055			
EDPR	202.02919				EDPR	361.65825			
MUSCLE FIBER TENDERNESS									
Equation	**β value**	**R^2**	**RMSE**	**Cp**	**Equation**	**β value**	**R^2**	**RMSE**	**Cp**
Intercept	3.68133	0.3066	1.021	4.00	Intercept	-0.71780	0.2694	1.048	4.00
ISTFPR	0.00802				ISTFPR	0.02202			
FSTFPR	-0.01026				FSTFPR	-0.01315			
EDPR	358.02627				EDPR	586.78016			
OVERALL TENDERNESS									
Equation	**β value**	**R^2**	**RMSE**	**Cp**	**Equation**	**β value**	**R^2**	**RMSE**	**Cp**
Intercept	3.36541	0.3343	1.011	4.00	Intercept	-1.35095	0.2936	1.042	4.00
ISTFPR	0.00749				ISTFPR	0.02317			
FSTFPR	-0.00930				FSTFPR	-0.01307			
EDPR	390.98070				EDPR	634.61514			

[1] Variable abbreviation explanation: ISTFPR=Initial Stiffness-Probe Compression; FSTFPR=Final Stiffness-Probe Compression; EDPR=Energy Dissipated-Probe Compression; R^2 = R-square; RMSE = Root Mean Squared Error; Cp = Mallock's Cp.

TABLE 27. Prediction equations for sensory traits using TA probe compression values[1] for pooled data at 4.4ºC (Phase 2).

	Raw data				Adjusted Data				
JUICINESS									
Equation	**β value**	**R^2**	**RMSE**	**Cp**	**Equation**	**β value**	**R^2**	**RMSE**	**Cp**
Intercept	4.63067	0.2604	0.618	4.00	Intercept	5.32439	0.2971	0.602	4.00
ISTFPR	0.06378				ISTFPR	0.07821			
FSTFPR	-0.07460				FSTFPR	-0.09415			
EDPR	107.99733				EDPR	73.52382			
CONNECTIVE TISSUE AMOUNT									
Equation	**β value**	**R^2**	**RMSE**	**Cp**	**Equation**	**β value**	**R^2**	**RMSE**	**Cp**
Intercept	11.02678	0.3812	0.464	4.00	Intercept	13.84779	0.5531	0.395	4.00
ISTFPR	0.07542				ISTFPR	0.07940			
FSTFPR	-0.10004				FSTFPR	-0.11568			
EDPR	-188.94455				EDPR	-328.68920			
MUSCLE FIBER TENDERNESS									
Equation	**β value**	**R^2**	**RMSE**	**Cp**	**Equation**	**β value**	**R^2**	**RMSE**	**Cp**
Intercept	9.79589	0.5129	0.548	4.00	Intercept	14.46320	0.7277	0.409	4.00
ISTFPR	0.11197				ISTFPR	0.13017			
FSTFPR	-0.14433				FSTFPR	-0.18269			
EDPR	-123.75272				EDPR	-369.39046			
OVERALL TENDERNESS									
Equation	**β value**	**R^2**	**RMSE**	**Cp**	**Equation**	**β value**	**R^2**	**RMSE**	**Cp**
Intercept	10.92353	0.5228	0.604	4.00	Intercept	15.60995	0.7073	0.473	4.00
ISTFPR	0.12745				ISTFPR	0.14377			
FSTFPR	-0.16558				FSTFPR	-0.20226			
EDPR	-183.83570				EDPR	-427.06157			

[1] Variable abbreviation explanation: ISTFPR=Initial Stiffness-Probe Compression; FSTFPR=Final Stiffness-Probe Compression; EDPR=Energy Dissipated-Probe Compression; R^2 = R-square; RMSE = Root Mean Squared Error; Cp = Mallock's Cp.

TABLE 28. Prediction equations for sensory traits using TA probe compression values[1] for pooled data at 10ºC (Phase 2).

	Raw data				Adjusted Data				
JUICINESS									
Equation	**β value**	**R^2**	**RMSE**	**Cp**	**Equation**	**β value**	**R^2**	**RMSE**	**Cp**
Intercept	8.42455	0.5585	0.413	4.00	Intercept	7.40434	0.5611	0.412	4.00
ISTFPR	0.13102				ISTFPR	0.10688			
FSTFPR	-0.16222				FSTFPR	-0.13103			
EDPR	-148.64747				EDPR	-84.68309			
CONNECTIVE TISSUE AMOUNT									
Equation	**β value**	**R^2**	**RMSE**	**Cp**	**Equation**	**β value**	**R^2**	**RMSE**	**Cp**
Intercept	9.39372	0.6438	0.533	4.00	Intercept	8.13120	0.6674	0.515	4.00
ISTFPR	0.21464				ISTFPR	0.18818			
FSTFPR	-0.25812				FSTFPR	-0.22393			
EDPR	-169.79147				EDPR	-81.39377			
MUSCLE FIBER TENDERNESS									
Equation	**β value**	**R^2**	**RMSE**	**Cp**	**Equation**	**β value**	**R^2**	**RMSE**	**Cp**
Intercept	9.53293	0.6675	0.756	4.00	Intercept	7.65629	0.6748	0.747	4.00
ISTFPR	0.30411				ISTFPR	0.26848			
FSTFPR	-0.36849				FSTFPR	-0.32073			
EDPR	-176.37310				EDPR	-72.91513			
OVERALL TENDERNESS									
Equation	**β value**	**R^2**	**RMSE**	**Cp**	**Equation**	**β value**	**R^2**	**RMSE**	**Cp**
Intercept	9.80868	0.6993	0.695	4.00	Intercept	8.11712	0.7019	0.692	4.00
ISTFPR	0.29831				ISTFPR	0.25924			
FSTFPR	-0.36268				FSTFPR	-0.31144			
EDPR	-182.69149				EDPR	-89.94746			

[1] Variable abbreviation explanation: ISTFPR=Initial Stiffness-Probe Compression; FSTFPR=Final Stiffness-Probe Compression; EDPR=Energy Dissipated-Probe Compression; R^2 = R-square; RMSE = Root Mean Squared Error; Cp = Mallock's Cp.

TABLE 29. R-square values of prediction equations for sensory traits utilizing Warner-Bratzler shear force values, segregated by temperature treatment (Phase 2).

Sensory Traits	All Temperatures	-6.6°C	4.4°C	10°C
JUICINESS				
R^2 =	0.0506	0.0470	0.0023	0.3855
CONNECTIVE TISSUE AMOUNT				
R^2 =	0.5699	0.5963	0.4892	0.6642
MUSCLE FIBER TENDERNESS				
R^2 =	0.5418	0.5499	0.4267	0.6519
OVERALL TENDERNESS				
R^2 =	0.5477	0.5612	0.4493	0.6486

[1] Variable abbreviation explanation: R^2 = R-square; MSE = Mean Square Error.

APPENDIX D

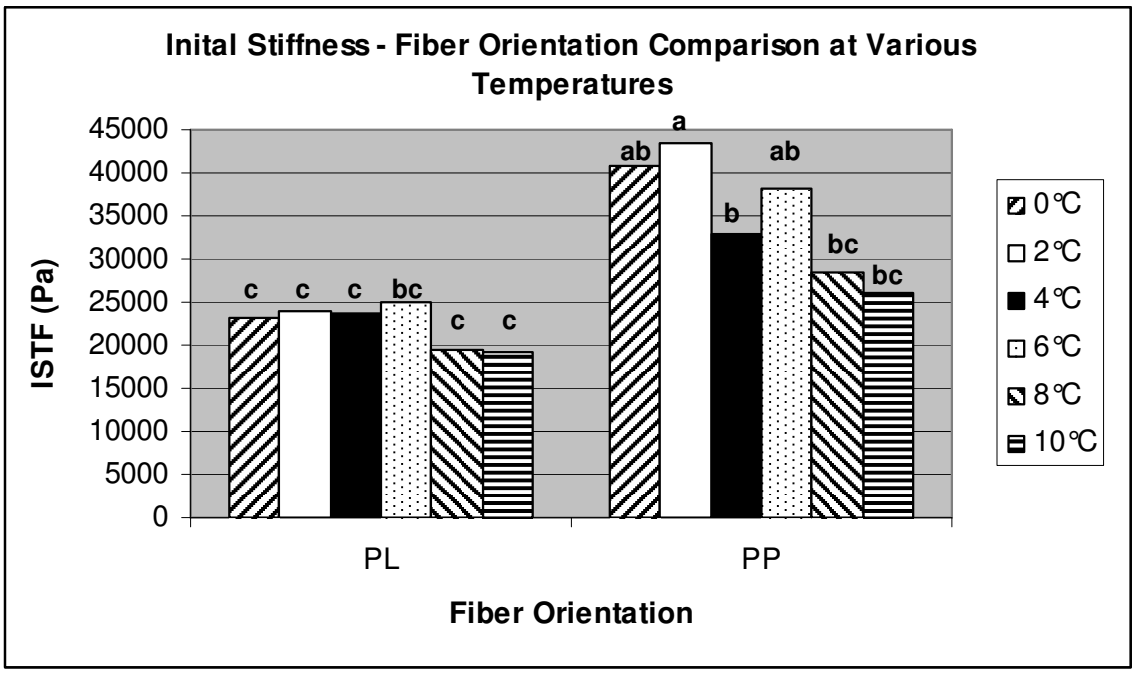

FIGURE 8. Comparison of initial stiffness mean values of each fiber orientation at each of the various holding temperatures.

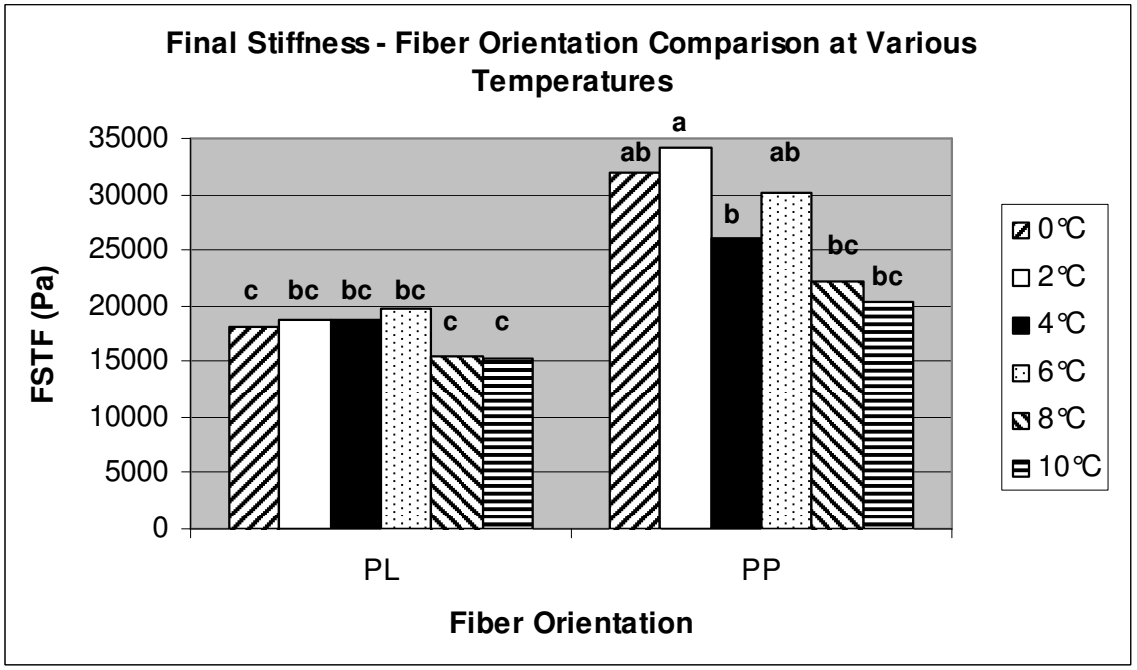

FIGURE 9. Comparison of final stiffness mean values of each fiber orientation at each of the various holding temperatures.

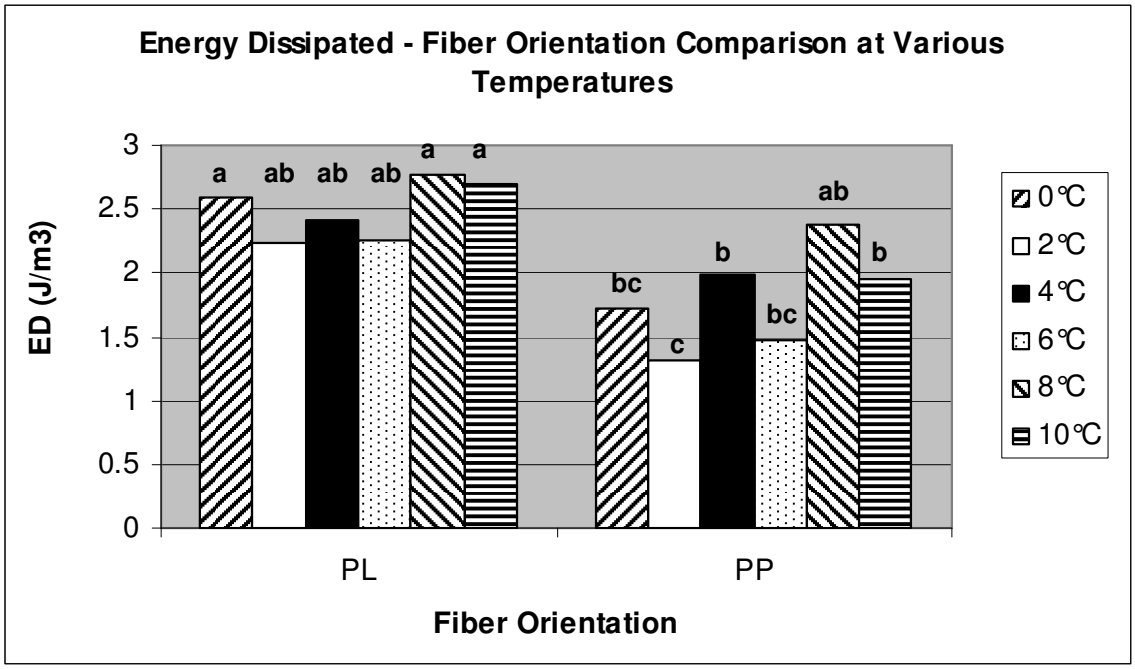

FIGURE 10. Comparison of energy dissipated values of each fiber orientation at each of the various temperatures.

APPENDIX E

TA.XT2 Program Software set up for cubed compression

1. Open Texture Expert Program

Choose T.A. (on main menu)
Choose T.A. Settings

2. Set Texture Analyzer Settings:

Test Mode and Options:
Measure Force in Compression
Hold Until Time

Parameters:
Post test speed: 10 mm/s
Pre test speed: 10 mm/s
Test speed: 10 mm/s
Rupture Test Distance: 1%
Distance: 3%
Force: 1.49 N
Time: 240 sec
Count: 5

Trigger:
Type: Auto
Force: 0.05 N
Stop at: Final
Auto Tare: X (Yes)

Break:
Detect: Stop Level
Sensitivity: 14.99 N

Units:
Force: Newtons
Distance: % Strain

3. Save settings to C drive

Saved as c:\te_uk\meat.set

4. **Load c:\te_uk\meat.set**

5. **Calibrate probe & force**

   Choose T.A. (on main menu)

6. **To run Texture Expert:**

   Choose: T.A.(main menu)
   Run A Test

   Archive As:
   Auto Save: X (Yes)
   File ID: give your file an ID
   File Number: give your sample an ID number
   Drive: choose where you want your data saved

   Pretest:
   Clear previous graphs X (Yes)

   Acquisition Rate:
   50 pps

7. **Process Data**

   Save Configuration
   Save type: Comma delimited
   All points
   Time & distance & force

MatLab Program for cubed compression

```
%  mainprog.m - 11/19/02 - Randi Boleman.
%  This is the principal program to process raw files (.lis) from XTRAD.
%  It processes the data to obtain strain relaxation functions:
%
%  Eijkl(t)=c1*exp(-c2*t)+c3*exp(-c4*t)+c5*exp(-c6*t)+c7
%
%  Strain level eps(0)=0.03
%  PART 1
%  1.  Calculate the sample.
%
%  PART 2
%  Collocation of the sample.
%
%  PART 2
%  2.  Runs 'opfun' script to obtain the coefficients of the prony series.
%          s=c(1)*exp(c(2)*t)+c(3)*exp(c(4)*t)+c(5)*exp(c(6)*t)+c(7)
%          t=time
%          s=stress/eps(0)
%          c(i)=prony series coefficient
%
%  3.  Calculates the prony series/creep compliance using collocated data.
%
%  NOTE:  This script runs in conjunction with preprog1, a shell script that:
%          Renames the input working files as archi?
%          Loads the corresponding area sizes for the files
%          Loads the sample name for the graphic
%          Stores archi1.out (averaged geometry sample) as sample_name.avg
%          Stores archi2.out (prony series coefficient) as sample_name.pro
%
%
%  The areas requested correspond to the experimentally determined surfaces of
%  the cubes of meat where the probe was acting on.
%
%
%  prony(i)=prony series coefficients
%
%
%
%
%
%
```

```
%
%
%%%%%%%%%%%%%%%%%%%%%%%%%%
%  PART 1
%%%%%%%%%%%%%%%%%%%%%%%%%%
%
%
%  fid=fopen ('filename','r'); opens filename and reads it only
%  declare a dummy matrix, which I call a, 'a=fscanf(fid,'%g %g','%g',[3 12000]);
clear all;
fid = fopen('875PL50.prn','r');
a = fscanf(fid,'%g %g %g',[3 12000]);
%  a=a' moves data from being in rows to columns;
a = a';
%  declare a variable, a, a=load(PLO2000), which is 200PL0;
%
%
%  t=a(:,3L; time=filename(force:time is in 3rd column);
t=a(:,3);
%
%  s11=filename(:,1) - '1' because force in 1st column;
s11=a(:,1);
%  e11=filename(:,2) - '2' because distance in 2n column;
e11=a(:,2);
%
%  area1=2.54*2.54 because of the sample being 2.54cm3;
%  convert cm to m;
area1=.0254*.0254;
%
%  25.4 mm = 2.54 cm - length of one side of sample;
for i=1:12000
            e11(i)=e11(i)/25.4;  %this gives the strain value;
end
%
for i=1:12000
   s11(i)=(s11(i)/1000)*9.81/(area1);  %this gives stress value and converts g to N;
end
%
for i=1:12000
   E11(i)=s11(i)/(e11(i));  %this divides stress by strain to give relaxation modulus (E);
end
%
%
E11=E11';  %transform from row to column;
```

```
%  average=[t s]
save 875PL50.out %average -ascii
%
%
%
%%%%%%%%%%%%%%%%%%%%
%  PART 2
%%%%%%%%%%%%%%%%%%%%
%
%
t1=t(1:10); %t1 reads the 1st 10 values of t;
E111=E11(1:10);  %E111 reads the 1st 10 values of E11;
p1=polyfit(t1,E111,1);
f=polyval(p1,t1);
f1=polyval(p1,.2);
%
%
t2=t(75:105); %t2 reads the 2nd 10 values of t;
E112=E11(75:105);  %E112 reads the 2nd 10 values of E11;
p2=polyfit(t2,E112,1);
f=polyval(p2,t2);
f2=polyval(p2,2);
%
%
t3=t(975:1005); %t3 reads the 3rd 10 values of t;
E113=E11(975:1005);  %E113 reads the 3rd 10 values of E11;
p3=polyfit(t3,E113,1);
f=polyval(p3,t3);
f3=polyval(p3,20);
%
%
t4=t(9975:10005); %t4 reads the 4th 10 values of t;
E114=E11(9975:10005);  %E114 reads the 4th 10 values of E11;
p4=polyfit(t4,E114,1);
f=polyval(p4,t4);
f4=polyval(p4,200);
%
%
rho(1)=.25;
rho(2)=2.5;
rho(3)=25;
b(1)=f1-f4; %vector matrix to define E1 thru E3 - E4;
b(2)=f2-f4;
b(3)=f3-f4;
```

```
A(1,1)=exp(-.2/rho(1)); %A(1,1) is first term in matrix & prony series;
A(1,2)=exp(-.2/rho(2));
A(1,3)=exp(-.2/rho(3));
A(2,1)=exp(-2/rho(1));
A(2,2)=exp(-2/rho(2));
A(2,3)=exp(-2/rho(3));
A(3,1)=exp(-20/rho(1));
A(3,2)=exp(-20/rho(2));
A(3,3)=exp(-20/rho(3));
E=inv(A)*b'; %takes the inverse of A, multiplies by b to obtain the spring coefficients
(E) in prony series;
%
%  creates vector for time (tt) with corresponding relaxation values;
for tt=1:200
   relax(tt)=f4+E(1)*exp(-tt/rho(1))+E(2)*exp(-tt/rho(2))+E(3)*exp(-tt/rho(3));
   time(tt)=tt;
end
%
%
%
%
%%%%%%%%%%%%%%%%%%%%
%  PART 3
%%%%%%%%%%%%%%%%%%%%
%
%
%
%
%
prony=[E(1) 1/rho(1) E(2) 1/rho(2) E(3) 1/rho(3) f4];
fit=prony(1)*exp(prony(2)*t1)+prony(3)*exp(prony(4)*t1)+prony(5)*exp(prony(6)*t1)
+prony(7);
%
save 875PL50A.out prony -ascii
```

```
%  creep 11/19/02  Randi Boleman.
%  This script produces the cubic roots and the coefficients necessary
%  to obtain the creep compliance D(t) from the stress relaxation E(t).
%
%          E(t)=c1*exp(-c2*t)+ c3*exp(-c4*t)+ c5*exp(-c6*t)+ c7            (1)
%          E'(t)=-c1*c2*exp(-c2*t) -c3*c4*exp(-c4*t) -c5*c6*exp(-c6*t)
%
%  The Laplace transform of dE(t)/dt (E'(t))
%
%          L{E'(t)}=E(0)-c1*c2/(s+c2)-c3*c4/(s+c4)-c5*c6/(s+c6), (2)
%
%  where,
%          E(0)=c1+c3+c5+c7(3)
%
%  and,
%          L{E'(t)}=sL{E(t)}  (4)
%
%  also,
%          Carson{E(t)}*Carson{D(t)}=1=> L{D'(t)}=1/L{E'(t)}    (5)
%                              **********************
%
%  then,
%
%          D'(s)=[(s+c2)(s+c4)(s+c6)]/[E(0)(s+c2)(s+c4)(s+c6)-c1c2(s+c4)(s+c6)-
c3c4(s+c2)(s+c6)-c5c6(s+c2)(s+c4)]
%
%  This is the quotient of two polynomials, say Q(s)/P(s).
%  Find the cubic roots of P(s), i.e. r1, r2, r3 =>
%
%          D'(s)=K0+d1/(s-r1)+d2/(s-r2)+d3/(s-r3)
%
%  where,
%          K0=lim(s->oo)Q(s)/P(s)=1/[lim(s->oo)E'(s)]=1/E(0)
%                          ******
%  and,
%          di=lim(s->(ri))[!(s)/P(s)](s-ri)
%          I=1,2,3
%
%  then,
%          d1=Q(r1)/[E(0)(r1-r2)(r1-r3)]
%          d2=Q(r2)/[E(0)(r2-r1)(r2-r3)]
%          d3=Q(r3)/[E(0)(r3-r1)(r3-r2)]
%
%  resulting,
```

```
%           D'(s)=sD(s) =>
%
%           D(s)=D0/s+d1/(s(s-r1)+d2/(s(s-r2)+d3/(s(s-r3))
%
%  finally,
%           ************************************************************
%           D(t)=K0+(d1/r1)(1-exp(-r1*t))+(d2/r2)(1-exp(-r2*t)) +(d3/r3)(1-exp(-r3*t))
%           ************************************************************
%
%           Res=[K0 D1 r1 D2 r2 D3 r3]
%
%
%
%  fid=fopen ('filename','r'); opens filename and reads it only
%  declare a dummy matrix, which I call a, 'prony=fscanf(fid,'%g %g %g %g %g' %g
%g',[1 7]); has 7 values
clear all;
fid = fopen('895PP40A.out','r');
prony = fscanf(fid,'%g %g %g %g %g %g %g',[1 7]);
%
for i=1
            c(i,1)=prony(i,1);
            c(i,2)=prony(i,2);
            c(i,3)=prony(i,3);
            c(i,4)=prony(i,4);
            c(i,5)=prony(i,5);
            c(i,6)=prony(i,6);
            c(i,7)=prony(i,7);

            E0(i)=c(i,1)+c(i,3)+c(i,5)+c(i,7);
            K0(i)=1/E0(i);

%  Find P(s) and roots r1,r2 and r2
            p1=[1 c(i,2)];
            p2=[1 c(i,4)];
            p3=[1 c(i,6)];

            p1p2=conv(p1,p2);
            p1p3=conv(p1,p3);
            p2p3=conv(p2,p3);

            p1p2t=[0 p1p2];
            p1p3t=[0 p1p3];
            p2p3t=[0 p2p3];
```

```
        p1p2p3=conv(p1p2,p3);

        P=E0(i)*p1p2p3-c(i,1)*c(i,2)*p2p3t-c(i,3)*c(i,4)*p1p3t-c(i,5)*c(i,6)*p1p2t;

        r=roots(P);
        r1(i)=r(1,1);
        r2(i)=r(2,1);
        r3(i)=r(3,1);

        Q=polyval(p1p2p3,r);
        d1=Q(1,1)/(E0(i)*(r1(i)-r2(i))*(r1(i)-r3(i)));
        d2=Q(2,1)/(E0(i)*(r2(i)-r1(i))*(r2(i)-r3(i)));
        d3=Q(3,1)/(E0(i)*(r3(i)-r1(i))*(r3(i)-r2(i)));

        D1(i)=d1/(-r1(i))
        D2(i)=d2/(-r2(i))
        D3(i)=d3/(-r3(i))

        end

Res=[K0' D1' r1' D2' r2' D3' r3'];
fif=fopen('totcreepux.out','a');
fprintf(fif,'%g %g %g %g %g %g %g\n',Res);
fclose(fif);
```

```
%
%  final.m - 11/19/02 - Randi Boleman.
%
%  This is the program that calculates trains (using the elastic Boussinesq solution:
%  concentrated force acting on an infinite plate), energy dissipated, and stiffness.
%  The calculations require the use of homogenized stresses and strains.
%
%  The inputs required are D1111(t) -along myofibers-, D2222(t) -across myofibers-,
and
%  D1122(t) which are provided % in that order in the file "totcreepux".
%
%  NOTES:
%  *******
%  The creep compliance terms are termed "pl" for D2222, "pp" for D1111,
%  and "plpp" for D1122.  X1-x3 is the plane of isotropy, myofibers run along x2.
%
%
%
%  THE FIRST SET WILL CALCULATE MECHANICS OF MASTICATION
ALONG THE MYOFIBERS.
%
%  THE SECOND SET WILL CALCULATE MECHANICS OF MASTICATION
ACROSS THE MYFIBERS.
%
%
clear all;
fid = fopen('totcreepux895.out','r');
totcreepux = fscanf(fid,'%g %g %g %g %g %g %g %g %g %g %g %g %g %g',[1 14]);
time=[0.025 0.25];
t=time';
%
Poisson=.35;
%
for i=1
D0pl=totcreepux(i,1);
D1pl=totcreepux(i,2);
r1pl=totcreepux(i,3);
D2pl=totcreepux(i,4);
r2pl=totcreepux(i,5);
D3pl=totcreepux(i,6);
r3pl=totcreepux(i,7);
D0pp=totcreepux(i,8);
D1pp=totcreepux(i,9);
r1pp=totcreepux(i,10);
```

```
D2pp=totcreepux(i,11);
r2pp=totcreepux(i,12);
D3pp=totcreepux(i,13);
r3pp=totcreepux(i,14);
D0plpp=-Poisson*totcreepux(i,8);
D1plpp=-Poisson*totcreepux(i,9);
r1plpp=totcreepux(i,10);
D2plpp=-Poisson*totcreepux(i,11);
r2plpp=totcreepux(i,12);
D3plpp=-Poisson*totcreepux(i,13);
r3plpp=totcreepux(i,14);

%  D0plpp=totcreepux(i,15);
%  D1plpp=totcreepux(i,16);
%  r1plpp=totcreepux(i,17);
%  D2plpp=totcreepux(i,18);
%  r2plpp=totcreepux(i,19);
%  D3plpp=totcreepux(i,20);
%  r3plpp=totcreepux(i,21);
%  Calculation of space variables.

s22s22=(3.694e03)^2;

s11s11=(1.320e03)^2;

s11s22=3.694e03*1.320e03;


%  Mastication parallel to the myofibers.

for j=1:2


sgmabar22pl(j)=-3.694e03*t(j);

sgmabar11pl(j)=-1.320e03*t(j);

epsbar22pl(j)= -1.320e03*(t(j)*(D0plpp+D1plpp+ D2plpp+ D3plpp) -
D1plpp*exp(r1plpp*t(j))/r1plpp - D2plpp*exp(r2plpp*t(j))/r2plpp -
D3plpp*exp(r3plpp*t(j))/r3plpp + D1plpp/r1plpp + D2plpp/r2plpp + D3plpp/r3plpp) -
3.694e03*(t(j)*(D0pl+D1pl+D2pl+D3pl) - D1pl*exp(r1pl*t(j))/r1pl -
D2pl*exp(r2pl*t(j))/r2pl - D3pl*exp(r3pl*t(j))/r3pl + D1pl/r1pl + D2pl/r2pl +
D3pl/r3pl);
```

```
epsbar11pl(j)=-1.320e03*(t(j)*(D0pp+D1pp+D2pp+D3pp) - D1pp*exp(r1pp*t(j))/r1pp -
D2pp*exp(r2pp*t(j))/r2pp - D3pp*exp(r3pp*t(j))/r3pp + D1pp/r1pp + D2pp/r2pp +
D3pp/r3pp) -3.694e03*(t(j)*(D0plpp+D1plpp+D2plpp+D3plpp) -
D1plpp*exp(r1plpp*t(j))/r1plpp - D2plpp*exp(r2plpp*t(j))/r2plpp -
D3plpp*exp(r3plpp*t(j))/r3plpp + D1plpp/r1plpp + D2plpp/r2plpp + D3plpp/r3plpp);


stiffpl(j)=sgmabar22pl(j)/epsbar22pl(j);

workpl(j)=sgmabar11pl(j)*epsbar11pl(j)+sgmabar22pl(j)*epsbar22pl(j);

inistiffpl(i)=sgmabar22pl(1)/epsbar22pl(1);

finalstiffpl(i)=stiffpl(j);


%  Calculation of terms for total energy dissipated 'energypl'.

term1pl=D1pl*t(j)^2/2 - D1pl*r1pl^(-2)*exp(r1pl*t(j))+ D1pl*r1pl^(-2) + D1pl*r1pl^(-
1)*t(j);
term2pl=D2pl*t(j)^2/2 - D2pl*r2pl^(-2)*exp(r2pl*t(j))+ D2pl*r2pl^(-2) + D2pl*r2pl^(-
1)*t(j);
term3pl=D3pl*t(j)^2/2 - D3pl*r3pl^(-2)*exp(r3pl*t(j))+ D3pl*r3pl^(-2) + D3pl*r3pl^(-
1)*t(j);

term1plpp=D1plpp*t(j)^2/2 - D1plpp*r1plpp^(-2)*exp(r1plpp*t(j))+ D1plpp*r1plpp^(-
2) + D1plpp*r1plpp^(-1)*t(j);
term2plpp=D2plpp*t(j)^2/2 - D2plpp*r2plpp^(-2)*exp(r2plpp*t(j))+ D2plpp*r2plpp^(-
2) + D2plpp*r2plpp^(-1)*t(j);
term3plpp=D3plpp*t(j)^2/2 - D3plpp*r3plpp^(-2)*exp(r3plpp*t(j))+ D3plpp*r3plpp^(-
2) + D3plpp*r3plpp^(-1)*t(j);

term1pp=D1pp*t(j)^2/2 - D1pp*r1pp^(-2)*exp(r1pp*t(j))+ D1pp*r1pp^(-2) +
D1pp*r1pp^(-1)*t(j)
term2pp=D2pp*t(j)^2/2 - D2pp*r2pp^(-2)*exp(r2pp*t(j))+ D2pp*r2pp^(-2) +
D2pp*r2pp^(-1)*t(j)
term3pp=D3pp*t(j)^2/2 - D3pp*r3pp^(-2)*exp(r3pp*t(j))+ D3pp*r3pp^(-2) +
D3pp*r3pp^(-1)*t(j)


energypl(i)=0.5*(s22s22*(term1pl+term2pl+term3pl) +
s11s11*(term1pp+term2pp+term3pp) + s11s22*(term1plpp+term2plpp+term3plpp));

resultpl=[inistiffpl' finalstiffpl' energypl'];
```

```
% Mastication perpendicular to the myofibers

sgmabar22pp(j)=-3.694e03*t(j);

sgmabar11pp(j)=-1.320e03;

epsbar22pp(j)= -1.320e03*(t(j)*(D0plpp+ D1plpp+D2plpp+D3plpp) -
D1plpp*exp(r1plpp*t(j))/r1plpp - D2plpp*exp(r2plpp*t(j))/r2plpp -
D3plpp*exp(r3plpp*t(j))/r3plpp + D1plpp/r1plpp + D2plpp/r2plpp + D3plpp/r3plpp) -
3.694e03*(t(j)*(D0pp+D1pp+D2pp+D3pp) - D1pp*exp(r1pp*t(j))/r1pp -
D2pp*exp(r2pp*t(j))/r2pp - D3pp*exp(r3pp*t(j))/r3pp + D1pp/r1pp + D2pp/r2pp +
D3pp/r3pp);

epsbar11pp(j)=-1.320e03*(t(j)*(D0pl+ D1pl+D2pl+D3pl) -D1pl*exp(r1pl*t(j))/r1pl -
D2pl*exp(r2pl*t(j))/r2pl - D3pl*exp(r3pl*t(j))/r3pl + D1pl/r1pl + D2pl/r2pl + D3pl/r3pl)
-3.694e03*(t(j)*(D0plpp+D1plpp+D2plpp+D3plpp) - D1plpp*exp(r1plpp*t(j))/r1plpp -
D2plpp*exp(r2plpp*t(j))/r2plpp - D3plpp*exp(r3plpp*t(j))/r3plpp + D1plpp/r1plpp +
D2plpp/r2plpp + D3plpp/r3plpp);

stiffpp(j)=sgmabar22pp(j)/epsbar22pp(j);

workpp(j)=sgmabar11pp(j)*epsbar11pp(j)+sgmabar22pp(j)*epsbar22pp(j);

inistiffpp(i)=sgmabar22pp(1)/epsbar22pp(1);

finalstiffpp(i)=stiffpp(j);

energypp(i)=0.5*(s11s11*(term1pl+term2pl+term3pl) +
2*s11s22*(term1plpp+term2plpp+term3plpp) + s22s22*(term1pp+term2pp+term3pp));

resultpp=[inistiffpp' finalstiffpp' energypp'];

end
end

result=[resultpl resultpp]'

save result.out result -ascii
```

APPENDIX F

TA.XT2 Program Software set up for probe compression

1. **Open Texture Expert Program**

    Choose T.A. (on main menu)
        Choose T.A. Settings

2. **Set Texture Analyzer Settings:**

    Test Mode and Options:
        Measure Force in Compression
        Hold Until Time

    Parameters:
        Post test speed: 10 mm/s
        Pre test speed: 10 mm/s
        Test speed: 10 mm/s
        Rupture Test Distance: 1 mm
        Distance: 6.4 mm
        Force: 1.49 N
        Time: 0.25 sec
        Count: 5

    Trigger:
        Type: Auto
        Force: 0.05 N
        Stop at: Final
        Auto Tare: X (Yes)

    Break:
        Detect: Stop Level
        Sensitivity: 14.99 N

    Units:
        Force: Newtons
        Distance: Millimeters

3. **Save settings to C drive**

    Saved as c:\te_uk\meat2.set

4. **Load c:\te_uk\meat2set**

5. **Calibrate probe & force**

   Choose T.A. (on main menu)

6. **To run Texture Expert:**

   Choose: T.A.(main menu)
   Run A Test

   Archive As:
   Auto Save: X (Yes)
   File ID: give your file an ID
   File Number: give your sample an ID number
   Drive: choose where you want your data saved

   Pretest:
   Clear previous graphs X (Yes)

   Acquisition Rate:
   50 pps

7. **Process Data**

   Save Configuration
   Save type: Comma delimited
   All points
   Time & distance & force

MatLab Program for determining probe compression values

```
%  mainprog.m - 11/19/02 - Randi Boleman.
%  This is the principal program to process raw files (.lis) from XTRAD.
%  It processes the data to obtain strain relaxation functions:
%
%  Eijkl(t)=c1*exp(-c2*t)+c3*exp(-c4*t)+c5*exp(-c6*t)+c7
%
%  Strain level eps(0)=0.03
%  PART 1
%  1.  Calculate the sample.
%
%  PART 2
%  Collocation of the sample.
%
%  PART 2
%  2.  Runs 'opfun' script to obtain the coefficients of the prony series.
%       s=c(1)*exp(c(2)*t)+c(3)*exp(c(4)*t)+c(5)*exp(c(6)*t)+c(7)
%       t=time
%       s=stress/eps(0)
%       c(i)=prony series coefficient
%
%  3.  Calculates the prony series/creep compliance using collocated data.
%
%  NOTE:  This script runs in conjunction with preprog1, a shell script that:
%       Renames the input working files as archi?
%       Loads the corresponding area sizes for the files
%       Loads the sample name for the graphic
%       Stores archi1.out (averaged geometry sample) as sample_name.avg
%       Stores archi2.out (prony series coefficient) as sample_name.pro
%
%
%  The areas requested correspond to the experimentally determined surfaces of
%  the cubes of meat where the probe was acting on.
%
%
%  prony(i)=prony series coefficients
%

%%%%%%%%%%%%%%%%%%%%%%%%%%%%%%%%%%%%%%%%%%%%%%%%%%%%%%%%%%%%%%%%%%%%%%%%
%%%%%%%%%%%%%%%%%%%%%%%%%%%%%%%%%%%%%%%%%%%%%%%%%%%%%%%%%%%%%%%%%%%%%%%%
%  PART 1  READ IN RAW DATA
```

```
%%%%%%%%%%%%%%%%%%%%%%%%%%%%%%%%%%%%%%%%%%%%
%%%%%%%%%%%%%%%%%%%%%%%%%%%%%%%%%%%%%%%%%%

clear all;
fileroot = input('Enter fileroot: ','s');

filename = strcat(fileroot,'.CSV');

M = dlmread(filename,',',4,0);

M(1,1) = 0;

force = M(:,1)/1000*9.81;
displacement = M(:,2)/1000;
time = M(:,3);

[nrow,ncolumn] = size(M);

maxdispl = max(displacement);


%%%%%%%%%%%%%%%%%%%%%%%%%%%%%%%%%%%%%%%%%%%%
%%%%%%%%%%%%%%%%%%%%%%%%%%%%%%%%%%%%%%%%%%
%  PART 2  CALCULATE ENERGY INTRODUCED BY PROBE
%%%%%%%%%%%%%%%%%%%%%%%%%%%%%%%%%%%%%%%%%%%%
%%%%%%%%%%%%%%%%%%%%%%%%%%%%%%%%%%%%%%%%%%

%D=displacement(1:34);        %D reads the 1st 34 values of displacement;
%F=force(1:34);               %F reads the 1st 34 values of force;
%p1=polyfit(D,F,2);
%ff=polyval(p1,D);

count = 0;
etime = 0;

for i=1:nrow
   if displacement(i,1) == maxdispl
      count = count + 1;
      Energy(count) = 0.5*force(i)*displacement(i,1);      % Joules
      t(count) = etime;
      etime = etime + 0.02;
   end
end
```

```
p1=polyfit(t,Energy,3);
ff=polyval(p1,t);

[nrow2,ncolumn2] = size(Energy);

Einf = Energy(ncolumn2)*0.70;


%%%%%%%%%%%%%%%%%%%%%%%%%%%%%%%%%%%%%%%%%%%%%%%%%%%%%%%%%%%%%%%%%%%%%%%
%%%%%%%%%%%%%%%%%%%%%%%%%%%%%%%%%%%%%%%%%%%%%%%%%%%%%%%%%%%%%%%%%%%%%%%
%  PART 3  PERFORM COLLOCATION
%%%%%%%%%%%%%%%%%%%%%%%%%%%%%%%%%%%%%%%%%%%%%%%%%%%%%%%%%%%%%%%%%%%%%%%
%%%%%%%%%%%%%%%%%%%%%%%%%%%%%%%%%%%%%%%%%%%%%%%%%%%%%%%%%%%%%%%%%%%%%%%

radius = 0.001;

rho(1) = 0.0025;
rho(2) = 0.025;
rho(3) = 0.25;

val = 0.18;

EE(1) = p1(1)*(0.01*val)^3 + p1(2)*(0.01*val)^2 + p1(3)*(0.01*val) + p1(4);
EE(2) = p1(1)*(0.10*val)^3 + p1(2)*(0.10*val)^2 + p1(3)*(0.10*val) + p1(4);
EE(3) = p1(1)*(1.00*val)^3 + p1(2)*(1.00*val)^2 + p1(3)*(1.00*val) + p1(4);

b(1) = -(EE(1)-Einf)*2/3.141592*log(radius)/maxdispl^2;   %Vector matrix to define E1
thru E3 - E4;
b(2) = -(EE(2)-Einf)*2/3.141592*log(radius)/maxdispl^2;
b(3) = -(EE(3)-Einf)*2/3.141592*log(radius)/maxdispl^2;

f4 = -Einf*2/3.141592*log(radius)/maxdispl^2;

A(1,1) = exp((-0.01*val)/rho(1));       %A(1,1) is first term in matrix & prony series;
A(1,2) = exp((-0.01*val)/rho(2));
A(1,3) = exp((-0.01*val)/rho(3));
A(2,1) = exp((-0.10*val)/rho(1));
A(2,2) = exp((-0.10*val)/rho(2));
A(2,3) = exp((-0.10*val)/rho(3));
A(3,1) = exp((-1.00*val)/rho(1));
A(3,2) = exp((-1.00*val)/rho(2));
A(3,3) = exp((-1.00*val)/rho(3));
```

```
E=inv(A)*b';                    %takes the inverse of A, multiplies by b to obtain the spring
coefficients (E) in prony series;


for jj=1:200
   tt = jj*0.1;
   relax(jj)=f4+E(1)*exp(-tt/rho(1))+E(2)*exp(-tt/rho(2))+E(3)*exp(-tt/rho(3));
   time(jj)=tt;
end

%%%%%%%%%%%%%%%%%%%%%%%%%%%%%%%%%%%%%%%%%%%%%%%%%%%%%%%%%%%%%%%%%%%%%%%%%%%%
%  PART 4   STORE RELAXTION-LIKE MODULI
%%%%%%%%%%%%%%%%%%%%%%%%%%%%%%%%%%%%%%%%%%%%%%%%%%%%%%%%%%%%%%%%%%%%%%%%%%%%

prony = [E(1) 1/rho(1) E(2) 1/rho(2) E(3) 1/rho(3) f4];

%  creep 11/19/02  Randi Boleman.
%  This script produces the cubic roots and the coefficients necessary
%  to obtain the creep compliance D(t) from the stress relaxation E(t).
%
%       E(t)=c1*exp(-c2*t)+ c3*exp(-c4*t)+ c5*exp(-c6*t)+ c7                (1)
%       E'(t)=-c1*c2*exp(-c2*t) -c3*c4*exp(-c4*t) -c5*c6*exp(-c6*t)
%
%  The Laplace transform of dE(t)/dt (E'(t))
%
%       L{E'(t)}=E(0)-c1*c2/(s+c2)-c3*c4/(s+c4)-c5*c6/(s+c6),     (2)
%
%  where,
%       E(0)=c1+c3+c5+c7     (3)
%
%  and,
%       L{E'(t)}=sL{E(t)}      (4)
%
%  also,
%       Carson{E(t)}*Carson{D(t)}=1=> L{D'(t)}=1/L{E'(t)}        (5)
%                          **********************
%
%  then,
%
%       D'(s)=[(s+c2)(s+c4)(s+c6)]/[E(0)(s+c2)(s+c4)(s+c6)-c1c2(s+c4)(s+c6)-
c3c4(s+c2)(s+c6)-c5c6(s+c2)(s+c4)]
%
```

```
%  This is the quotient of two polynomials, say Q(s)/P(s).
%  Find the cubic roots of P(s), i.e. r1, r2, r3 =>
%
%       D'(s)=K0+d1/(s-r1)+d2/(s-r2)+d3/(s-r3)
%
%  where,
%       K0=lim(s->oo)Q(s)/P(s)=1/[lim(s->oo)E'(s)]=1/E(0)
%                          ******
%  and,
%       di=lim(s->(ri))[!(s)/P(s)](s-ri)
%       I=1,2,3
%
%  then,
%       d1=Q(r1)/[E(0)(r1-r2)(r1-r3)]
%       d2=Q(r2)/[E(0)(r2-r1)(r2-r3)]
%       d3=Q(r3)/[E(0)(r3-r1)(r3-r2)]
%
%  resulting,
%       D'(s)=sD(s) =>
%
%       D(s)=D0/s+d1/(s(s-r1)+d2/(s(s-r2)+d3/(s(s-r3))
%
%  finally,
%       ***************************************************************
%       D(t)=K0+(d1/r1)(1-exp(-r1*t))+(d2/r2)(1-exp(-r2*t)) +(d3/r3)(1-exp(-r3*t))
%       ***************************************************************
%
%       Res=[K0 D1 r1 D2 r2 D3 r3]
%
%

for i=1
        c(i,1)=prony(i,1);
        c(i,2)=prony(i,2);
        c(i,3)=prony(i,3);
        c(i,4)=prony(i,4);
        c(i,5)=prony(i,5);
        c(i,6)=prony(i,6);
        c(i,7)=prony(i,7);

        E0(i)=c(i,1)+c(i,3)+c(i,5)+c(i,7);
        K0(i)=1/E0(i);

%  Find P(s) and roots r1,r2 and r2
```

```
        p1=[1 c(i,2)];
        p2=[1 c(i,4)];
        p3=[1 c(i,6)];

        p1p2=conv(p1,p2);
        p1p3=conv(p1,p3);
        p2p3=conv(p2,p3);

        p1p2t=[0 p1p2];
        p1p3t=[0 p1p3];
        p2p3t=[0 p2p3];

        p1p2p3=conv(p1p2,p3);

        P=E0(i)*p1p2p3-c(i,1)*c(i,2)*p2p3t-c(i,3)*c(i,4)*p1p3t-c(i,5)*c(i,6)*p1p2t;

        r=roots(P);
        r1(i)=r(1,1);
        r2(i)=r(2,1);
        r3(i)=r(3,1);

        Q=polyval(p1p2p3,r);
        d1=Q(1,1)/(E0(i)*(r1(i)-r2(i))*(r1(i)-r3(i)));
        d2=Q(2,1)/(E0(i)*(r2(i)-r1(i))*(r2(i)-r3(i)));
        d3=Q(3,1)/(E0(i)*(r3(i)-r1(i))*(r3(i)-r2(i)));

        D1(i)=d1/(-r1(i))
        D2(i)=d2/(-r2(i))
        D3(i)=d3/(-r3(i))

        end

Res=[K0' D1' r1' D2' r2' D3' r3'];

filename = strcat(fileroot,'.out');

save(filename,'prony','-ASCII')



time=[0.025 0.25];
t=time';
%
```

```
Poisson=.35;
%
for i=1
D0pl=Res(i,1);
D1pl=Res(i,2);
r1pl=Res(i,3);
D2pl=Res(i,4);
r2pl=Res(i,5);
D3pl=Res(i,6);
r3pl=Res(i,7);
D0pp=Res(i,1);
D1pp=Res(i,2);
r1pp=Res(i,3);
D2pp=Res(i,4);
r2pp=Res(i,5);
D3pp=Res(i,6);
r3pp=Res(i,7);
D0plpp=-Poisson*Res(i,1);
D1plpp=-Poisson*Res(i,2);
r1plpp=Res(i,3);
D2plpp=-Poisson*Res(i,4);
r2plpp=Res(i,5);
D3plpp=-Poisson*Res(i,6);
r3plpp=Res(i,7);

%  D0plpp=totcreepux(i,15);
%  D1plpp=totcreepux(i,16);
%  r1plpp=totcreepux(i,17);
%  D2plpp=totcreepux(i,18);
%  r2plpp=totcreepux(i,19);
%  D3plpp=totcreepux(i,20);
%  r3plpp=totcreepux(i,21);
%  Calculation of space variables.

s22s22=(2.3616e01)^2;

s11s11=(8.448e00)^2;

s11s22=2.3616e01*8.448e00;


%  Mastication parallel to the myofibers.

for j=1:2
```

```
sgmabar22pl(j)=-2.3616e01*t(j);

sgmabar11pl(j)=-8.448e00*t(j);

epsbar22pl(j)= -8.448e00*(t(j)*(D0plpp+D1plpp+ D2plpp+ D3plpp) -
D1plpp*exp(r1plpp*t(j))/r1plpp - D2plpp*exp(r2plpp*t(j))/r2plpp -
D3plpp*exp(r3plpp*t(j))/r3plpp + D1plpp/r1plpp + D2plpp/r2plpp + D3plpp/r3plpp) -
2.3616e01*(t(j)*(D0pl+D1pl+D2pl+D3pl) - D1pl*exp(r1pl*t(j))/r1pl -
D2pl*exp(r2pl*t(j))/r2pl - D3pl*exp(r3pl*t(j))/r3pl + D1pl/r1pl + D2pl/r2pl +
D3pl/r3pl);

epsbar11pl(j)=-8.448e00*(t(j)*(D0pp+D1pp+D2pp+D3pp) - D1pp*exp(r1pp*t(j))/r1pp -
D2pp*exp(r2pp*t(j))/r2pp - D3pp*exp(r3pp*t(j))/r3pp + D1pp/r1pp + D2pp/r2pp +
D3pp/r3pp) -2.3616e01*(t(j)*(D0plpp+D1plpp+D2plpp+D3plpp) -
D1plpp*exp(r1plpp*t(j))/r1plpp - D2plpp*exp(r2plpp*t(j))/r2plpp -
D3plpp*exp(r3plpp*t(j))/r3plpp + D1plpp/r1plpp + D2plpp/r2plpp + D3plpp/r3plpp);


stiffpl(j)=sgmabar22pl(j)/epsbar22pl(j);

workpl(j)=sgmabar11pl(j)*epsbar11pl(j)+sgmabar22pl(j)*epsbar22pl(j);

inistiffpl(i)=sgmabar22pl(1)/epsbar22pl(1);

finalstiffpl(i)=stiffpl(j);


%  Calculation of terms for total energy dissipated 'energypl'.

term1pl=D1pl*t(j)^2/2 - D1pl*r1pl^(-2)*exp(r1pl*t(j))+ D1pl*r1pl^(-2) + D1pl*r1pl^(-
1)*t(j);
term2pl=D2pl*t(j)^2/2 - D2pl*r2pl^(-2)*exp(r2pl*t(j))+ D2pl*r2pl^(-2) + D2pl*r2pl^(-
1)*t(j);
term3pl=D3pl*t(j)^2/2 - D3pl*r3pl^(-2)*exp(r3pl*t(j))+ D3pl*r3pl^(-2) + D3pl*r3pl^(-
1)*t(j);

term1plpp=D1plpp*t(j)^2/2 - D1plpp*r1plpp^(-2)*exp(r1plpp*t(j))+ D1plpp*r1plpp^(-
2) + D1plpp*r1plpp^(-1)*t(j);
term2plpp=D2plpp*t(j)^2/2 - D2plpp*r2plpp^(-2)*exp(r2plpp*t(j))+ D2plpp*r2plpp^(-
2) + D2plpp*r2plpp^(-1)*t(j);
term3plpp=D3plpp*t(j)^2/2 - D3plpp*r3plpp^(-2)*exp(r3plpp*t(j))+ D3plpp*r3plpp^(-
2) + D3plpp*r3plpp^(-1)*t(j);
```

```
term1pp=D1pp*t(j)^2/2 - D1pp*r1pp^(-2)*exp(r1pp*t(j))+ D1pp*r1pp^(-2) +
D1pp*r1pp^(-1)*t(j)
term2pp=D2pp*t(j)^2/2 - D2pp*r2pp^(-2)*exp(r2pp*t(j))+ D2pp*r2pp^(-2) +
D2pp*r2pp^(-1)*t(j)
term3pp=D3pp*t(j)^2/2 - D3pp*r3pp^(-2)*exp(r3pp*t(j))+ D3pp*r3pp^(-2) +
D3pp*r3pp^(-1)*t(j)


energypl(i)=0.5*(s22s22*(term1pl+term2pl+term3pl) +
s11s11*(term1pp+term2pp+term3pp) + s11s22*(term1plpp+term2plpp+term3plpp));

resultpl=[inistiffpl' finalstiffpl' energypl'];

% Mastication perpendicular to the myofibers

sgmabar22pp(j)=-2.3616e01*t(j);

sgmabar11pp(j)=-8.448e00;

epsbar22pp(j)= -8.448e00*(t(j)*(D0plpp+ D1plpp+D2plpp+D3plpp) -
D1plpp*exp(r1plpp*t(j))/r1plpp - D2plpp*exp(r2plpp*t(j))/r2plpp -
D3plpp*exp(r3plpp*t(j))/r3plpp + D1plpp/r1plpp + D2plpp/r2plpp + D3plpp/r3plpp) -
2.3616e01*(t(j)*(D0pp+D1pp+D2pp+D3pp) - D1pp*exp(r1pp*t(j))/r1pp -
D2pp*exp(r2pp*t(j))/r2pp - D3pp*exp(r3pp*t(j))/r3pp + D1pp/r1pp + D2pp/r2pp +
D3pp/r3pp);

epsbar11pp(j)=-8.448e00*(t(j)*(D0pl+ D1pl+D2pl+D3pl) -D1pl*exp(r1pl*t(j))/r1pl -
D2pl*exp(r2pl*t(j))/r2pl - D3pl*exp(r3pl*t(j))/r3pl + D1pl/r1pl + D2pl/r2pl + D3pl/r3pl)
-2.3616e01*(t(j)*(D0plpp+D1plpp+D2plpp+D3plpp) - D1plpp*exp(r1plpp*t(j))/r1plpp -
D2plpp*exp(r2plpp*t(j))/r2plpp - D3plpp*exp(r3plpp*t(j))/r3plpp + D1plpp/r1plpp +
D2plpp/r2plpp + D3plpp/r3plpp);

stiffpp(j)=sgmabar22pp(j)/epsbar22pp(j);

workpp(j)=sgmabar11pp(j)*epsbar11pp(j)+sgmabar22pp(j)*epsbar22pp(j);

inistiffpp(i)=sgmabar22pp(1)/epsbar22pp(1);

finalstiffpp(i)=stiffpp(j);

energypp(i)=0.5*(s11s11*(term1pl+term2pl+term3pl) +
2*s11s22*(term1plpp+term2plpp+term3plpp) + s22s22*(term1pp+term2pp+term3pp));
```

```
resultpp=[inistiffpp' finalstiffpp' energypp'];

end
end

result=[resultpl resultpp]'

save result.out result -ascii
```

VITA

Randi Marburger Boleman is the wife of Christopher Thomas and daughter of Gary Marburger of Crystal City, Texas and Bonnie Ackermann of Cotulla, Texas. She was born on November 6, 1974 in Crystal City, where she spent her youth.

In 1993, Randi enrolled in Texas A&M University, where she graduated in 1997 with her Bachelor of Science in Animal Science. She continued her education by receiving a Master of Science in Food Science and Technology in 1999 under the guidance of Dr. Jimmy T. Keeton. As a result of her research, there is potential development of an online tenderness assessment without sample destruction that will be beneficial to the beef industry.

Randi is currently employed as Assistant Director and Registered Dietitian at Bryan Independent School District School Nutrition Services.

The author's permanent address is 2112 Maplewood Court, College Station, TX, 77845.